CRYSTALLIZATION OF FRUCTOSE FROM AQUEOUS SOLUTIONS

By

Lie-Ding Shiau

A DISSERTATION

Submitted to
Michigan State University
in partial fulfillment of the requirements
for the degree of

DOCTOR OF PHILOSOPHY

Department of Chemical Engineering

1988

ABSTRACT

CRYSTALLIZATION OF FRUCTOSE FROM AQUEOUS SOLUTIONS

By

Lie-Ding Shiau

The growth rates of fructose crystals formed by contact nucleation were studied in an unstirred solution using a photomicroscopic technique. The results indicated the existence of a distribution of apparent initial sizes and a distribution of growth rates. The crystals were found to follow the constant crystal growth (CCG) model, in which an individual crystal has an inherent, constant growth rate, but different crystals have different inherent rates in the same environment. Crystallization of fructose in the presence of glucose resulted in slower growth rates, but the CCG model was found to remain applicable.

A new model, taking both nucleation and supersaturation changes into account, was developed to relate the resulting crystal size distribution (CSD) from a batch crystallizer in the presence of growth rate dispersion (GRD) to the growth rate distribution based on the CCG assumption. The modeling equations were solved with a mass balance constraint to simulate the resulting CSD for a seeded, batch sucrose crystallizer. The model was tested using sucrose rate data since no such data were available for fructose. The effects of the presence of GRD on mean crystal size, production and coefficient of variation were examined.

A study of the nucleation and growth rates of fructose in a batch crystallizer was also conducted. The novel model previously developed was used to recover nucleation and growth rates from batch experiments in the presence of GRD. The procedure developed solved the general problem of data recovery from batch experiments and should be applicable to any batch study.

Finally, a recursion formula was developed to relate the resulting CSD from a cascade of mixed suspension, mixed product removal (MSMPR) crystallizers to the growth rate distributions of each stage in the presence of GRD based on the CCG assumption. The recursion formula was solved simultaneously with the mass balance to predict the CSD from a three-stage MSMPR sucrose crystallizer. Again, the sucrose data were used to test the model due to the wide availability of sucrose rate data. The effects of the presence of GRD on mean crystal size, production rate and coefficient of variation were also examined.

ACKNOWLEDGMENTS

I would like to thank my advisor, Professor Kris A. Berglund, for his guidance and encouragements throughout this research. I also want to thank Professors Daina M. Briedis, Charles A. Petty, Pericles Markakis and James F. Steffe for their useful comments and criticism.

Special thanks are given to my parents, Mr. and Mrs. Yue-Mau Shiau, and my wife, Shiow-Hwa, for their encouragements, moral support and love during this study.

TABLE OF CONTENTS

LIST OF TABLES

LIST OF FIGURES

CHAPTER 6:

CHAPTER 1

INTRODUCTION

1.1 Introduction

Crystallization is an important unit operation in the chemical industry for purification and separation. World wide production rates of crystalline materials such as sucrose, sodium chloride, and many fertilizer chemicals (ammonium phosphates, urea, potassium nitrate, etc.) all exceed 10^6 tons per year (vanDamme, 1973).

Crystal size distribution (CSD) is one of the most important properties of crystallization processes. It affects the end uses of the crystalline product and interacts strongly with the crystallization process itself (Randolph and Larson, 1971). White and Wright (1971) and Berglund and Murphy (1986) have shown that growth rate dispersion (GRD) is an extremely important phenomenon affecting the CSD. Using the results of batch sucrose crystallization, they showed conclusively that crystals of the same size can grow at different rates in identical environments.

Due to the high solubility of fructose in water, crystallization of fructose has been a major difficulty in its manufacture. Therefore, despite the large number of nucleation and growth studies with the sucrose-water system (Hartel et al., 1980; Bergund, 1980; Gwynn et al., 1980; Kuijvenhoven and deJong, 1982), few data are available on the fructose-water system.

The objectives of this research are to:

1. Determine the growth rate and GRD of fructose crystals formed by contact nucleation in unstirred solutions by the

photomicroscopic technique. The effects of glucose on the crystallization of fructose on the same phenomena will also be studied (Ch.3).

2. Develop a model to relate the resulting CSD from a batch crystallizer in the presence of GRD to the growth rate distribution. The model equations will be solved with a mass balance constraints to simulate the CSD for a seeded, batch sucrose crystallizer. Sucrose rate data will be used since no such data are available for fructose (Ch.4).
3. Determine the nucleation and growth rates from both pure fructose solution and fructose solution with the impurity glucose from a batch crystallizer in the presence of GRD based on the developed model (Ch.5).
4. Develop a model to relate the resulting CSD from a cascade of mixed suspension, mixed product removal (MSMPR) crystallizers in the presence of GRD to the growth rate distribution of each stage. The model equations will be solved simultaneously with the mass balance to predict the CSD for a three-stage MSMPR sucrose crystallizer. Again, the sucrose rate data will be used due to the wide availability of sucrose rate data in the literature (Ch.6).

1.2 Literature Cited

Berglund, K.A. "Growth and Size Dispersion Kinetics for Sucrose Crystals in the Sucrose-Water System", M.S. Thesis, Colorado State University, Ft. Collins. Co(1980).

Berglund, K.A.; Murphy, V.G., Ind. Eng. Chem. Fundam., 1986, 25, 174.

Gwynn, S.M.; Hartel, R.W.; Murphy, V.G., "Contact Nucleation in the Crystallizati of Sucrose", AIChE Mtg., Chicago (November 16-20, 1980).

Hartel, R.W.; Berglund, K.A.; Gwynn, S.M.; Schierholz, P.M.; Murphy, V.G., AIChE Symp. Ser., 1980, 76(193), 65.

Kuijvenhoven, L.J.; deJong, E.J., "The Kinetics of Continuous Sucrose Crystallization", Industrial Crystallization 81, edited by S.J. Jancic and E.J. deJong, North Holland Publishing Co., 253 (1982).

Randolph, A.D.; Larson, M.A., "Theory of Particulate Processes", Academic Press, New York (1971).

White, E.T.; Wright, P.G., Chem Eng. Progr. Symp. Sers., 1971, 67(110), 53.

vanDamme M.A., "Crystal Growth: An Introduction (Edited by Hartman, P.)", North-Holland, Amsterdam (1973).

2.1

Use

cor

com

ber

cry

enc

(Bo

nec

fru

is

con

glu

whe

a r

glu

are

con

adv

hig

The

diab

CHAPTER 2

LITERATURE SURVEY

2.1 Background

Uses of Fructose

Fructose, also called levulose or fruit sugar, is a monosaccharide constituting one-half of the sucrose molecule. It is one of the most common natural sugars and occurs, for example, in sweet fruits and berries, as well as in honey. Despite its widespread occurrence, crystalline fructose has not been made commercially available at low enough cost to be competitive with sucrose or other sweeteners (Bollenback 1983). A major area where significant improvement is necessary to achieve lower costs is in the crystallization step of fructose from aqueous solutions (Dwivedi, 1980).

Pure fructose is a white, hygroscopic, crystalline substance and is not to be confused with the high fructose corn syrups which may contain 42-90 wt % fructose. The nonfructose part of these syrups is glucose plus small amounts of glucose polymers (Bollenback, 1983). When compared to the perceived sweetness of sucrose (100), fructose has a relative sweetness of 170-180. In contrast to sucrose and fructose, glucose has a relative sweetness of 70-80. Special dietary purposes are realized due to its high sweetening power that theoretically allows consumption of less sweetner, i.e, fewer food calories. A further advantage of fructose in foods is based on fructose not promoting as high a rise in blood insulin as glucose or sucrose (Külz, 1874). Therefore, fructose-based foods may be helpful in the diets of diabetics and those with disturbances of glucose metabolism.

Ba

bi

wh

li

wa

hi

so

so

fo

di

pr

oc

di

di

an

as

ar

et

cr

lo

lo

ca

Basic Properties

Fructose is highly soluble in water as is evidenced by its solubility relation (Bates, 1942).

$$c = 0.150103t^2 - 0.814t + 333.023 \quad (1)$$

where

c = gm fructose/100 gm water

t = °c

Fructose is much more soluble in water than sucrose or glucose as listed in Table 1 (Watanabe, 1978). For instance, at 50°C, 100 gm water can dissolve 662 gm fructose as opposed to 260 gm sucrose. This high solubility results in the viscosity of saturated aqueous fructose solution being much higher than that of saturated aqueous sucrose solution (at 50°C, 4000-5000 c.p. for fructose as opposed to 102 c.p. for sucrose (Wantanabe, 1978)). The high viscosity leads to difficulties in the study of the crystallization of fructose and is probably one reason for the few kinetic studies of the system.

An additional consideration of crystalline fructose is that it occurs in the forms of anhydrous fructose, the hemihydrate, and the dihydrate (Young et al., 1952; Yamauchi, 1975). The hemihydrate and dihydrate tend to crystallize out of solution more easily than anhydrous fructose under some conditions. The hemihydrate crystallizes as spherulitic aggregates of fine needles (Young et al., 1952), which are difficult to handle and have a melting point of about 68°C (Jones et al., 1952). The dihydrate somewhat resembles anhydrous fructose in crystal habit, although its crystals are usually two or five times longer than they are wide (Young et al., 1952). However, due to its low melting point of about 21.3°C (Young et al., 1952) the dihydrate can cause a high quality crystalline product to degrade to a sticky

Table 1. Solubility of sugars in 100g water

Temp.	Fructose	Sucrose	Glucose
20°C	368g	204g	86.5g
25	408	211	111
30	446	219	121
35	487	229	138
40	539	238	158
45	573	249	191
50	662	260	242
55	740	273	272

mass. The only commercially acceptable crystalline product is anhydrous fructose with the melting point 102~104°C.

Impurities

Glucose is the major impurity likely to be present in fructose syrup formed during corn wet mining due to the production of fructose from glucose using glucose isomerase (Bollenback, 1983). The effects of glucose on the nucleation and growth of anhydrous fructose crystals have not be reported in the literature.

Other important impurities include the difructoses and difructose dianhydrides, which are formed *in situ* under industrial crystallization conditions. Forsberg et al. (1975) demonstrated that the formation of these difructoses and difructose dianhydrides caused a decrease in the the overall yield. At least eight difructose dianhydrides have been reported and their structures differ in the configuration of each fructose moiety and the linkage between them (Shallenberger, 1982; Defaye and Pedersen, 1985). Watanabe (1978) reported that the polymers of fructose formed during the evaporation process retarded the crystallization of fructose and the polymerization was not observed in the range of pH 4.4-5.5, while it was accelerated at pH 3.4 and less.

2.2 Nucleation

Introduction

Nucleation is the formation of a crystalline structure from solution. It is believed that nucleation can occur by primary or by secondary means (Mullin, 1972). Primary nucleation is due to a series of bimolecular collisions in a highly supersaturated solution and can be classified as homogeneous or heterogeneous. Homogeneous nucleation

is b

inso

nucl

subs

solu

Bots

of n

iden

Lars

Conta

but a

al.,

adsor

is by definition a spontaneous generation of nuclei in which no foreign insoluble particles such as dust are present. Heterogeneous nucleation, however, occurs as a result of the presence of some foreign substance which provides a nucleation site.

Secondary nucleation requires the presence of growing crystals in solutions and occurs at much lower supersaturation (Bauer et al., 1974; Botsaris, 1976). In general, secondary nucleation is the main source of nuclei in most industrial crystallizers and several types have been identified (Ottens and deJong, 1973; Botsaris, 1976; Estrin, 1976; Larson, 1982):

1. initial breeding: when dry crystals are added to a supersaturation solution and the small crystalline particles on crystal surfaces detach in solution and become nuclei.
2. needle breeding: when micro-dendrites, formed on the crystal surface at high supersaturation, break off.
3. fluid shear: when nuclei are formed by the high fluid shear between crystal and solution.
4. contact nucleation (collision breeding): when the crystal is brought into contact with walls of the container, the stirrer or pump impeller, or other crystals. In most crystallizers, the dominant type of nucleation is contact nucleation (Bauer et al., 1974; Garside and Davey, 1980).

Contact Nucleation

The actual mechanism of contact nucleation is not well understood, but at least two possible mechanisms have been proposed (Johnson et al., 1972): (1) removal of pre-ordered crystalline structures from the adsorption layer near the crystal surface and (2) some mechanical

breakage (micro-attrition) of the crystal surface. In principle, both mechanisms can occur simultaneously. Clontz and McCabe (1971) developed an experimental apparatus wherein the contact energy could be controlled by allowing a solid rod to fall on a specific face of a growing crystal fixed in a flowing stream of solution. Their work as well as that of their coworkers (Johnson et al., 1972; Tai et al., 1975) indicated that more nuclei were formed at higher supersaturations. In addition, energy of contact and hardness of contacter were found important.

Botsaris (1976) suggested that needle-like dendrites on the surface of a growing crystal may be the source of nuclei. When these dendrites are broken away by fluid shear or mechanical forces they become nuclei. Gilmer and Bennema (1972) showed through a computer analysis of a growth model that macroscopically smooth crystals may indeed have these microscopic irregularities. Khambaty and Larson (1978) showed that as the frequency of contact was increased a critical value was attained such that the crystal needed a regeneration time. The dependence of number of nuclei generated on supersaturation and the existence of the regeneration time of the crystal surface imply that contact nucleation results from a more complicated process than straightforward mechanical breakage on the crystal surface.

Direct observation of micro-attrition at a crystal surface was first reported by Garside and Larson (1978). Experiments were conducted using a photomicroscopic cell in which a parent crystal was contacted and nuclei could be photographed during the experiment. The same photomicroscopic technique was extended and used by Berglund (1981) and Berglund and Larson (1981a). Berglund et al. (1983) found that only a very light contact of a growing crystal of potassium

nitrate by a stainless steel rod was necessary to form contact nuclei. It might indicate that a pre-ordered crystalline structure could be removed from the surface in contact nucleation; however, the actual mechanism still needs to be investigated further in detail. A study of the mechanisms of contact nucleation is not within the scope of this work.

2.3 Growth Rate Dispersion

Definition

MaCabe's ΔL law (1929) states that at any instant all crystals in a well-mixed vessel grow at the same linear growth rates. Later size-dependent growth was reported in certain materials (McCabe and Stevens, 1951; Canning and Randolph, 1967; Abegg et al., 1968), but it was still assumed that at any instant all crystals of the same size grow at the same rate. However, the results obtained by White and Wright (1971) from the crystallization of sucrose and aluminum trihydroxide showed that crystals initially all of one size and growing under the same conditions exhibit variations in growth rate. This phenomenon was termed as growth rate dispersion (GRD) and was found to produce an spread in product crystal sizes.

The phenomenon of GRD has been identified as a significant factor in the establishment of the crystal size distribution (CSD) in crystallizers with two methods of describing GRD presented in the literature. The first, in which it is assumed that the growth rate of an individual crystal fluctuates with time, is referred to as the random fluctuation (RF) model (Randolph and White, 1977). In the second, based on the contact nucleation studies of Berglund and Larson (1981), Ramanarayanan (1982), and Berglund et al. (1983), an individual

crystal is assumed to have an inherent, constant growth rate, but different crystals can have different inherent rates. This model will be referred to as the constant crystal growth (CCG) model.

Random Fluctuation Model

Random fluctuations of growth rate have been reported from single crystal growth studies over long periods (up to several days) (Cartier et al., 1959; Human et al., 1982; vanEnckevort, 1982). The Burton-Cabrera-Frank (BCF) growth theory (Burton et al., 1951) appears to give a qualitative explanation of the phenomenon: the origin of the GRD lies in the imperfect growth of crystal surfaces and the dislocation density on crystal surfaces. Thus, changes in the dislocation networks occur as individual crystals form and overgrow imperfection. In addition to that, collisions of crystals with each other and crystallizer internals also could result in changes in the dislocation network of a crystal, and lead to the random fluctuation of growth rates (Zumstein and Rousseau, 1987).

Constant Crystal Growth Model

The photomicroscopic technique first used by Garside and Larson (1978) for the study of contact nuclei allowed observation of individual crystals during their growth. By use of this technique, the CCG model was found to be applicable in a variety of organic and inorganic solutions for periods of at least a few hours, such as citric acid monohydrate-water (Berglund and Larson, 1981), ammonium dihydrogen phosphate-water (Ramanarayanan, 1982), potassium nitrate-water (Berglund et al., 1983), sucrose-water (Shanks and Berglund, 1985), potash alum-water (Mathis-Lilley and Berglund, 1985), ammonium

dihydrogen phosphate-water (Garside and Ristic, 1983). Based on the BCF surface diffusion mechanism, the most likely cause for the presence of GRD is a variation in dislocation density on the surface of various nuclei resulting in different growth rate.

2.4 Modeling Growth Rate Dispersion in a Batch Crystallizer: Constant Supersaturation and Negligible Nucleation

Modeling Based on Random Fluctuation Model

White and Wright (1971) conducted batch experiments in which they grew an initially monosized distribution of sucrose crystals. By sampling their crystallizer at subsequent times, they observed that the CSD widened with time and that there was a reasonably linear relationship between the variance of the CSD and the mean size, that is

$$\Delta\sigma^2 = P\Delta\bar{L} \tag{2}$$

where $\Delta\sigma^2$ is the increase in variance of the sample size distribution over that of the seed size distribution (If the seeds are all of one size, the initial variance is zero). $\Delta\bar{L}$ is the increase in mean size and P is a proportionality factor, termed as the dispersion parameter.

Since increase in variance and increase in mean size are linked, the size dispersion effect can be described simply by the single parameter, P. That is, for a given amount of growth, as measured by the increase in mean size, the increase in variance can be evaluated, and so the standard deviation and thus the size dispersion function are known.

Randolph and White (1977) attributed the phenomenon of size spreading of a narrow CSD to fluctuations in growth rates. They introduced the concept of growth rate diffusivity (D_G), which was developed as an analogue to Taylor dispersion, in their modeling

procedure. Upon solution of the population balance developed by Randolph and Larson (1971) for a batch crystallizer, the following result was obtained.

$$\frac{\Delta\sigma^2}{\Delta t} = 2D_G \tag{3}$$

So a plot of the variance of the CSD vs. time should yield a straight line with a slope equal to twice the growth rate diffusivity. By definition,

$$\bar{G} = \frac{\Delta\bar{L}}{\Delta t} \tag{4}$$

and

$$P = \frac{\Delta\sigma^2}{\Delta\bar{L}} \tag{5}$$

Therefore, the relationship between D_G and P can be correlated as

$$D_G = \frac{P\bar{G}}{2} \tag{6}$$

Modeling Based on Constant Growth Model

According to the CCG model, the final size of the crystal in the crystallizer is equal to its initial size plus the amount of growth that the crystal has occured in the crystallizer. Ramanarayanan et al. (1984) developed a statistical-mathematical model to account for the three factors affecting crystal size distribution (CSD) under a given growth environment, namely, the birth size, the growth rate, and the residence time of the crystals. This model can be used to determine the growth kinetic parameters from batch crystallization experiments.

Starting with the CCG model,

$$L = L_o + Gt \tag{7}$$

where

L = crystal size at t

L_o = initial crystal size

G = growth rate

t = time

and taking the expected values for both sides,

$$\bar{L} = \bar{L}_o + \bar{G}t \tag{8}$$

the variance of the crystal population can be written as:

$$\sigma_L^2 = \sigma_{L_o}^2 + \sigma_G^2 t^2 \tag{9}$$

In the above equations it is assumed that the variables L_o, G and t are random independent variables. Thus, by monitoring the crystal population in a batch crystallizer, a plot of the mean size of the population vs. time is a straight line with a slope equal to the mean growth rate of the crystals, and a plot of the variance of the population with square of the time is a straight line with the slope corresponding to the variance of the GRD.

Blem and Ramanarayanan (1987) analyzed batch crystallization experiments with the ammonium dihydrogen phosphate (ADP)-water system based on the above model and concluded:

1. Secondary contact nuclei of ADP are born into a finite size range indicating birth size dispersion (BSD).
2. The mean and the variance of the CSD follow the statistical-mathematical extension of the CCG model.
3. The mean growth rate and the growth rate dispersion parameter can be determined from <u>in situ</u> CSD measurements using linear plots of the mean particle size vs. time and the variance vs. time squared, respectively, in a batch crystallizer.

4. It was observed in the range of experiments that the mean growth rate and the growth rate dispersion parameter are dependent on supersaturation and can be correlated with a power law.

Modeling Based on the Superimposing of the Two Models

Berglund and Murphy (1986) analyzed growth rate dispersion using the two competing models from experiments on sucrose crystals. They concluded that the RF model and the CCG model fit the CSD data equally well and that the superimposing of the two models into a more general model should be explored. Zumstein and Rousseau (1987) superimposed the two models and developed a mathematical model that characterizes, in terms of the growth dispersion parameters, the effects of both growth rate dispersion mechanisms on the CSD in batch and continuous crystallizers. From the model, the relative importance of each mechanism can be determined in the analysis of CSD data. The model developed was based on the concept that crystals are introduced into the system with a distribution of time-averaged growth rates and, due to the changes in the dislocation networks of the crystals, individual crystal growth rates fluctuate about their original values during the growth period.

Upon the solution of the population balance developed by Randolph and Larson (1971) for a batch crystallizer, the time dependence of the mean and the variance of the CSD are therefore:

$$\bar{L}(t) = \bar{L}_o + \bar{G}t \tag{10}$$

$$\sigma_L^2(t) = \sigma_{L_o}^2 + \sigma_G^2 t + 2t \int_o^\infty f(G) D_G dG \tag{12}$$

where

$\bar{G}$ = mean time-average growth rate

D_G = growth rate diffusivity parameter

f(G) = probability density function for G

If D_G is not a function of growth rate, the final term in Eq. 10 reduces to $2D_G t$. If there is no distribution of growth rates, σ_G^2 is zero; on the other hand, the parameter D_G is zero when no fluctuation in crystal growth rates occur. In other words, Eq. 10 reduces to the expression given by Randolph and White for growth rate dispersion due to the random growth rate fluctuation mechanism, and it also reduces to the expression given by Ramanarayanan et al. (1985) for systems in which only the growth rate distribution mechanism exits.

From the batch crystallization of potassium alum nuclei resulting from initial breeding (Zumstein and Rousseau, 1987), the experimental data indicated that the growth rate distribution model fits the data much better than the corresponding model based on growth rate fluctuation. In order to determine if both mechanisms for growth rate dispersion were significant, a partial F-test was used to test the null hypothesis: random growth rate fluctuations are not important given that crystals have a distribution of growth rates. The null hypothesis was rejected at the 95% confidence limit, indicating that addition of the random growth rate fluctuation mechanism to the model does improve the fit to the data.

Since the source of growth rate dispersion appears to be the dislocation networks of individual crystals, the magnitude of its influence may vary between different seed populations and the dislocation networks of crystal obtained from initial breeding are

expected to be quite different from those of much larger, well-formed crystals used in previous studies.

2.5 Modeling Growth Rate Dispersion in a Batch Crystallizer: Variable Supersaturation and Non-negligible Nucleation

Modeling Based on Random Fluctuation Model

For a batch crystallizer considering the dispersion effects due to random fluctuations in growth rate, Randolph and White (1977) developed the following population balance equation.

$$\frac{\partial n}{\partial t} + G \frac{\partial n}{\partial L} = D_G \frac{\partial^2 n}{\partial L^2} \tag{12}$$

where

n = the population density of crystals

L = characteristic size of crystal

G = mean time-averaged growth rate

D_G = growth rate diffusivity

The above equation requires are initial condition and two boundary conditions.

$$\text{B.C.} \qquad L = 0; \quad B^\circ = n^\circ G - D_G \left(\frac{\partial n}{\partial L} \right)_{L \to 0}$$

$$L \to \infty; \quad n \to 0$$

where

B° = nucleation rate

n° = zero size population density

However, the initial population density n(L,0) for a batch crystallizer is not well defined. If the crystallizer is initially seeded, n(L,0) may be denoted by an initial seed distribution function

$N_s(L)$. However, in an unseeded system, initial nucleation can occur by several mechanisms, and one cannot realistically use a zero initial condition for the size distribution (Wey, 1986). In this case, Baliga and Larson (1970) suggested the use of the size distribution of crystals in suspension at the time of the first appearance of crystals as the initial population density. Melikhov and Berliner (1981) and Lakatos et al. (1984) have employed this approach to simulate the CSD for batch crystallizers which could describe size spread of produced crystals in consequence of random fluctuations in growth rate.

2.6 Modeling Growth Rate Dispersion in a Continuous Crystallizer

The Population Balance

Crystallizers of the continuous mixed-suspension, mixed-product-removal (MSMPR) type are widely used in industry and the laboratory. If the assumptions of (a) perfect mixing; (b) no classification at withdrawal; (c) negligible breakage or agglomeration; (d) uniform shape factor; (e) the ability to represent all crystals by a characteristic dimension L are all valid, the steady state population balance developed by Randolph and Larson (1971) reduces to

$$\frac{d(nG)}{dL} + \frac{n}{\tau} = 0 \qquad (13)$$

where

G = growth rate

n = population density

τ = residence time

Integration of this equation enables the CSD to be determined. Based on the assumptions of size-independent crystal growth (MaCabe's ΔL law), all crystals with equal growth rates (i.e., no growth rate

dispersion), and all nuclei formed at a near-zero size, Eq. 12 is integrated (Randolph and Larson, 1971).

$$n = n^\circ \exp\left[-\frac{L}{G\tau}\right] \tag{14}$$

where

n° = zero size population density

A semilogarithmic relation is predicted between crystal population density and size. When the model holds, G can be determined from the slope and n° from the intercept of the ln n vs. L plot. Finally, the zero size population density n° is related to the kinetics of nucleation in the following way (Randolph and Larson, 1971). Let the nucleation rate B° be represented by

$$B^\circ = \left[\frac{dN}{dt}\right]_{L \to 0} \tag{15}$$

where

N = cumulative number distribution

Note that the growth rate G may be thought of as the differential $\frac{dL}{dt}$. Thus,

$$\left[\frac{dN}{dt}\right]_{L \to 0} = \left[\frac{dN}{dL} \cdot \frac{dL}{dt}\right]_{L \to 0} \tag{16}$$

Remembering that

$$\left[\frac{dN}{dL}\right]_{L \to 0} = n^\circ \tag{17}$$

gives

$$B^\circ = n^\circ G \tag{18}$$

Therefore, the nucleation rate can be determined from both the slope and the intercept in the ln n vs. L plot.

However, evidence from continuous sucrose crystallization experiments (Hartel et al., 1980; Kuijvenhoven and deJong, 1982) have shown that at lower crystal size (< 50μm) orders of magnitude more crystals

are present than are predicted by this relation. Clearly any or all of the assumptions may be in error. When curvature occurs, the slope no longer has a single value and the intercept must be determined by some means of nonlinear extrapolation. In order to develop an unambiguous kinetic model, it is necessary to understand the causes for the curvature. The results studied by Girolami and Rousseau (1985) show that the apparent relationship between growth rate and crystal size that has been observed for potassium alum is a manifestation of growth rate dispersion; moreover, it is likely that size-dependent growth kinetics reported for other systems is the result of this phenomenon. The reason for the apparent relationship between growth and size is as follows: with growth rate dispersion, crystals grown in a batch system are classified into sizes by their growth rates, and following the growth of crystals at a given size one observes the effects of growth rate dispersion rather than size-dependent kinetics. Berglund and Larson (1984) used probability transform techniques to develop a model for a continuous MSMPR crystallizer that accounts for size dependent growth, growth rate dispersion (where crystal of the same size may have different growth rates), and initial size distribution. The study made use of data taken previously in contact nucleation experiments with the citric acid monohydrate-water system. From the modeling studies of continuous mixed suspension, mixed product removal (MSMPR) crystallizers operating in the contact nucleation regime, found that the curvature in the semilogarithmic population density crystal size plots can be explained on the basis of growth rate dispersion coupled with an initial size distribution of the nuclei. Furthermore, it was found the initial size distribution has a small effect, while the growth rate distribution has a large effect on the predicted crystal

size distribution (CSD). When the two distributions were combined into a bivariate distribution which allows a linear dependence of growth rate on initial size, little change was observed.

The modeling results combined with previous experimental results on the citric acid monohydrate-water system (Berglund, 1981) suggest that the most important factor contributing to nonideality in the CSD from a continuous MSMPR crystallizer is growth rate dispersion. It is, therefore, concluded that this factor should be the focus in future work to control CSD.

Modeling Based on Random Fluctuation Model

Randolph and White (1977) defined a growth diffusivity to model the size spreading of a narrow CSD due to fluctuations in growth rates. Thus, the population flux is given by both convection and dispersion terms as

$$F = nG - D_G \frac{dn}{dL} \tag{19}$$

where

F = the population flux

n = population density

G = mean time-averaged growth rate

D_G = growth rate diffusivity

L = crystal size

When the above expression is introduced into the population balance equation for an MSMPR crystallizer, a second-order ordinary differential equation results. Thus,

$$G \frac{dn}{dL} + \frac{n}{\tau} = D_G \frac{d^2n}{dL^2} \tag{20}$$

where

τ = residence time

Introduction of the second-order term due to size dispersion requires two boundary conditions as follows.

$$\text{B.C.} \quad L = 0; \quad B^\circ = n^\circ G - D_G \left(\frac{dn}{dL} \right)_{L \to 0}$$

$$L \to \infty; \quad n \to 0$$

The previously observed linear increase in squared variance of CSD with time in batch crystallizers was correctly predicted with this diffusion model.

Solution of the continuous crystallization equations with the diffusivity term added indicates that the size dispersion phenomenon is unobservable with the wide CSD of the MSMPR crystallizer but could be an important factor in configurations producing a narrow CSD. A possible method for control of the CSD is the use of cascade crystallizers to approximate a plug flow residence time distribution. Randolph and Tan (1978) solved the simultaneous population and mass balance equations together with power law kinetics of nucleation and growth rate to predict the CSD in presence of GRD from a multistage classified recycle crystallization process based on the same concept. They found that the distribution is narrowed with increasing recycle of classified crystals. Production rate increases when recycling more undersize particle due to the increase in specific surface area. The phenomenon of size dispersion due to growth rate fluctuations limits the ultimate narrowness of CSD that can be obtained in a staged classified recycle sugar crystallizer.

Modeling Based on the Constant Crystal Growth Model

Larson et al.(1985) presented a model which relates the CSD from

a MSMPR crystallizer to the distribution of growth rates based on CCG model. The jth moment about the origin of the CSD is related to the jth moment about the origin of the growth rate distribution as follows:

$$M_L(j) = j!\tau^j M_G(j) \tag{21}$$

Noting that

$$M_L(j) = \int_o^\infty L^j f_L(L)\, dL \tag{22}$$

$$M_G(j) = \int_o^\infty G^j f_G(G) dG \tag{23}$$

where

$f_L(L)$ = probability density function for L

$f_G(G)$ = probability density function for G

L = crystal size

G = growth rate

τ = residence time

For j=1 and j=2,

$$M_L(1) = \tau M_G(1) \tag{24}$$

and

$$M_L(2) = 2\tau^2 M_G(2) \tag{25}$$

From Eqs. 24 and 25, the coefficient of variation of the size distribution (CV_L) can be related to the coefficient of variation of the growth rate distribution (CV_G) by

$$CV_L = \sqrt{cV_G^2 + 1} \tag{26}$$

Therefore, the crystal size distribution can be calculated from prior knowledge of the growth rate distribution. Even a limited knowledge of only the coefficient of variation and the mean growth rate permits an approximation of the expected crystal size distribution.

Conversely, estimates of the mean and variance of the growth rate distribution can be determined from the moments of the CSD from an MSMPR crystallizer. Bujac (1976) is the first to note that several types of nuclei are present. Daudey (1987) pointed out that the likely source of contact nuclei are "true" contact nuclei (fast growers) and attrition fragments (slow growers). Based on pilot scale crystallization experiments with the sucrose-water system, Berglund and deJong (1988) indicate that two populations of nuclei are present in continuous experiments. Their analysis shows that a distribution of growth rates within a growth rate population is of little consequence in causing curvature in semilogarithmic population density vs. size plots when more than one type of nuclei is present. In this case the separation of the growth rate distribution (i.e., the relative magnitude of their mean growth rates) is the most important parameter.

Modeling Based on the Superimposing of the Two Models

Zumstein and Rousseau (1987) included both the CCG model and the RF model to simulate the CSD in a continuous MSMPR crystallizer and a constant-supersaturation batch crystallizer. From the model, the relative importance of each mechanism can be evaluated in the analysis of CSD data. Their results indicate that both the growth rate distribution and random growth rate fluctuation mechanisms cause an increase in the spread of the CSD obtained from a batch crystallizer and can be separately observed experimentally by monitoring the increase in the variance of the CSD during growth periods. However, only the growth rate distribution mechanism can be experimentally observed in a continuous crystallizer since it causes an increase in the spread of the CSD, which is seen as upward curvature in the

population plot. Random growth rate fluctuations may damp out the effect of the growth rate distribution and thereby cause growth rate dispersion to be unobservable in a continuous crystallizer.

2.7 Summary

Since photomicroscopic experiments have confirmed that the CCG model applies to a variety of oganic and inorganic systems (Berglund and Larson, 1981; Ramanarayanan ,1982; Garside and Ristic, 1983), they provide the impetus for using the CCG approach in crystallizer modeling. Berglund and Larson (1984) and Larson et al. (1985) related the CSD from a single MSMPR crystallizer to the distribution of growth rates based on the CCG model. Ramanarayanan et al. (1984) and Zumstein and Rousseau (1987) developed batch crystallizer models based on the same CCG assumption limited to the case of constant supersaturation and negligible nucleation. While nucleation could be accounted for in the MSMPR crystallizer models, it was not in the batch ones. However, nucleation and supersaturation changes are inevitable in most industrial batch crystallization process. Therefore, a model taking these changes into account is needed and will be explored (Ch.4). In addition, the model for a single-stage MSMPR crystallizer by Larson et al. (1985) will be extended to a cascade of multi-stage MSMPR crystallizers (Ch.6).

2.8 Literature Cited

Abegg, C.F.; Stevens, J.D.; Larson, M.A., AIChE J., 1968, 14, 118.

Baliga, J.B.; Larson, M.A., paper presented at 63rd AICHE Annual Meeting, Chicago, Ill, November 1970.

Bates, F.J.,"Polarimetry, Saccharimetry and the Sugars", U.S. Government Printing Off., Washington, DC (1942).

Bauer, L.G.; Larson, M.A.; Dallons, V.J., Chem. Eng. Sci., 1974, 29, 1253.

Berglund, A.A., "Formation and Growth of Contact Nuclei", Ph.D. thesis, Iowa State University, Ames, IA (1981).

Berglund, K.A.; deJong, E.J., submitted for publication to AIChE Journal (1988).

Berglund, L.A.; Larson, M.A., "Growth and Growth Dispersion of Contact Nuclei", paper presented at 2nd World Cong. Chen. Eng., Montreal (1981a).

Berglund, K.A.; Larson, M.A., AIChE J., 1984, 30(2), 280.

Berglund, K.A.; Kaufman, E.L.; Larson, M.A., AIChE J., 1983, 29(5), 867.,

Berglund, K.A.; Murphy, V.G., Ind. Eng. Chem. Fundam., 1986, 25, 174.

Blem, K.E.; Ramanarayanan, K.A., AIChE J., 1987, 33(4), 677.

Bollenback, G.N.,"Kirk-Othmer Encyclopedia of Chemical Technology", 3rd Ed., Vol. 21, John Wiley and Sons, New York, New York (1983).

Botsaris, G.D.,"Industrial Crystallization (edited by Mullin, J.W.)", Plenum Press, New York, p3 (1976).

Bujac, P.D.B.,"Industrial Crystallization (edited by Mullin, J.W.)", Plenum Press, New York, p23 (1976).

Burton, W.K.; Cabrera, N; Frank, F.C., Phil. Trans. Roy. Soc., 1951, 243 (A866). 299.

Canning, T.F.; Randolph, A.E., AIChE J., 1967, 13, 5.

Cartier, R.; Pindzola, D.; Bruins, P., Ind. Eng. Chem., 1959, 51, 1409.

Clontz, N.A.; McCabe, W.L., Chem. Eng. Progr. Sym. Ser., 1971, 67(110), 6.

Daudey, P.J., "Crystallization of Ammonium Sulfate-Secondary Nucleation and Growth Kinetics in Suspension", Ph.D. Dissertation, Technical University of Delft, Delft, The Netherlands (1987).

Defaye, J.; Pedersen, C., Carbohydr. Res., 1985, 136, 53.

Dwivedi, B.K.; Raniwala, S.K., U.S. Patent No. 4199373, April 22, 1980.

Estrin, J.,"Preparation and Properties of Solid State Materials", Vol 2, W.R. Wilcox, ed., p. 1, Marcel Bekker, Inc., New York, NY (1976).

Forsberg, K.H.; Hamalainen, L.; Melaja, A.J.; Virtanen, J.J., U.S. Patent No. 3883365, May 13, 1975.

Garside, J.; Davey, R.J., Chem. Eng. Comm., 1980, 4, 393.

Garside, J.; Davey, R.J., J. Cryst. Growth, 1978, 43, 694.

Garside, J.; Ristic, R.I., J. Cryst. Growth, 1983, 61, 215.

Gilmer, G.H.; Bennema, P., J. Cryst. Growth, 1972, 13/14, 148.

Girolami, M.W.; Rousseau, R.W., AIChE J., 1985, 31(11), 1821.

Human, H.J.; vanEnckevork, W.J.P.; Bennema. P.,"Industrial Crystallization (edited by Jancic, S.J. and deJong, E.J.)", North-Holland, Amsterdam, p387 (1982).

Johnson, R.T.; Rousseau, R.W.; McCabe, W.L., AIChE Sym. Ser., 1972, 68(121), 31.

Jones, F.T.; Young, F.E.; Black, D.R., J. Phy. Chem., 1952, 20, 649.

Khambaty, S., Larson, M.A., Ind. Eng. Chem. Fundam., 1978, 17, 160.

Kuijvenhoven, L.J.; deJong, E.J.,"Industrial Crystallization (edited by S.J. Jancic and E.J. deJong)", North Holland Publishing Co., p253 (1982).

Külz, E. 1874. "Beitrag zur Pathologic und Terapie des Diabetes Mellitus", p. 130, Marburg, Cited in Huttunen, J.K. 1971. Fructose in medicine. Postgrad. Med J. 47: 654.

Lakatos, B.; Varga, E.; Halasz, S.; Blickle,T,"Industrial Crystallization (edited by S.J. Jancic and E.J. deJong),Elsevier Science Publishers B.B., Amsterdam, - Printed in The Netherlands, p185 (1984).

Larson, M.A.,"Industrial Crystallization edited by S.J. Jancic and E.J. deJong), North Holland Publishing Company, Amsterdam, The Netherlands, p55 (1982).

Larson, M.A; White, E.T.; Ramanarayanan, K.A.; Berglund, K.A., AIChE J., 1985, 31(1), 90.

Mathis-Lilley, J.J.; Berglund, K.A., AIChE J. 1985, 31(5), 865.

McCabe, W.L., Ind. Eng. Chem., 1929, 21, 30.

McCabe, W.L.; Stevens, R.P., Chem. Eng. Progr., 1951, 47, 168.

Melikhov, I.V.; Berliner, L.B., Chem. Eng. Sci., 1981, 36, 1021.

Mullin, J.W.,"Crystallization", Butterworths, London (1972).

Ottens, E.P.K.; deJong, E.J., Ind. Eng. Chem. Fundam., 1973, 12(2) 179.

Ramanarayanan, K.A., "Production and Growth of Contact Nuclei", Ph.D. Dissertation, Iowa State U., Ames Iowa (1982).

Ramanarayanan, K.A.; Athreya K.; Larson. M.A., AIChE Sym. Ser., 1984, 80(240), 76.

Randolph, A.D.; Larson, M.A.,"Theory of Particulate Processes", Academic Press, New York (1971).

Randolph, A.D.; Tan, C.S., Ind. Eng. Chem. Process Des. Dev., 1978, 17(2), 189.

Randolph, A.D.; White, E.T., Chem Eng. Sci., 1977, 32, 1067.

Shallenberger, R.S.,"Advanced Sugar Chemistry", The AVI Publishing Company, Inc. Westport, CN (1982).

Shanks, B.H.; Berglund, K.A., AIChE J., 1985, 31(1), 152.

Tai, C.Y., McCabe, W.L.; Rousseau, R.W., AIChE J., 1975, 21(2), 351.

vanEnckevort, W.J.P., Verification of crystal growth models by detailed surface microtopography and X-ray diffraction topography. Ph.D. thesis, University of Nijmegen 1982.

Wantanabe, T., Seito Gigutsu Kenkgu Kaishi, 1978, 28, 70.

Wey, J.S., Chem. Eng. Commun., 1985, 35, 231.

White, E.T.; Wright, P.G., Chem. Eng. Progr. Symp. Ser., 1971, 67(110), 53.

Yamauchi, T., U.S. Patent No. 3928062, Dec. 23, 1975.

Young, F.E.; Jones, F.T.; Lewis, H.J., J. Phy. Chem., 1952, 56, 738.

Zumstein, R.C.; Rousseau, R.W., AIChE J., 1987, 33(1), 121.

Zumstein, R.C.; Rousseau, R.W., AIChE J., 1987, 33(11), 1921.

CHAPTER 3

GROWTH KINETICS OF FRUCTOSE CRYSTALS FORMED BY CONTACT NUCLEATION IN PURE AND GLUCOSE-CONTAINING FRUCTOSE SOLUTIONS*

3.1 Abstract

The growth kinetics of fructose crystals formed by contact nucleation were studied in unstirred solutions using a photomicroscopic technique. The results indicated the existence of a distribution of apparent initial sizes and a distribution of growth rates. The crystals were found to follow the constant crystal growth (CCG) model, in which an individual crystal has an inherent, constant growth rate, but different crystals have different inherent rates under the same environment. Crystallization of fructose in the presence of glucose resulted in slower growth rates, but the CCG model was found to remain applicable.

3.2 Introduction

Despite the large number of recent secondary nucleation and growth rate studies with the sucrose-water system (Hartel et al., 1980; Kuijvenhoven and deJong, 1982; Berglund, 1980; Gwynn et al., 1980; Shanks and Berglund; 1985), little data is available on the fructose-water system. Fructose is much more soluble in water than sucrose

* The pure fructose solution studies were published as a paper in AIChE J., 1987, 33(6), 1028. The glucose-containing fructose solution studies are a portion of a larger paper submitted to J. of Crystal Growth.

(Watanabe, 1987; Bates, 1942), e.g., at 50°C, 100 gm water can dissolve 662 gm fructose as opposed to 260 gm sucrose. This high solubility results in the viscosity of saturated aqueous fructose solution being much higher than that of saturated aqueous sucrose solution, e.g., at 50°C, 4000-5000 c.p. for fructose as opposed to 102 c.p. for sucrose (Watanabe, 1978). In addition, the presence of glucose in fructose syrup may retard crystal growth. Residual glucose is often found after glucose isomerase conversion of glucose to fructose and subsequent ion exchange enrichment (Vanninen and Dotty, 1979). The presence of glucose and the high viscosity of fructose solutions lead to difficulties in the study of the crystallization of fructose and are probably the reasons for the few kinetic studies of the system.

For the case of a continuous mixed suspension, mixed product removal (MSMPR) crystallizer, Randolph and Larson (1971) have developed the population balance technique. Based on the assumptions of size-independent crystal growth, all crystals with equal growth rate (i.e. no growth rate dispersion), and all nuclei formed at a near-zero, a semilogarithmic relation is predicted between crystal population density and size. When the model holds and a straight line is produced, the growth rate is determined from the slope and the nucleation rate is determined from both the slope and the intercept. However, evidence from continuous sucrose crystallization experiments (Hartel et al., 1980; Kuijvenhoven and deJong, 1982), has shown that at lower crystal sizes ($< 50\ \mu m$) more crystals (orders of magnitude more) are present than are predicted by this relation. Therefore, one or more of the assumptions may be in error. The most likely violations are the non-zero birth size for nuclei and growth rate dispersion (Berglund, 1981).

The phenomenon of growth rate dispersion (GRD) is a significant factor in the control of the crystal size distribution (CSD) in crystallizers. Two methods of modeling growth rate dispersion have been presented in the literature. The first, in which it is assumed that the growth rate of an individual crystal fluctuates in the course of time is referred to as the random fluctuation (RF) model (Randolph and white, 1977). In the second, based on the contact nucleation studies of Berglund (1981), Berglund and Larson (1982), and Ramanarayanan et al. (1982), it is assumed that an individual crystal has an inherent, constant growth rate, but different crystals have different inherent growth rates. This model will be referred to as the constant crystal growth (CCG) model.

Gwynn et al. (1980) studied contact nucleation in the sucrose-water system and confirmed that contact nucleation is the primary source of new particles. In addition, it was found that contact nuclei of sucrose have an initial size distribution, not zero size as required by the MSMPR crystallizer model. Shanks and Berglund (1985) observed size-independent growth and compliance with the CCG model for contact nuclei in the sucrose-water system. Furthermore, they postulated that curvature in semilogarithmic population density-size plots from continuous sucrose crystallization is probably due to growth rate dispersion.

Since fructose is a monosaccharide constituting half of the sucrose molecule, it is reasonable that similar phenomenon may exist with respect to nucleation and growth in the two systems. It is the objective of this work to perform photomicroscopic experiments on the fructose-water system to study these nucleation and growth

characteristics. In addition, the influence of impurity glucose on the nucleation and growth of fructose crystals will be also investigated.

3.3 Experimental Appatatus

The experimental apparatus and techniques were the same as those used for the aqueous sucrose system by Shanks and Berglund (1985). A schematic diagram of the cell with a description of features is shown in Figure 1. In contact nucleation experiments the growth rates of crystals in an unstirred cell were studied. Since the aqueous fructose solutions were highly viscous, there should be no significant difference whether agitation in growth cell was provided or not. Contact nuclei were created by sliding the parent crystal along a glass plate in the growth cell. The growth of nuclei was monitored photographically through a microscope. The experimental conditions and the number of nuclei analyzed are given in Table 1 and Table 2.

3.4 Data Analysis

The raw data obtained from each experiment consisted of a series of photographs. The negatives of the photographs were projected to enlarge them for measurement. An image analyzer was used to determine the area of each crystal in the enlargement. The characteristic size was taken as the equivalent circular diameter, which can be transformed to the geometric mean size by multiplying by $\sqrt{\pi}/2$. The sizes were then plotted against time with the slope equal to mean growth rate and intercept equal to apparent initial sizes.

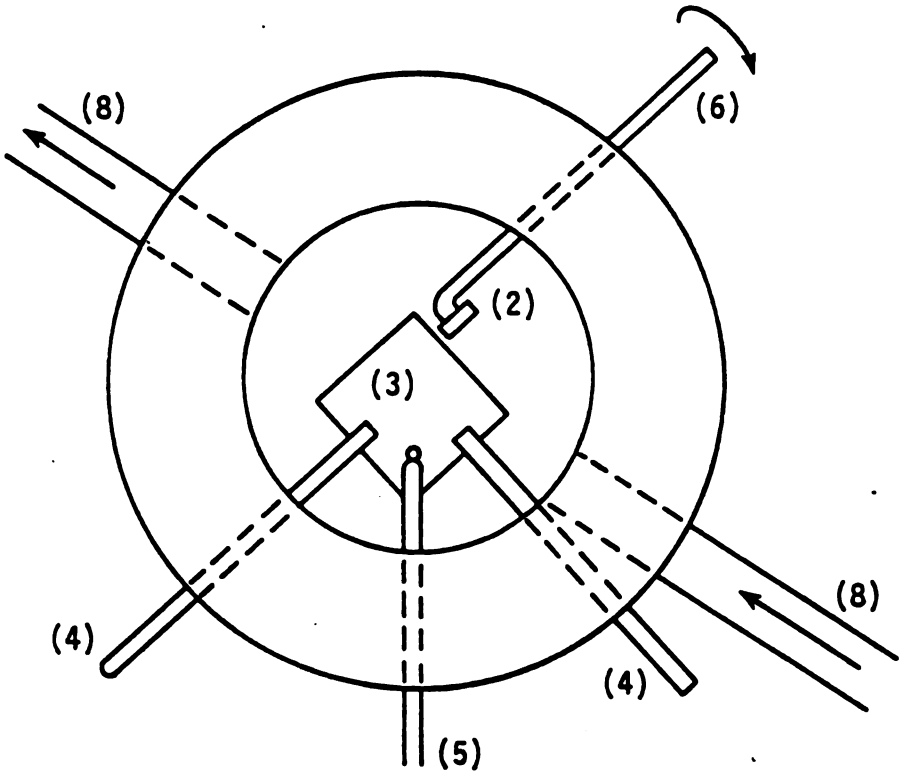

TOP VIEW

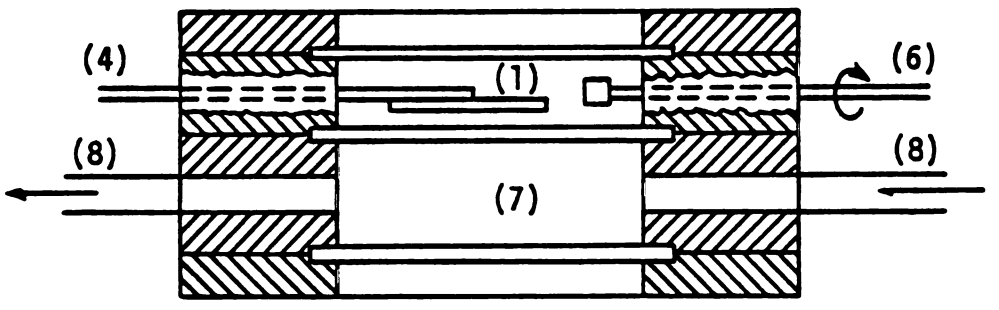

SIDE VIEW

Figure 1. Schematic diagram of nucleation cell with the features: (1) chamber containing solution; (2) parent crystal; (3) glass cover slip where parent crystal is slid; (4) support rods for glass cover slip; (5) thermistor; (6) movable rod holding parent crystal; (7) chamber containing constant temperature water; and (8) water inlet and outlet.

Table 1. Conditions and number of nuclei analyzed for photomicroscopic experiments with the fructose-water system

Run	Supercooling, °C	Temperature, °C	No. of nuclei analyzed
1	1	30	16
2	3	30	12
3	5	30	11
4	7	30	17
5	1	40	11
6	3	40	12
7	5	40	12
8	7	40	12
9	3	50	20
10	5	50	15
11	7	50	13
12	9	50	14

Table 2. Conditions and number of nuclei analyzed for photomicroscopic experiments with the fructose-glucose-water system at 40°C

Run	Supercooling, °C	Impurity/Water ratio gm/gm	No. of nuclei analyzed
1	1	0.05	12
2	3	0.05	13
3	5	0.05	15
4	7	0.05	11
5	9	0.05	14
6	1	0.3	13
7	3	0.3	12
8	5	0.3	11
9	7	0.3	15
10	9	0.3	12
11	11	0.3	13
12	5	0.6	14
13	7	0.6	13
14	9	0.6	13
15	11	0.6	16
16	5	0.9	18
17	7	0.9	16
18	9	0.9	12
19	11	0.9	15

3.5 Results and Discussion

Pure Fructose Solutions

Figure 2 shows examples of size versus time plots for some individual crystals at 40°C. It is evident, and confirmed by high correlation coefficients, that a linear relation exists between the size and time. Since the slope of the line is equal to growth rate, these plots imply a single, size-independent growth rate. The lines also have different slopes indicating a distribution of growth rates, i.e., growth rate dispersion. Furthermore, the variation in intercept, which corresponds to an initial size distribution (Gwynn et al., 1980), is apparent. In Figure 3, the growth rate is plotted against the apparent initial size for each nucleus formed and grown at 40°C. Little correlation is present as evidence by the large amount of scatter. This indicates a distribution of apparent initial sizes and a distribution of growth rates. Similar plots have been observed for the data taken at 30 and 50°C. These results indicate that the CCG model describes this system.

Figure 4 shows the relationship between mean growth rate and relative supersaturation ratio at different temperatures studied. The solubility data was taken from Circular C440 of the National Bureau of Standards (Bates, 1943).

Since the mean growth rate can be expressed in terms of a power law model and the temperature dependence of the kinetic model can be analyzed in terms of the Arrhenius relation, the mean growth rate can be written as

$$\bar{G} = A \exp\left(-E_G/RT\right) S^n \qquad (1)$$

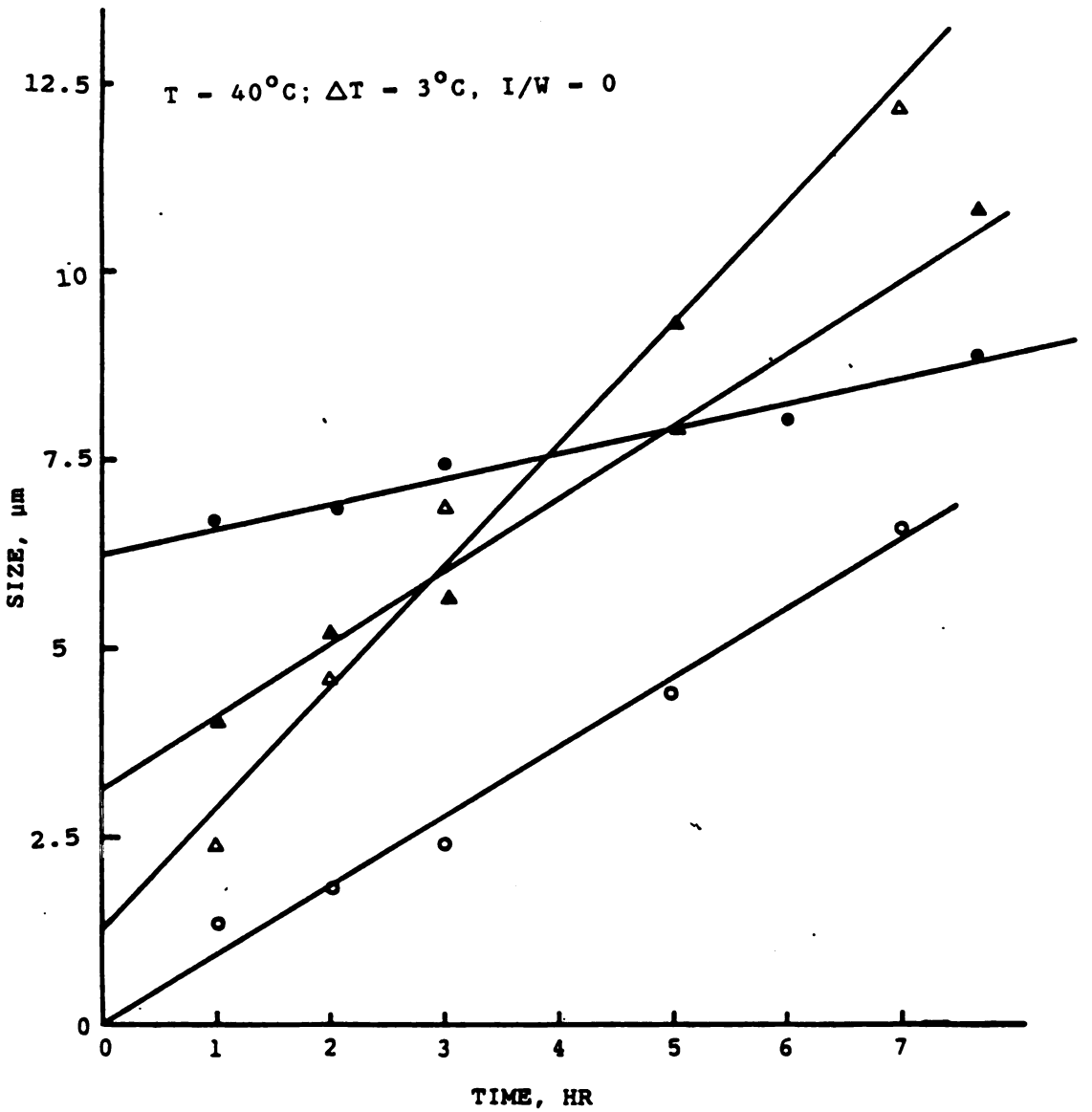

Figure 2. Examples of size versus time data for contact nuclei of fructose in the pure solution.

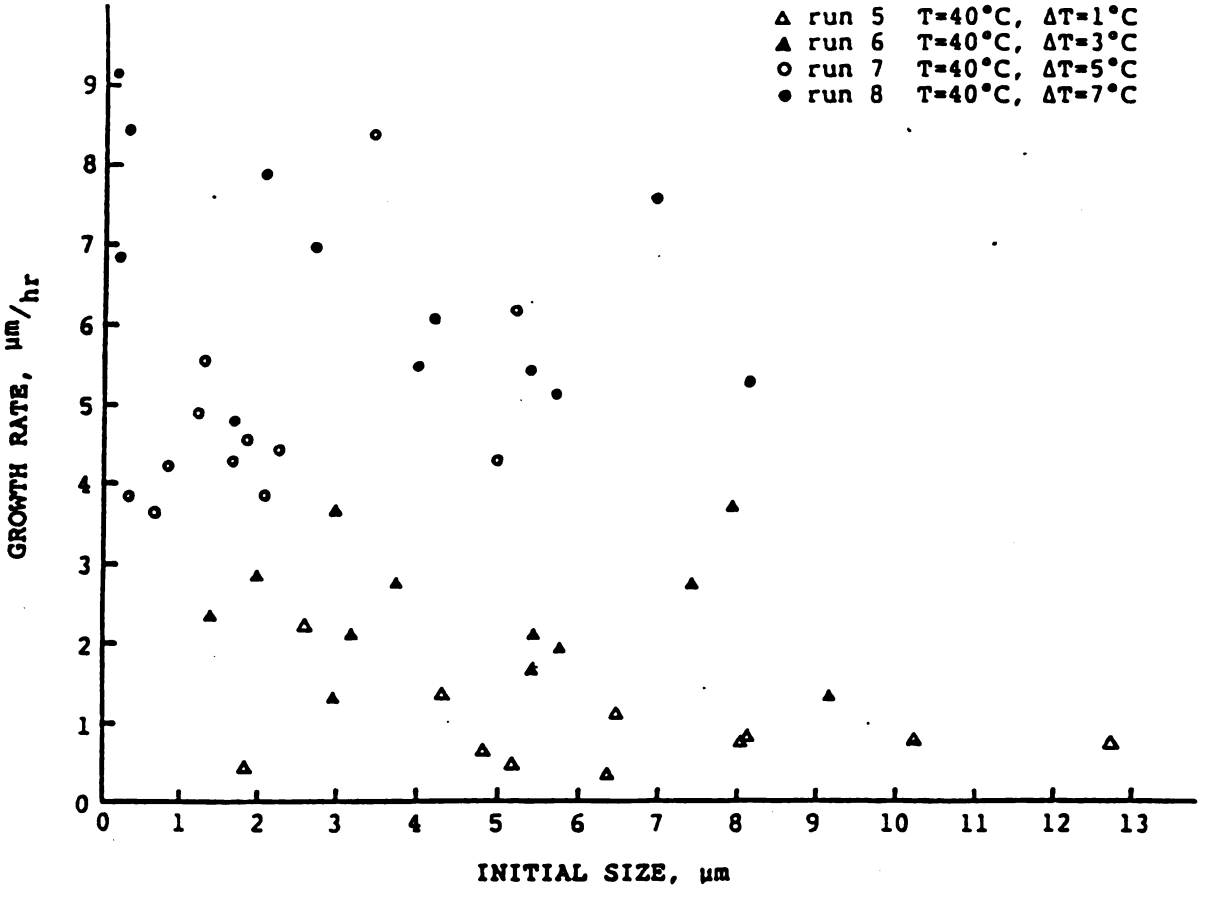

Figure 3. Growth rate versus apparent initial size for contact nuclei of fructose in the pure solution.

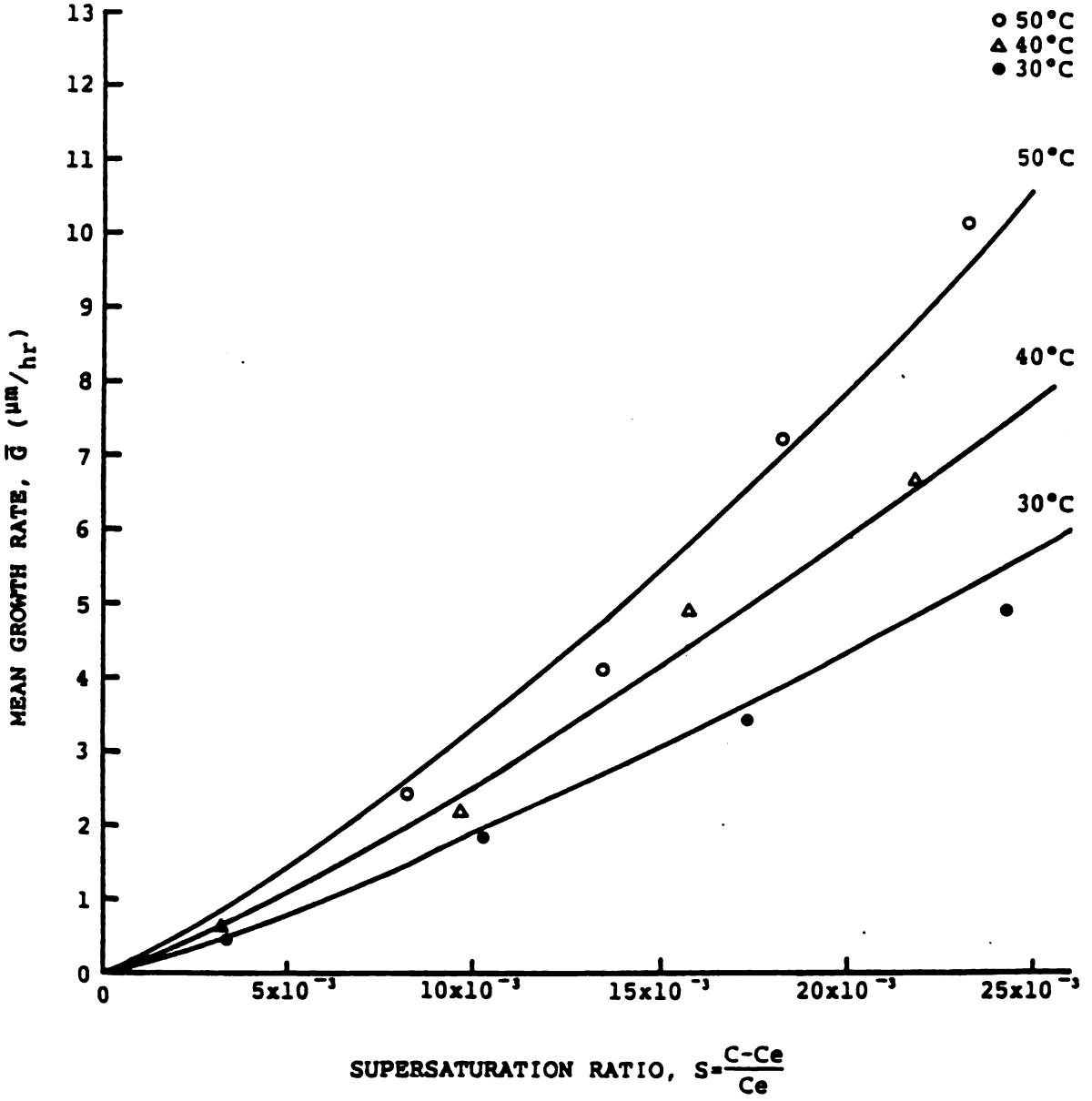

Figure 4. Mean growth rate versus relative supersaturation for contact nuclei of fructose in the pure solution.

The data in Figure 4 were fitted to the above eqation with the following result,

$$\bar{G} = 1.4 \times 10^{7} \exp(-6.1/RT)\ S^{1.3} \qquad (2)$$

Upon comparison to sucrose growth rates, it is apparent that the rate for fructose is much slower. The mass transfer engineering crystal growth model presented by Ohara and Reid (1973) predicts a value of one for a volume-diffusion controlled process. The Burton-Cabrera-Frank (BCF) surface diffusion and dislocation model (Burton et al., 1951) predicts a value of 1 for n at high supersaturation and value of 2 at low supersaturation. For the range of relative superaturation studied, S is small (0.0032-0.024); n would be expected to have the value of 2 in a surface-integration controlled process. However, n was found to have the value of 1.3, which may indicate that both volume diffusion and surface integration are important. This is further supported by the value of activation energy.

Smythe (1967) stated that the activation energy for the volume diffusion process in sucrose crystal growth is between 7 and 9 kcal/g-mol. In this work an activation energy of 6.1 kcal/g-mol was obtained for the growth rate. Since the exact value of the activation energy for the volume diffusion of fructose solution is not avalable in the literature, it is difficult to determine whether the crystal growth is diffusion-controlled or surface-integration controlled. However, for a purely diffusion-controlled process no growth rate dispersion should be observed, since growth rate dispersion is thought to be a surface phenomenon. Since 6.1 kcal/g-mol is near the range of 7 and 9 kcal/g-mol, it can be expected that both volume diffusion and surface integration play important roles here. This also suggests that growth

rate dispersion can be observed in systems when volume diffusion is thought to dominate.

To estimate the parameters of the growth rate distribution, the variance of growth rates was calculated at each experimental condition as shown in Figure 5. The result of fitting the data is

$$\sigma_G^2 = 0.17\ \bar{G}^{1.4} \tag{3}$$

When the above result is compared with $\sigma_G^2 = 0.83\ \bar{G}^{1.7}$ for the sucrose-water system (Berglund and Murphy, 1986) - for which it has been shown that growth rate is not mass-transfer limited - it is evident that the variance of the growth rate distribution in the fructose-water system is smaller than that in the sucrose-water system. However, there is still similarity between these two systems, since the exponents are greater than one for both systems.

Glucose-containing Fructose Solutions

Solutions containing glucose were prepared by adding glucose to pure fructose solutions. The concentration of impurity was expressed as ratio of impurity to water (I/W). Since the influence of impurity on fructose solubility is not clear, the same solubility as in the pure system was used in the impure system.

Figure 5 shows examples of size versus time plots for several crystals grown in the presence of glucose. It was demonstrated that the growth rate of a single crystal was constant while different crystals had different growth rates. The phenomena of size-independent growth and growth rate dispersion were observed for all impurity concentrations. Thus the CCG model used in the pure fructose system was also employed in the glucose-containing fructose solutions.

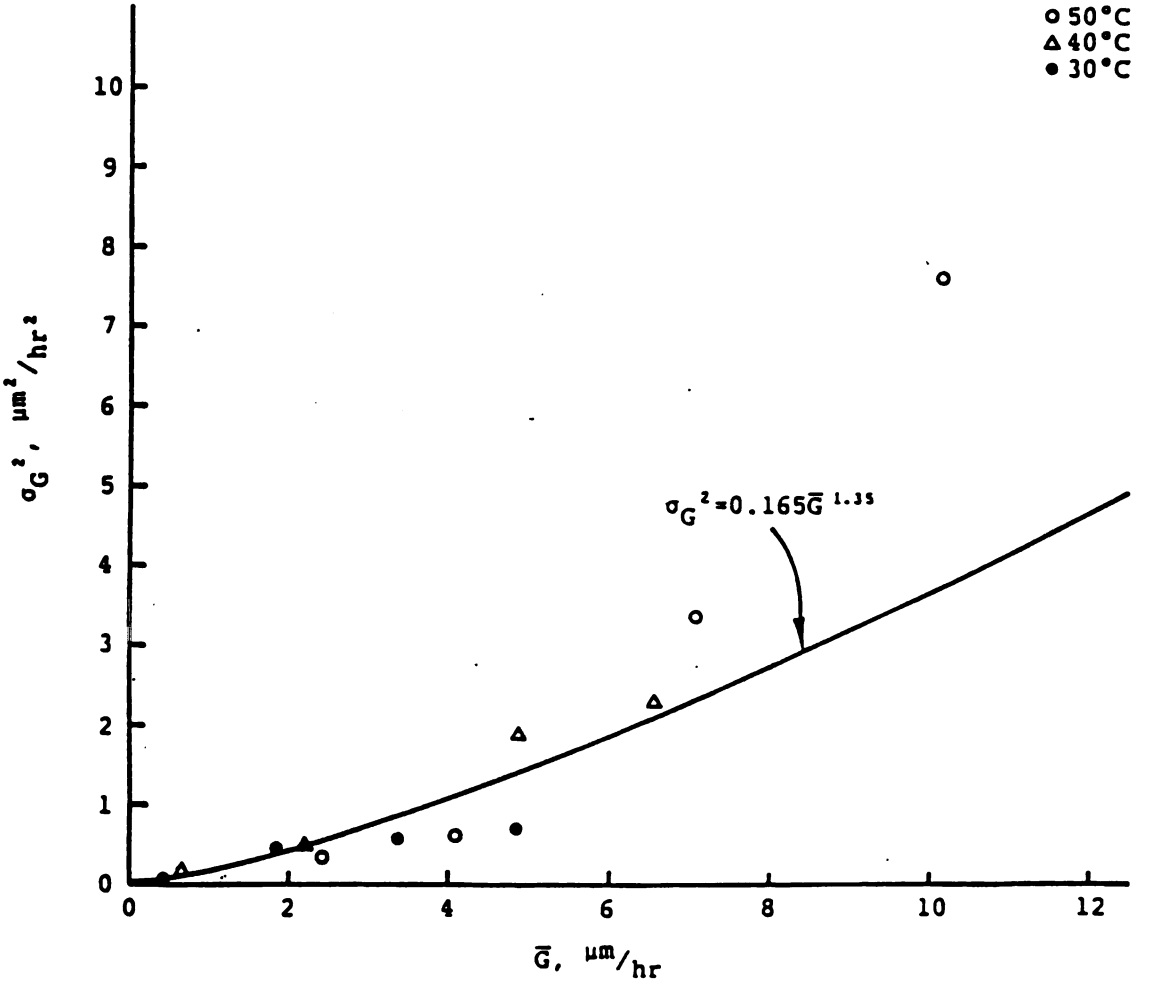

Figure 5. Variance of the growth rate distribution versus mean growth rate for contact nuclei of fructose in the pure solution.

The relationship between mean growth rate and relative supersaturation at different values of impurity/water (I/W) ratio is shown in Figure 6. The mean growth rate was decreased to 25 to 50 % of that in the pure system by the presence of glucose at concentrations ranging from 0.05 to 0.9 in terms of I/W ratio. This can be described by the following equation

$$\bar{G} = A \exp(-E_G/RT) [S-2.7\times10^{-4}(I/W)^{0.89}]^n \exp(-0.0098I/W) \quad (4)$$

Here A, E_G and n are assumed to be the same as in the pure fructose system.

It was observed that nuclei generated in a solution of high supersaturation, which was calculated from solubility data for the pure system, would dissolve at a temperature lower than the supposed saturation temperature of the solution. Nuclei will be generated and grow only when supersaturation reaches a critical value. The critical value increases as impurity/water ratio is increased. This phenomenon suggests that solubility of fructose increases with an increase of glucose concentration. In the equation of mean growth rate, the term $2.71\times10^{-4}(I/W)$ is subsracted from S to account for the increase of the solubility.

Besides the solubility change, the presence of glucose could also affect volume diffusion in solution and/or surface integration of crystal molecule. The need for the inclusion of exp(-0.0098I/W) in the model may represent these effects.

Figure 7 shows the variance of the growth rate distribution at $40^{\circ}C$. A power law model was used to fit the data resulting in the following equation

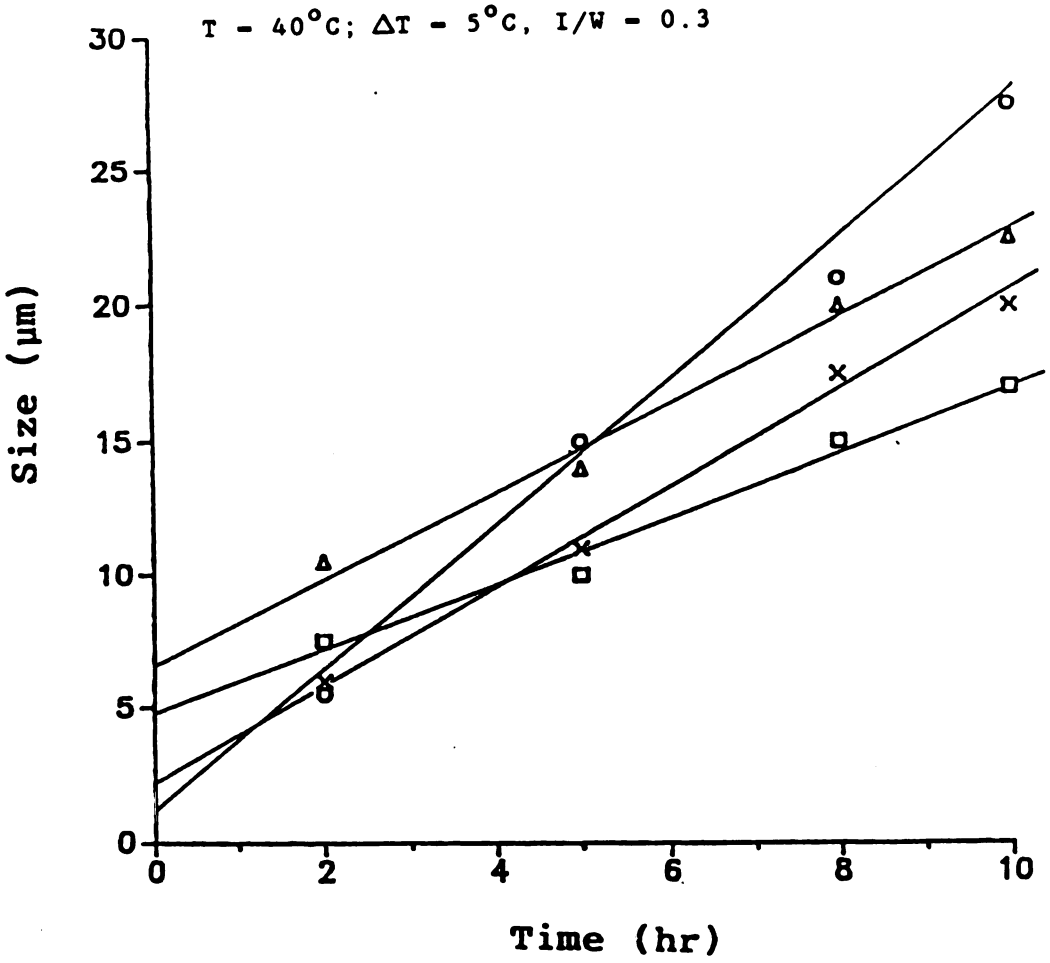

Figure 6. Examples of size versus time data for contact nuclei of fructose in glucose-containing fructose solution.

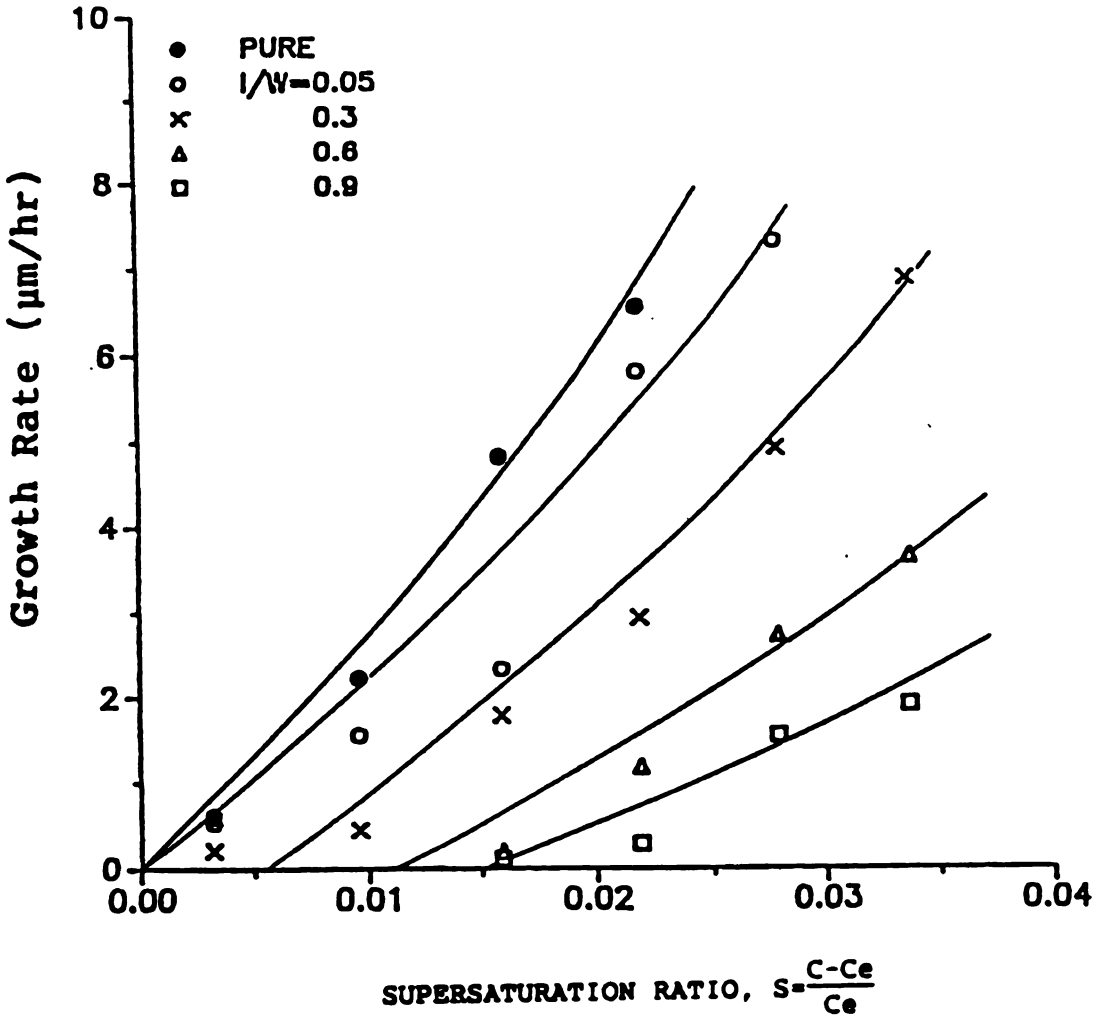

Figure 7. The influence of glucose on the relationship between mean growth rate versus relative supersaturation.

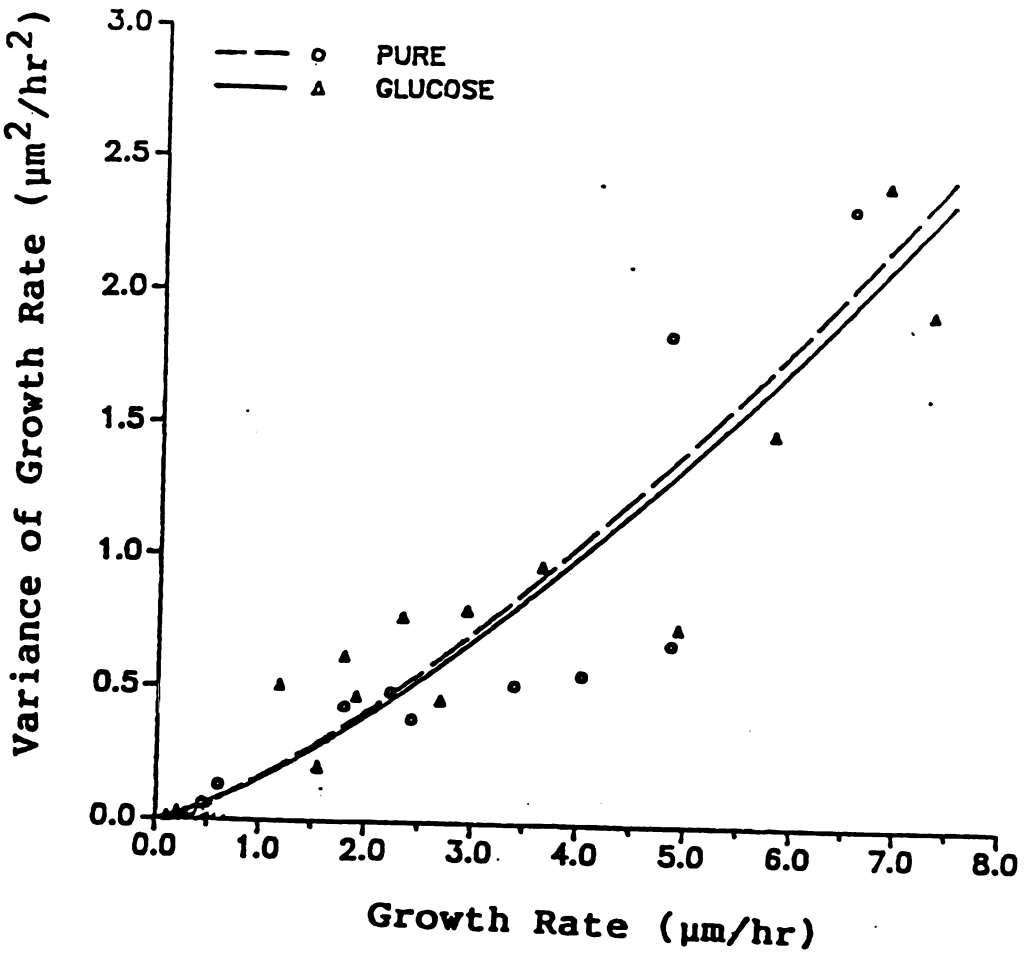

Figure 8. The influence of glucose on the variance of the growth rate distribution.

$$\sigma_G^2 = 0.156\ \bar{G}^{1.36} \qquad (5)$$

No significant difference of the variance of growth rate distribution was found between pure and glucose-impure systems.

3.6 Conclusions

THe growth rate of fructose crystals in the pure fructose solution and the glucose-containing fructose solution was size-independent, with growth rate dispersion among different crystals.

An activation energy for mean growth of 6.1 kcal/gm-mol was found for the pure fructose solution. This might indicate that both volume diffusion and surface integration are important.

Growth inhibition was observed in the glucose-containing solution. It is probably caused by an increase of fructose solubility by glucose.

The variance of growth rate distribution increases as growth rate is increased for both pure and impure system. The studies show no significant difference in the variance of growth rate distribution between the two systems.

3.7 Nomenclature

A = frequency factor, μm/hr

C = concentration, gm fructose/ 100 g solution

C_e = saturation concentration, gm fructose/ 100 g solution

E_G = activation energy, kcal/g-mol

$\bar{G}$ = mean liner crystal growth rate, μm/hr

I = impurity, g

n = growth rate order

R = ideal gas constant, 1.987 x 10^{-3}kcal/g-mol

S = relative supersaturation (= $(C-C_e)/C_e$)

T = temperature, K

W = water, g

Greek Symbol

σ_G^2 = variance of growth rate distribution, $\mu m^2/hr^2$

3.8 Literature Cited

Bates, F.J., "Polarimetry, Saccharimetry and the Sugars", United States Government printing Office, Washington (1942).

Berglund, K.A., "Formation and Growth of Contact Nuclei", Ph.D. Dissertation, Iowa State University, Ames, IA (1981).

Berglund, K.A.; Larson, M.A. "Growth and Growth Dispersion of Contact Nuclei", paper presented at 2nd world Cong. Chem, Eng., Montreal (1981).

Berglund, K.A.; Larson, M.A., AIChE J., 1984, 30(2), 280.

Berglund, K.A.; Larson, M.A., "Growth of Contact Nuclei of Citric Acid Monohydreate," AIChE Sym. Serm, 215 (78) 9 (1982).

Berglund, K.A. et al., AIChE J., 1983, 29(5), 867.

Berglund, K.A., "Growth and Size Distribution Kinetics for Sucrose Crystals in the Sucrose-Water System", M.S. Thesis, Colorado State University, Ft, Collins, CO (1980).

Berglund, K.A.; Murphy, V.G., Ind. Eng. Chem. Fundam., 1986, 25, 174.

Gwynn, S.M.; Hartel, R.W.; Murphy, V.G., "Contact Nucleation in the Crystallization of Sucrose", AIChE Mtg., Chicago (November 16-20, 1980).

Hartel, R.W. et al., AIChE Sym. Ser., 1980, 193(76), 65.

Kuijvenhoven, L.J.; deJong, E.J., "The Kinetics of Continuous Sucrose Crystallization", Industrial Cryystallization 81, edited by S.J. Jancic and E.J. deJong, North Holland Publishing Co., 253 (1982).

Larson, M.A. et al., AIChE J., 1985, 31(1), 90.

Ramanarayanan, K.A.; Berglund, K.A.; Larson, M.A, "Growth Kinetics in the presence of Growth Rate Dispersion from Batch Crystallizers", AIChE Mtg., Los Angeles (November 14-18, 1982).

Randolph, A.D.; Larson, M.A., "Theory of Particulate Processes", Academic Press, New York (1971).

Randolph, A.D.; White,E.T., Chem. Eng. Sci., 1977, 32, 1067.

Shank,B.H.; Berglund,K.A., AIChE J., 1985, 31, 152.

Vanninen,E.; Dotty,T,"Sugar: Science and Technology", applied Science Publishers, London (1979).

Watanabe,T., "Studies on the Crystallization of Fructose", Seito Gigutsu, 1978, 28, 70.

CHAPTER 4

A MODEL FOR A SEEDED BATCH CRYSTALLIZER: VARIABLE SUPERSATURATION, NUCLEATION, AND GROWTH RATE DISPERSION*

4.1 Abstract

A model is developed to relate the resulting crystal size distribution (CSD) from a seeded batch crystallizer with variable supersaturation during nucleation to the seed size distribution, the initial size distribution of subsequently generated nuclei, and the growth rate distribution. This model employs the constant crystal growth (CCG) model, in which an individual crystal has an inherent, constant growth rate, but different crystals might have different inherent growth rates. The model is solved with a mass balance constraint to generate the resulting CSD for a seeded, batch sucrose crystallizer.

4.2 Introduction

The phenomenon of growth rate dispersion (GRD) has been identified as a significant factor in the establishment of the crystal size distribution (CSD) in crystallizers. Two methods of describing GRD have been presented in the literature. The first, in which it is assumed that the growth rate of an individual crystal fluctuates with time, is referred to as the random fluctuation (RF) model (Randolph and White, 1977). In the second, based on the contact nucleation studies of Berglund and Larson (1981), Ramanarayanan (1982), and Berglund et

* a paper submitted to AIChE Journal

al. (1983), an individual crystal is assumed to have an inherent, constant growth rate, but different crystals have different inherent growth rates. This model will be referred to as the constant crystal growth (CCG) model.

Since Randolph and White (1977) first proposed RF model, numerous researchers have employed the same approach to simulate the CSD for both MSMPR (Randolph and Tan, 1978) and batch crystallizers (Melikhov and Berliner, 1981; Lakatos et al., 1984). However, photomicroscopic experiments have confirmed that the CCG model applies to a variety of organic and inorganic solutions, such as citric acid monohydrate-water (Berglund and Larson, 1981), Ammonium dihydrogen phosphate-water (Ramanarayanan, 1982), potassium nitrate-water (Berglund et al. 1983), sucrose-water (Shanks and Berglund, 1985), potash alum-water (Mathis-Lilley and Berglund, 1985), ammonium dihydrogen phosphate-water (Garside and Ristic, 1983), and fructose-water (Shiau and Berglund, 1987). These studies provide the impetus for using the CCG approach in crystallizer modeling.

Berglund and Larson (1984), Larson et al. (1985), Shiau and Berglund (1987), Zumstein and Rousseau (1987), and Berglund and deJong (1988) related the CSD from a single or multi-stage MSMPR crystallizer to the distribution of growth rates based on the CCG model. Ramanarayanan et al. (1984) and Zumstein and Rousseau (1987) developed batch crystallizer models limited to the case of constant supersaturation and negligible nucleation. While nucleation could be accounted for in the MSMPR crystallizer models, it was not in the batch ones. However, nucleation and supersaturation changes are inevitable in most industrial batch crystallization process; therefore, a model taking these changes into account is needed.

The objective of this paper is to develop a general relationship among the initial size distribution of nuclei, the seed CSD, the growth rate distribution, and the product CSD based on CCG model for a seeded batch crystallizer in the case of non-constant supersaturation and non-negligible nucleation. Special cases of the model equations are considered for a number of realistic situations.

Two example calculations have been performed to predict the product CSD from a seeded, batch crystallizer with nucleation. The model equation is solved simultaneously with the mass balance for power law growth and nucleation kinetics. The data used in the examples are taken from the studies of sucrose crystallization by Berglund (1980), Hartel (1980), and Berglund and Murphy (1986).

4.3 Model

A seeded batch crystallizer contains two types of crystals, seeds and subsequently generated nuclei, which can be represented by S crystals and N crystals, respectively (Jones and Mullin, 1974). This model will comprise one part representing the S crystals and the other part of the subsequently generated N crystals. The following assumptions are made in developing this model:

1. Crystal breakage and agglomeration are negligible.
2. The nuclei generated have an initial size distribution, which could be a function of supersaturation, but is independent of growth rate distribution.
3. The growth rate of a crystal is independent of its size.
4. The CCG model is assumed applicable.

N Crystals

For a well-mixed, batch crystallizer, the number of nuclei generated at time t is given by

$$dn_N(t) = B^0(t)\, dt \tag{1}$$

Let $f_G(t;g)$ represent the distribution of growth rates for the crystals at t such that $f_G(t;g)dg$ is the fraction of the total number of crystals at t having a growth rate of g. Further, let $f_{L_{N_o}}(t;\ell_{N_o})$ represent the distribution of initial sizes for the crystals generated at t such that $f_{L_{N_o}}(t;\ell_{N_o})d\ell_{N_o}$ is the fraction of the total number of nuclei generated at t having an initial size of ℓ_{N_o}. Thus, the number of crystals, generated at t with a growth rate g and an initial size ℓ_{N_o}, is given by

$$dn_N(t;\ell_{N_o},g) = B^0(t)dt \cdot f_G(t;g)dg \cdot f_{L_{N_o}}(t;\ell_{N_o})d\ell N_o \tag{2}$$

The size of crystals, generated at t with a growth rate g and an initial size ℓ_{N_o}, at T is given by

$$\ell_N(T;\ell_{N_o},g) = \ell_{N_o}(t) + \int_t^T g(\theta)d\theta \tag{3}$$

where g is a function of θ and changes from t to T. Raising both sides to the jth power yields

$$\ell_N(T;\ell_{N_o},g)^j = (\ell_{N_o}(t) + \int_t^T g(\theta)d\theta)^j \tag{4}$$

Expanding the righthand side of Equation 4 in a binomial series yields

$$\ell_N(T;\ell_{N_o},g)^j = \sum_{r=0}^{j} \binom{j}{r} \ell_{N_o}(t)^{j-r} \cdot [\int_t^T g(\theta)d\theta]^r \tag{5}$$

Therefore, the jth moment of crystals, generated at t with a growth rate g and an initial size ℓ_{N_o}, about the origin of CSD at T can be written as

$$\ell_N(T;\ell_{N_o},g)^j \cdot dn_N(t;\ell_{N_o},g)$$

$$= B^o(t)dt \cdot f_G(\theta;g)dg \cdot f_{L_{N_o}}(t;\ell_{N_o})d\ell_{N_o} \cdot \ell_N(T;\ell_{N_o},g)^j$$

$$= B^o(t)dt \cdot f_G(\theta;g)dg \cdot f_{L_{N_o}}(t;\ell_{N_o})d\ell_{N_o} \cdot \sum_{r=0}^{j} \binom{j}{r} \ell_{N_o}(t)^{j-r} \cdot [\int_t^T g(\theta)d\theta]^r$$

$$= B^o(t)dt \cdot \sum_{r=0}^{j} \binom{j}{r} \ell_{N_o}(t)^{j-r} \cdot f_{L_{N_o}}(t;\ell_{N_o})d\ell_{N_o} \cdot f_G(\theta;g)dg \cdot [\int_t^T g(\theta)d\theta]^r \tag{6}$$

where, $f_G(t;g)$ has been replaced with $f_G(\theta;g)$ since $f_G(\theta;g)$ and g are functions of θ, which changes from t to T. Taking $f_G(\theta;g)dg$ inside the integral sign gives

$$f_G(\theta;g)dg\cdot\left[\int_t^T g(\theta)d\theta\right]^r = \left[\int_t^T \left(g(\theta)^r\cdot f_G(\theta;g)dg\right)^{\frac{1}{r}} d\theta\right]^r \tag{7}$$

Substituting Equation 7 into Equation 6 yields

$$\ell_N(T;\ell_{N_o},g)^j\cdot dn_N(t;\ell_{N_o},g)$$

$$- B^o(t)\,dt\cdot\sum_{r=0}^{j}\binom{j}{r}\ell_{N_o}(t)^{j-r}\cdot f_{N_o}(t;\ell_{N_o})d\ell_{N_o}\cdot\left[\int_t^T \left(g(\theta)^r\cdot f_G(\theta;g)dg\right)^{\frac{1}{r}} d\theta\right]^r \tag{8}$$

Thus, the jth moment of crystals, generated at t with all possible growth rates and all possible initial sizes, about the origin of CSD at T can be written as

$$\ell_N(T)^j\cdot dn_N(t) = \int_{(\ell_{N_o})}^{\infty}\int_{(g)}^{\infty} B^o(t)dt\cdot\sum_{r=0}^{j}\binom{j}{r}\ell_{N_o}(t)^{j-r}\cdot f_{L_{N_o}}(t;\ell_{N_o})d\ell_{N_o}\cdot\left[\int_{(\theta)}^{T}\left(g(\theta)^r\cdot f_G(\theta;g)dg\right)^{\frac{1}{r}}dr\right]^r \tag{9}$$

Noting that $\ell_{N_o}(t)$ and $G(\theta)$ are independent random variables, Equation 9 can be written as

$$\ell_N(T)^j\cdot dn_N(t) = B^o(t)dt\cdot\sum_{r=0}^{j}\binom{j}{r}\int_{(\ell_{N_o})}^{\infty}\ell_{N_o}(t)^{j-r}\cdot f_{L_{N_o}}(t;\ell_{N_o})d\ell_{N_o}$$

$$\cdot\left[\int_{(\theta)}^{T}\left(\int_{(g)}^{\infty} g(\theta)^r\cdot f_G(\theta;g)dg\right)^{\frac{1}{r}}d\theta\right]^r$$

$$- B^0(t)dt \cdot \sum_{r=0}^{j} \binom{j}{r} M_{L_{N_o}}(t;j-r) \cdot \left[\int_{t}^{T} M_G(\theta;r)^{\frac{1}{r}} d\theta\right]^r \tag{10}$$

where

$$M_{L_{N_o}}(t;j-r) = \int_o^\infty \ell_{N_o}(t)^{j-r} \cdot f_{L_{N_o}}(t;\ell_{N_o})d\ell_N \tag{11}$$

$$M_G(\theta;r) = \int_o^\infty g(\theta)^r \cdot f_G(\theta;g)dg \tag{12}$$

Therefore, the jth moment of all the nuclei, generated from 0 to T, about the origin of CSD at T is given by

$$M'_{L_N}(T;j) = \int_0^T \ell_N(T)^j \cdot dn_N(t)$$
$$= \int_0^T \left\{ B^0(t) \cdot \sum_{r=0}^{j} \binom{j}{r} M_{L_{N_o}}(t;j-r) \cdot \left[\int_{t}^{T} M_G(\theta;r)^{\frac{1}{r}} d\theta\right]^r \right\} dt \tag{13}$$

since

$$M'_{L_{N_o}}(T;0) = \int_0^T B^0(t)dt \tag{14}$$

The normalized jth moment of all the crystals at T is

$$M_{L_N}(T;j) = \frac{1}{\int_o^T B^0(t)dt} \int_0^T \left\{ B^0(t) \cdot \sum_{r=0}^{j} \binom{j}{r} M_{L_{N_o}}(t;j-r) \right.$$

$$\cdot \left[\int_t^T M_G(\theta;r)^{\frac{1}{r}}\, d\theta\right]^r \Bigg\} dt \tag{15}$$

Special case I: constant growth conditions, constant nucleation conditons

$$M_{L_N}(T;j) = \sum_{r=0}^{j} \frac{1}{r+1} \cdot \binom{j}{r} M_{L_{N_o}}(T;j-r) \cdot M_G(T;r) \cdot T^r \tag{16}$$

Special case II: monosized initial size distribution of nuclei ($\ell_{N_o} \neq 0$)

$$M_{L_N}(T;j) = \frac{1}{\int_0^T B^o(t)dt} \int_0^T \left\{ B^o(t) \cdot \sum_{r=0}^{j} \binom{j}{r} \ell_{N_o}^{\,j-r} \cdot \left[\int_t^T M_G(\theta;r)^{\frac{1}{r}}\, d\theta\right]^r \right\} dt \tag{17}$$

Special case III: crystals are born at zero size ($\ell_{N_o} = 0$)

$$M_{L_N}(T;j) = \frac{1}{\int_0^T B^o(t)dt} \int_0^T \left\{ B^o(t) \cdot \left[\int_t^T M_G(\theta;r)^{\frac{1}{r}}\, d\theta\right]^r \right\} dt \tag{18}$$

Special case IV: special case I + special case II

$$M_{L_N}(T;j) = \sum_{r=0}^{j} \frac{1}{r+1} \cdot \binom{j}{r} \ell_{N_o}^{\,j-r} \cdot M_G(T;r) \cdot T^r \tag{19}$$

Special case V: special case I + special case III

$$M_{L_N}(T;j) = \frac{M_G(T;j) \cdot T^j}{j+1} \tag{20}$$

S crystals

The number of seeds, charged into the crystallizer at t=0 with a growth rate g and an intial size ℓ_{s_o}, is given by

$$dn_S(0;\ell_{s_o},g) = N_{s_o} \cdot f_G(0,g)dg \cdot f_{L_{s_o}}(0;\ell_{s_o}) \tag{21}$$

Where N_{s_o} is the total number of seeds charged into the crystallizer at t=0, and $f_{L_{s_o}}(0;\ell_{s_o})$ represents the distribution of initial sizes for the seeds charged into the crystallizer at t=0 such that $f_{L_{s_o}}(0;\ell_{s_o})d\ell_{s_o}$ is the fraction of the seeds having an initial size of ℓ_{s_o}. $f_G(0;g)$ represents the distribution of growth rates for the seeds at t=0 such that $f_G(0;g)dg$ is the fraction of the seeds having a growth rate of g at t=0.

The size of seeds, charged into the crystallizer at t=0 with a growth rate g and an initial size ℓ_{s_o} at T is given by

$$\ell_s(T;\ell_{s_o},g) = \ell_{s_o}(o) + \int_o^T g(\theta)d\theta \tag{22}$$

So,

$$\ell_s(T;\ell_{s_o},g)^j = [\ell_{s_o}(o) + \int_o^T g(\theta)d\theta]^j \tag{23}$$

Expanding the righthand side of Equation 23 in a binomial series yields

$$\ell_s(T;\ell_{s_o},g)^j = \sum_{r=0}^{j} \binom{j}{r} \ell_{s_o}(o)^{j-r} \cdot [\int_o^T g(\theta)d\theta]^r \tag{24}$$

Therefore, the jth moment of seeds, with a growth rate g and initial size ℓ_{s_o}, about the origin of CSD at T is

$$\ell_s(T;\ell_{s_o},g)^j \cdot dn_s(\ell_o,g)$$

$$= N_{s_o} \cdot f_G(\theta;g)dg \cdot f_{L_{s_o}}(0,\ell_{s_o})d\ell_{s_o} \cdot \ell_s(T;\ell_{s_o},g)^j$$

$$= N_{s_o} \cdot f_G(\theta,g)dg \cdot f_{L_{s_o}}(0;\ell_{s_o})d\ell_s \cdot \sum_{r=0}^{j} \binom{j}{r} \ell_{s_o}(o)^{j-r} \cdot [\int_o^T g(\theta)d\theta]^r$$

$$= N_{s_o} \cdot \sum_{r=0}^{j} \binom{j}{r} \ell_{s_o}(o)^{j-r} \cdot f_{L_{s_o}}(o;\ell_{s_o})d\ell_s \cdot f_G(\theta;g)dg \cdot [\int_o^T g(\theta)d\theta]^r \tag{25}$$

Here, $f_g(0;g)$ has been replaced with $f_G(\theta;g)$ since $f_G(\theta;g)$ and g are functions of θ, which changes from 0 to T. Taking $f_G(\theta;g)dg$ inside the intergral sign yields

$$f_G(\theta;g)dg \cdot [\int_o^T g(\theta)d\theta]^r = [\int_o^T (g(\theta)^r \cdot f_G(\theta;g)dg)^{\frac{1}{r}} d\theta]^r \tag{26}$$

Substituting Equation 26 into Equation 25 yields

$$\ell_s(T;\ell_{s_o},g)^j \cdot dn_s(\ell_o,g) = N_{s_o} \cdot \sum_{r=0}^{j}\binom{j}{r} \ell_{s_o}(o)^{j-r} \cdot f_{L_{s_o}}(o;\ell_{s_o})$$

$$\cdot [(g(\theta)^r \cdot f_G(\theta;g)dg)^{\frac{1}{r}} d\theta]^r \qquad (27)$$

Thus, the jth moment of all the seeds (with all possible growth rates and all possible initial sizes) about the origin of CSD at T is

$$M'_{L_s}(T;j) = \int_{(\ell_{s_o})}^{\infty}\int_{(g)}^{\infty} N_{s_o} \cdot \sum_{r=0}^{j}\binom{j}{r}\ell_{s_o}(o)^{j-r} \cdot f_{L_{s_o}}(o;\ell_{s_o})d\ell_{s_o}$$

$$\cdot [\int_{(\theta)}^{T} (g(\theta)^r \cdot f_G(\theta;g)dg)^{\frac{1}{r}} d\theta]^r \qquad (28)$$

Noting that $\ell_{s_o}(o)$ and $g(\theta)$ are independent random variables, Equation 28 can be rewritten as

$$M'_{L_s}(T;j) = N_{s_o} \cdot \sum_{r=0}^{j}\binom{j}{r} \int_{(\ell_{s_o})}^{\infty} \ell_{s_o}(o)^{j-r} \cdot f_{L_{s_o}}(o;\ell_{s_o})d\ell_{s_o}$$

$$\cdot [\int_{(\theta)}^{T} (\int_{(g)}^{\infty} g(\theta)^r \cdot f_G(\theta;g)dg)^{\frac{1}{r}} d\theta]^r$$

$$= N_{s_o} \cdot \sum_{r=0}^{j}\binom{j}{r} M_{L_{s_o}}(0;j-r) \cdot [\int_0^T M_G(\theta;r)^{\frac{1}{r}} d\theta]^r \qquad (29)$$

where

$$M_{L_{s_o}}(0;j-r) = \int_o^\infty \ell_{s_o}(o)^{j-r} \cdot f_{L_{s_o}}(o;\ell_{s_o}(d\ell_{s_o}) \tag{30}$$

Since N_{s_o} is the total number of seeds, the normalized jth moment of all the seeds at T is

$$M_{L_s}(T;j) = \sum_{r=0}^{j} \binom{j}{r} M_{L_{s_o}}(0;j-r) \cdot [\int_0^T M_G(\theta;r)^{\frac{1}{r}} d\theta]^r \tag{31}$$

Special case I: constant growth condition

$$M_{L_s}(T;j) = \sum_{r=0}^{j} \binom{j}{r} M_{L_{s_o}}(0;j-r) \cdot M_G(r)T^r \tag{32}$$

Which is the same form as developed by Ramanarayanan et al. (1984) for a seeded batch crystallizer with constant supersaturation and negligible nucleation.

Special case II: monosized seed size distribution ($\ell_s \neq 0$)

$$M_{L_s}(T;j) = \sum_{r=0}^{j} \binom{j}{r} \ell_{s_o}{}^{j-r} \cdot [\int_0^T M_G(\theta;r)^{\frac{1}{r}} d\theta]^r \tag{33}$$

Special case III: special case I + special case II

$$M_{L_s}(T;j) = \sum_{r=0}^{j} \binom{j}{r} \ell_{s_o}{}^{j-r} \cdot M_G(r) \cdot T^r \tag{34}$$

N + S crystals

Combining Equations (9) and (18), the normalized jth moment of all the crystal, including N crystals and S crystals, about the origin of CSD at T is

$$M_{L_{N+S}}(T;j) = \frac{1}{\int_0^T B^0(t)dt + N_{s_o}} \left[\int_0^T B(t)dt \cdot M_{L_N}(T;j) + N_{s_o} \cdot M_{L_S}(T;j)\right] \quad (35)$$

4.4 Application of the Model

In the case of considering GRD based on the above model for a well-mixed, batch crystallizer, the CSD modeling equations can be summarized as follows:

Population balances (moment form):

for N crystals: Eq. (15)

for S crystals: Eq. (31)

for both N crystals and S crystals: Eq. (35)

Mass balance:

$$W_2(T) = W_2(0) + W_s - M_T(T) \cdot V(T)$$

Growth Kinetics:

Berglund and Murphy (1986) and Shiau and Berglund (1987) measured the mean growth kinetics and the variance of growth rate distribution for sucrose and fructose, respectively. In both cases, the mean growth

rate has an Arrhenius form and the variance of growth rate distribution can be represented as a power law expression as follows:

$$\bar{G}(T) = A\, e^{\frac{-E_G}{R \cdot TEMP}}\, S(T)^m$$

$$\sigma_G^2(T) = a\, \bar{G}(T)^b$$

In terms of the moment form,

$$M_G(T;1) = \bar{G}(T)$$

and

$$M_G(T;2) = \bar{G}(T)^2 + \sigma_G^2(T)$$
$$= \bar{G}(T)^2 + a\bar{G}(T)^b$$

In applying the model coupled with the mass balance equation, the third moment of growth rate distribution needs to be estimated from the knowledge of the first and second moments. In most cases, the growth rate distribution can be fit to a Gamma distribution allowing the two parameters $\alpha(T)$ and $\beta(T)$ for the Gamma distribution to be calculated from the mean and variance, thus

$$\beta(T) = \frac{\sigma_G^2(T)}{\bar{G}(T)}$$

$$\alpha(T) = \frac{\bar{G}(T)}{\beta(T)}$$

the third moment then may be written

$$M_G(T;3) = \alpha(T) \cdot (\alpha(T) + 1) \cdot (\alpha(T) + 2) \cdot \beta(T)^3$$

Slurry density:

$$M_T(T) = \rho \cdot k_v \cdot M_{L_{N+S}}(T;3) \cdot Num_{N+S}(T)$$

Nucleation kinetics:

$$B^0(T) = k_N(T) \cdot M_T(T)^I \cdot S(T)^J$$

Free liquor volume:

$$V(T) = \frac{V_T}{1 + k_v \cdot M_{L_{N+S}}(T;3) \cdot Num_{N+S}(T)}$$

Number of N crystal and S crystals per unit free liquor volume:

for N crystals: $\int_0^T B^0(t)dt$

for S crystals: $\frac{N_{s_o}}{V(T)}$

for both N crystals and S crystals: $Num_{N+S}(T) = \int_0^T B^0(t)dt + \frac{N_{s_o}}{V(T)}$

4.5 Example Calculations

Example 1: A seeded, isothermal batch crystallizer with nucleation

The crystallizer is initially seeded with crystals of uniform size. The conditions employed in this example are listed in Table 1. The crystallizer was simulated at a constant temperature of 40°C.

GRD will result in some crystals of greater size and some of smaller size; however, crystals of greater size consume the solute faster than crystals of smaller size. Therefore, GRD results in a greater solute consumption. Figure 1 shows the desupersaturation

Table 1. Conditions employed in the examples of a batch crystallizer for sucrose.

Parameters	Quantity
sucrose crystal density, g/cm 3	1.588
initial concentration, g sucrose/100 g soln	73
sucrose solution, g	5000
seed size, μm	100
seed loading, g	50
birth size of nuclei, μm	0
saturated sucrose concentration at a given temperature (TEMP), where C* is in g sucrose/100 g soln and T is in ^{o}C (Bates, 1942)	$c^{*}=62.77+0.1760\ TEMP+0.000344\ TEMP^{2}$
the mean growth rate kinetics, where $\bar{G}$ is in μm/min, TEMP is in ^{o}K, and C is sucrose concentration in g sucrose /100 g soln (Berglund, 1980)	$\bar{G} = 7.99\times10^{10} \exp \frac{(-13600)}{R\cdot TEMP} \cdot (C-C^{*})^{2}$
the variance of growth rate distribution where $\bar{G}$ is in μm/min and σ_G^2 is $\mu m^2/min^2$ (Berglund and Murphy, 1986)	$\sigma_G^2 = 0.286\bar{G}^{1.74}$
nucleation rate, where B^{o} is in #/cm^3-min, $\bar{G}$ is in μm/min and M_T is suspension density in g/cm^3 (Hartel, 1980)	$B^{o} = 2.4\times10^{-8}\ \bar{G}^{1.5} M_T$

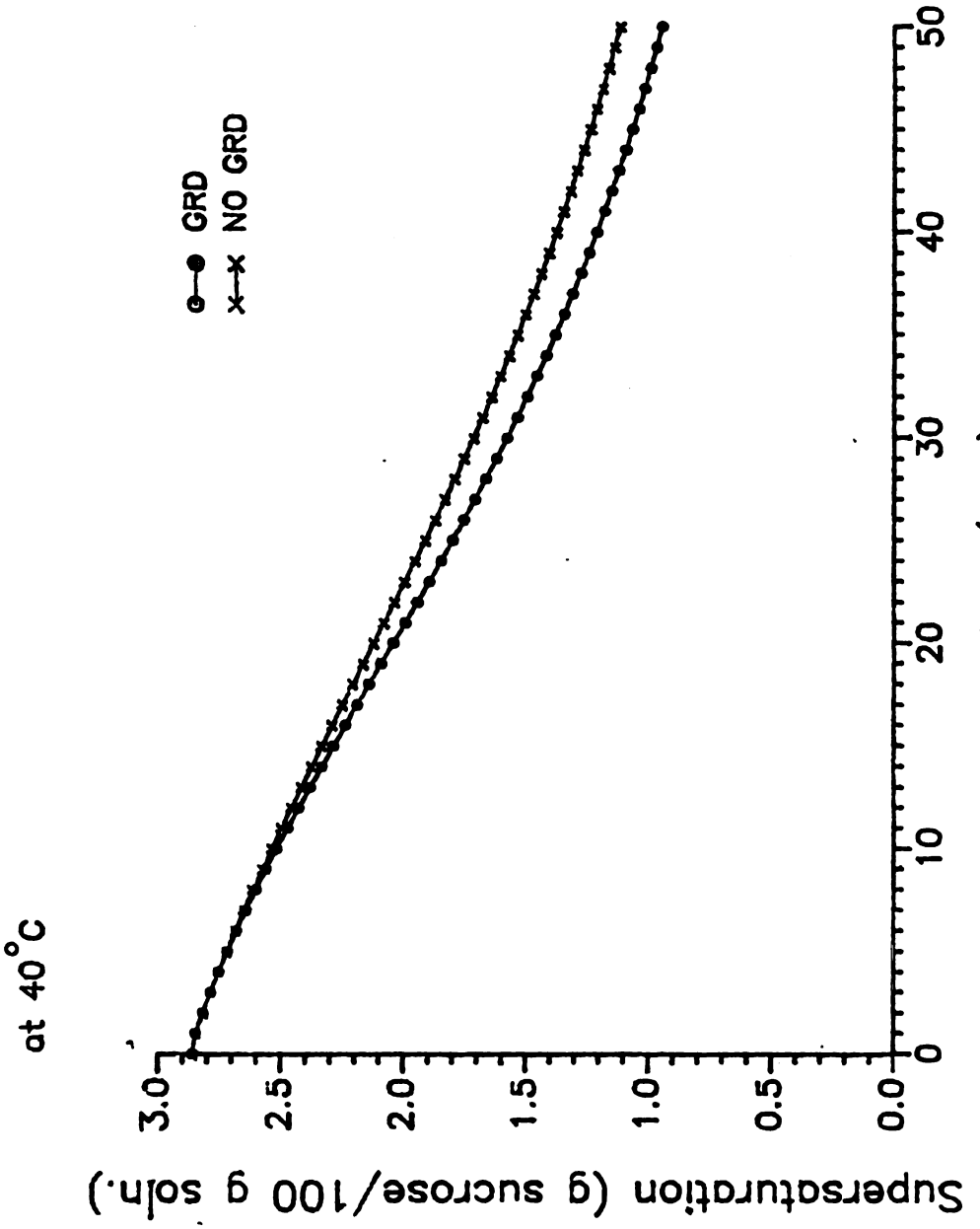

Figure 1. Supersaturation versus time for both GRD and no GRD at a constant temperature of 40°C in Example 1.

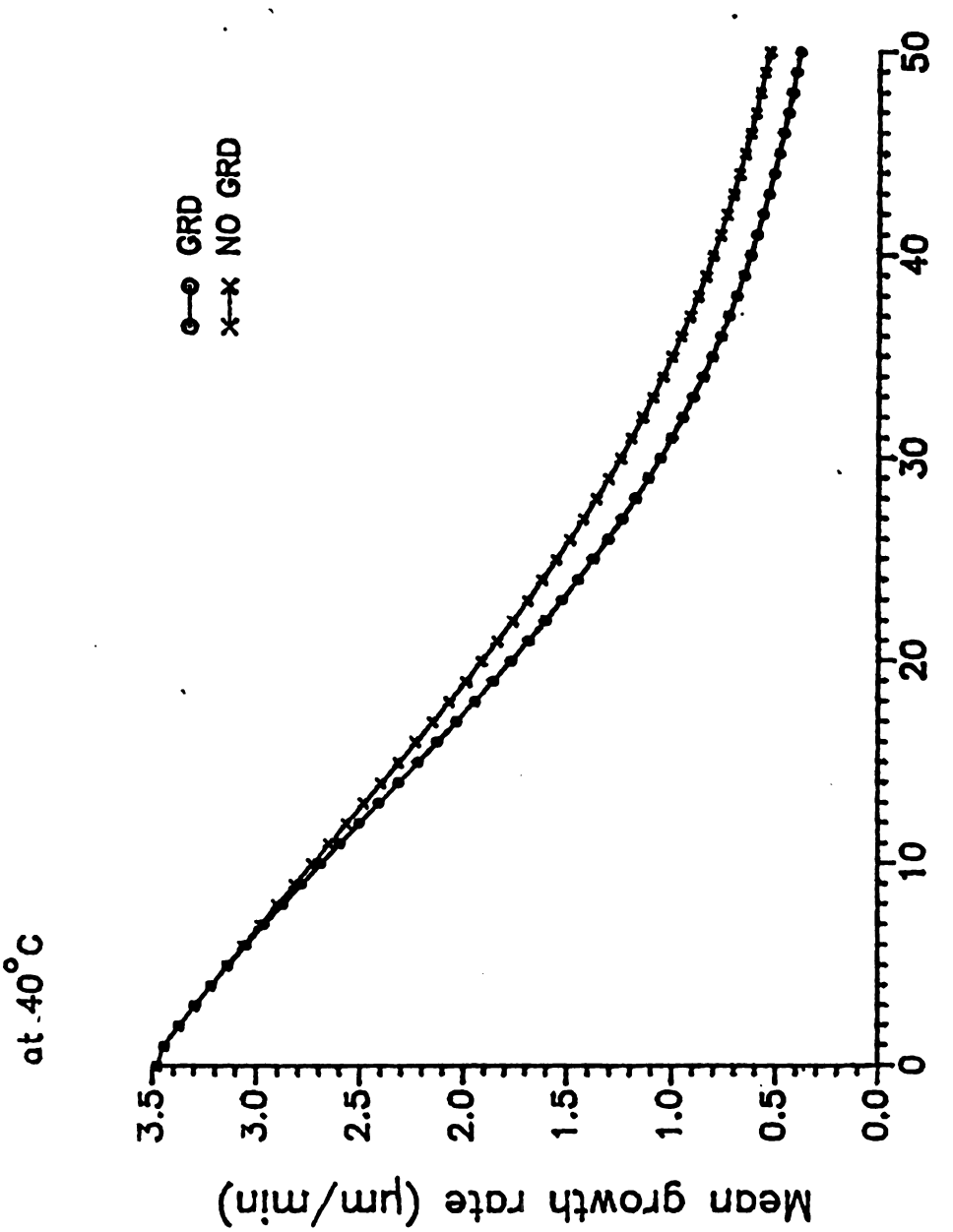

Figure 2. Mean growth rate versus time for both GRD and no GRD at a constant temperature of 40°C in Example 1.

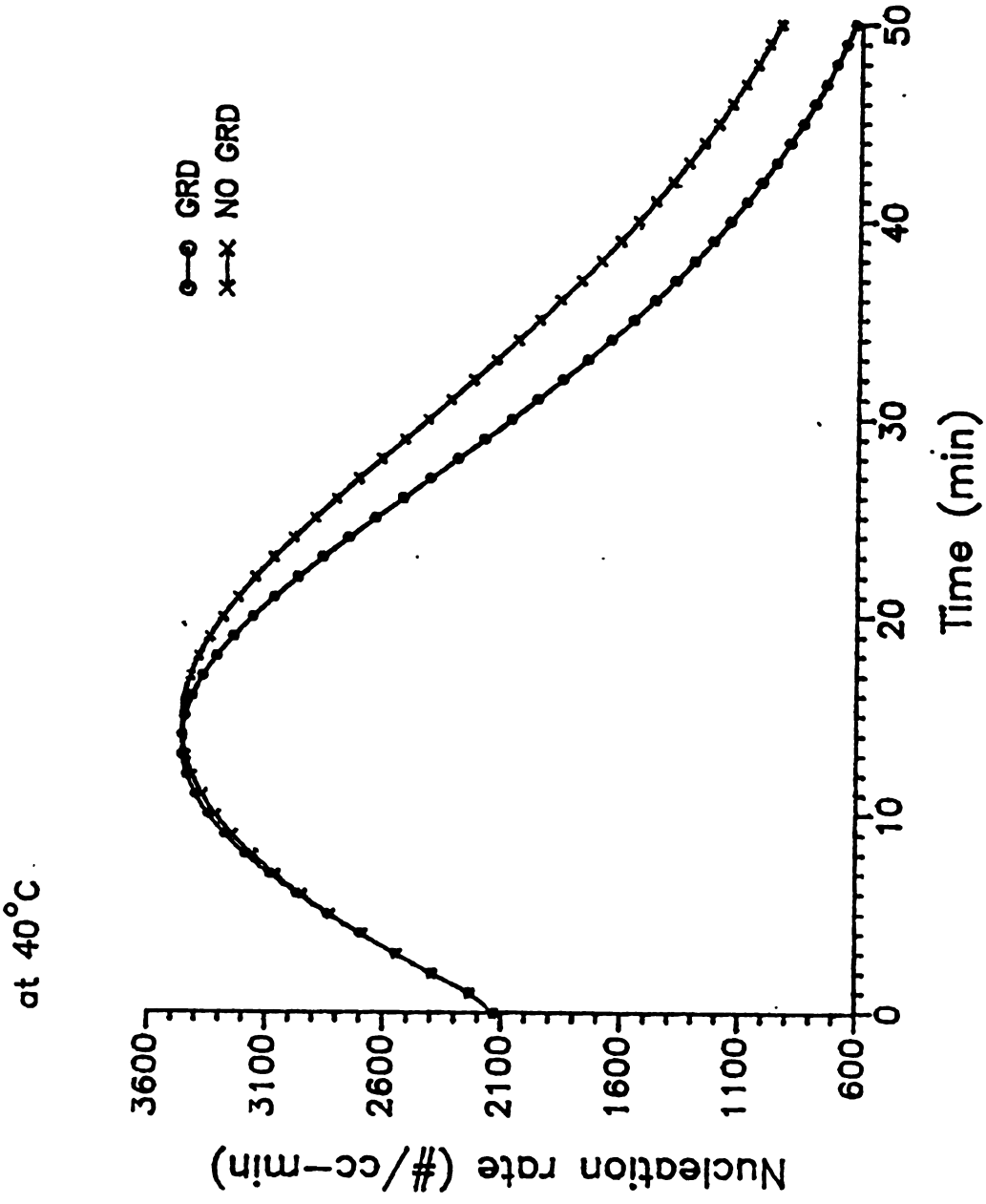

Figure 3. Nucleation rate versus time for both GRD and no GRD at a constant temperature of 40°C in Example 1.

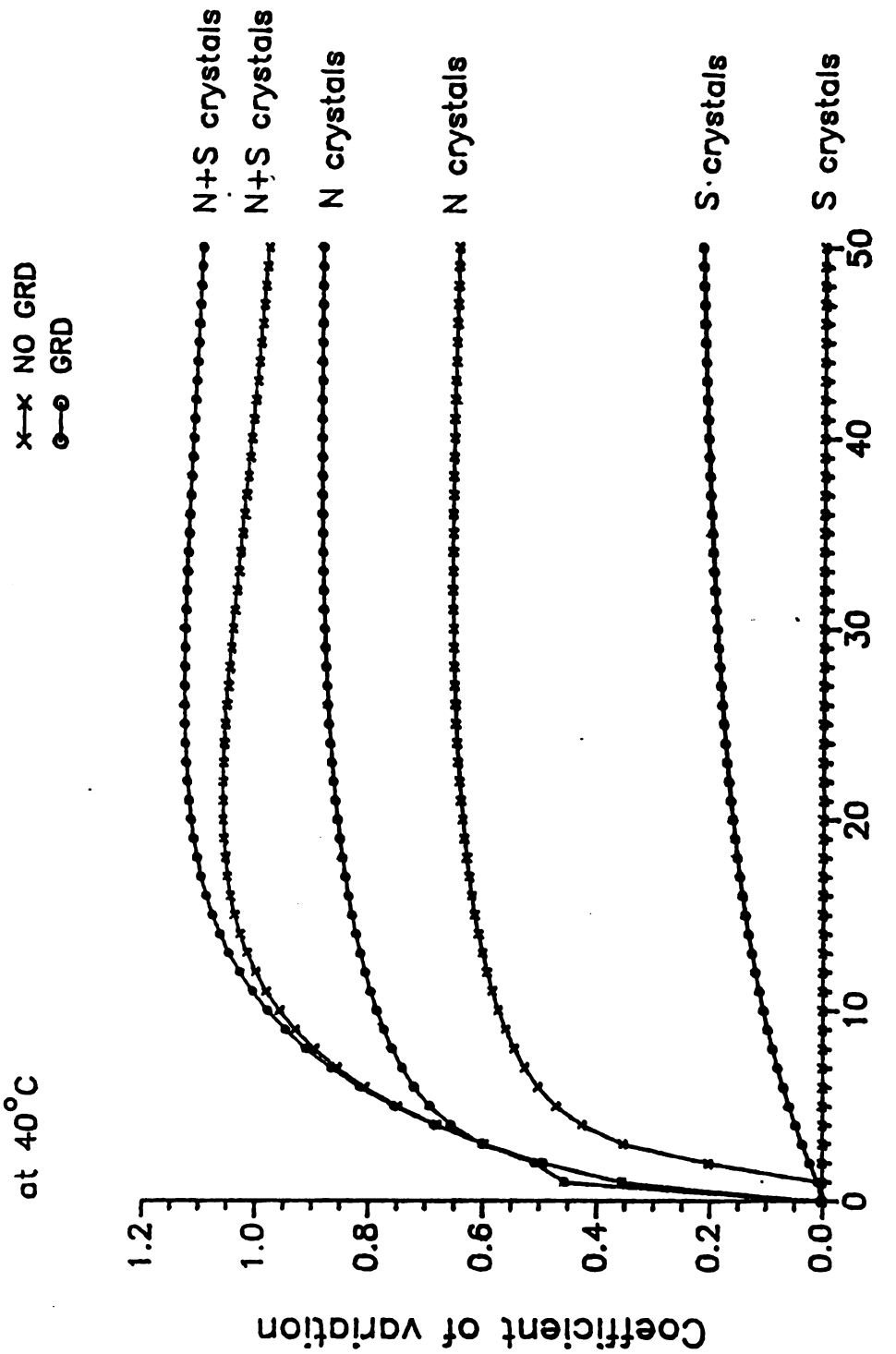

Figure 4. C.V. on a number basis for N, S, and N+S crystals versus time for both GRD and no GRD at a constant temperature of 40°C in Example 1.

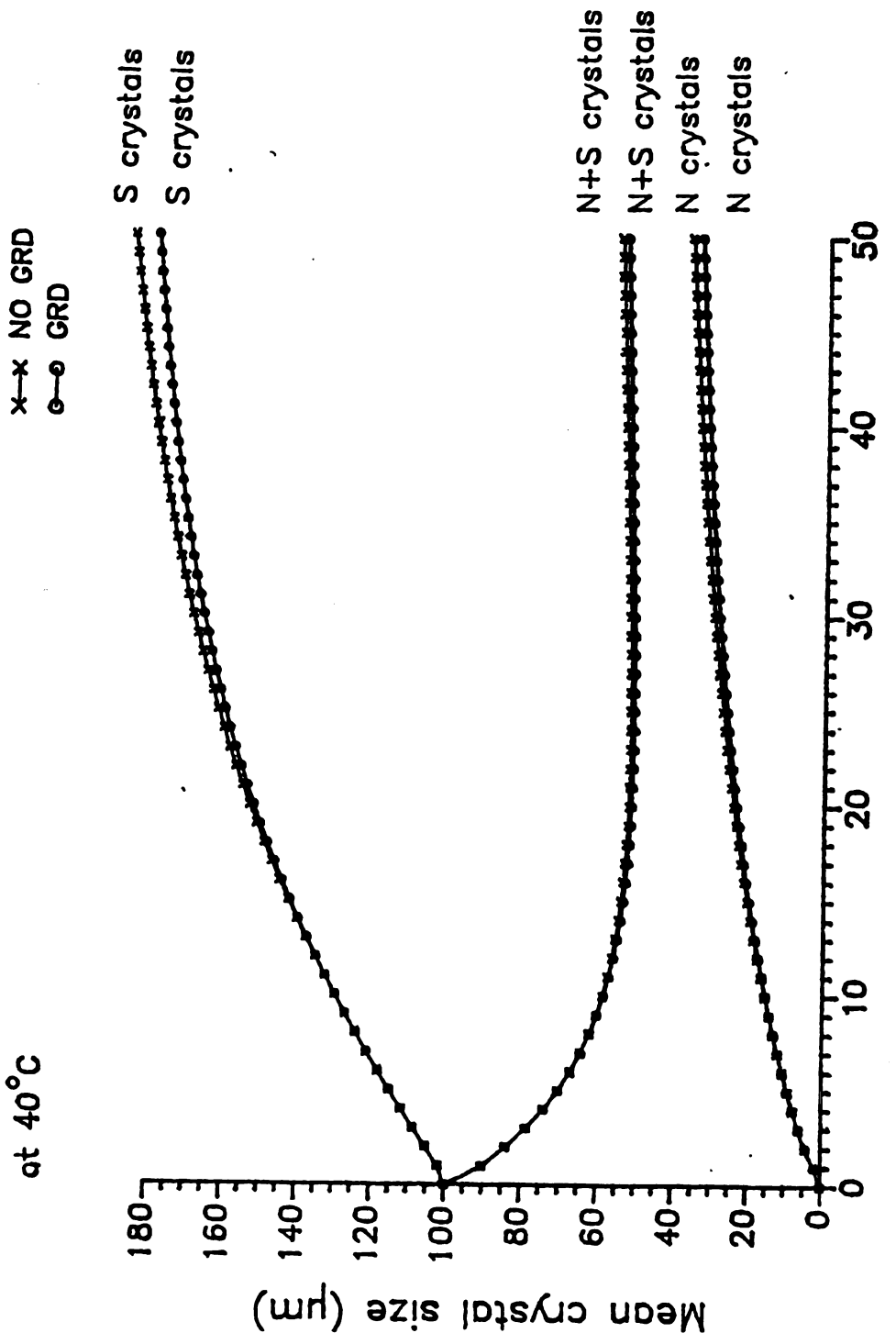

Figure 5. Mean crystal size on a number basis for N, S, and N+S crystals versus time for both GRD and no GRD at a constant temperature of 40°C in Example 1.

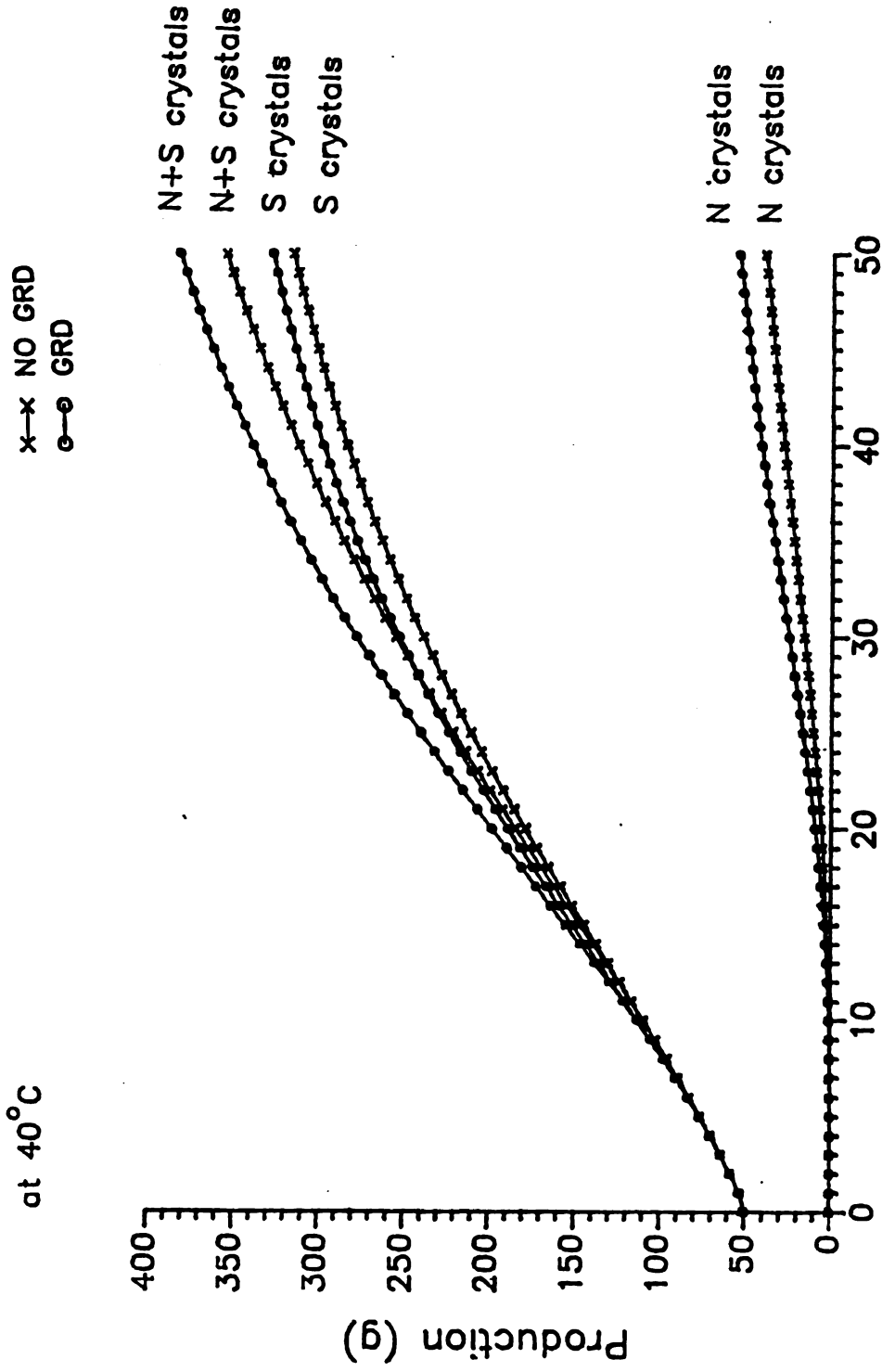

Figure 6. Production for N, S, and N+S crystals versus time for both GRD and no GRD at a constant temperature of 40°C in Example 1.

curves, in which supersaturation in the case of GRD decreases faster than that in the case of no GRD. Consequently, mean growth rate in the case of GRD decreases faster than that in the case of no GRD (Figure 2). The nucleation rate increases to a maximum and decreases for both cases since mean growth rate decreases and suspension density increases in the crystallization process (Figure 3).

Coefficients of variation on a number basis in the case of GRD are always greater than those in the case of no GRD, and the difference between GRD and no GRD are quite significant (Figure 4). Since GRD would result in a smaller mean growth rate as shown in Figure 2, mean crystal sizes on a number basis for S crystals, N crystals, and S+N crystals in the case of GRD are a little smaller than those in the case of no GRD (Figure 5). On the other hand, GRD has the opposite result on the production as shown in Figure 6. Since GRD results in a greater solute consumption, production in the case of GRD would be greater than that in the case of no GRD for S, N, and S+N crystals.

It seems that GRD has smaller effects on mean growth rates and production with greater effects on coefficients of variation for S, N, and S+N crystals. It must be kept in mind that the above example was only simulated in a relative short period for supersaturation of 1.0 ~ 3.0 g sucrose/100 g soln due to the limited applicability of nucleation, growth rate, and growth rate dispersion kinetics. The effects of GRD on product performances are expected to be more significant during a longer time period.

Example 2: A seeded, constant level of supersaturation batch crystallizer with nucleation

Batch crystallizers are usually operated at a controlled level of

supersaturation to yield crystals of better quality. The conditions in this example are the same as those in example 1 listed in Table 1. The crystallizer was simulated at a constant level of supersaturation of 1.5 g sucrose/100 g soln.

Since GRD results in a greater solute consumption, cooling rate in the case of GRD has to be faster than that in the case of no GRD in order to keep a constant level of supersaturation, i.e., operating temperature in the case of GRD decreases faster than that in the case of no GRD (Figure7). Consequently, mean growth rate in the case of GRD decreases faster than that in the case of no GRD (Figure 8). Since suspension density increases and supersaturation is kept constant in the crystallization process, nucleation rate increases for both GRD and no GRD cases (Figure 9). Coefficients of variation on a number basis in the case of GRD are always greater than those in the case of no GRD, and the difference between GRD and no GRD are once again quite significant (Figure 10). Since GRD would result in a smaller mean growth rate (Figure 8), mean crystal sizes on a number basis for S crystals, N crystals, and S+N crystals in the case of GRD are a little smaller than those in the case of no GRD (Figure 11). On the other hand, GRD has the opposite result on the production (Figure 12). Since GRD results in a greater solute consumption, production in the case of GRD is greater than in the case of no GRD for S, N, and S+N crystals.

It has been found that GRD has smaller effects on mean growth and production and greater effects on coefficient of variation for S, N, and S+N crystals similar to Example 1. Again, the simulation was only for a relative short period at a temperature between 40-47^{o}C due to the

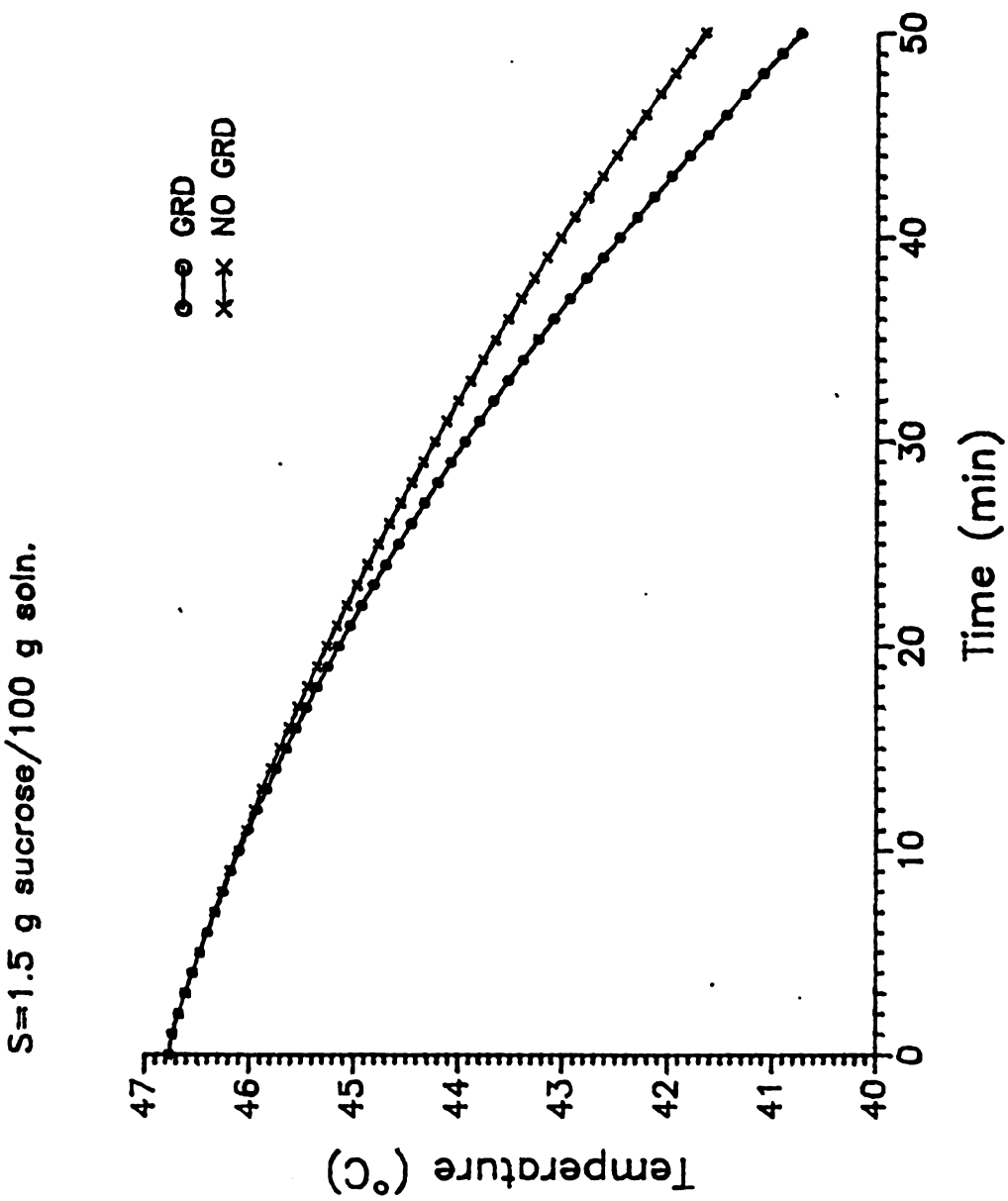

Figure 7. Cooling temperature versus time for both GRD and no GRD at a constant level of supersaturation of 1.5 g sucrose/100 g soln in Example 2.

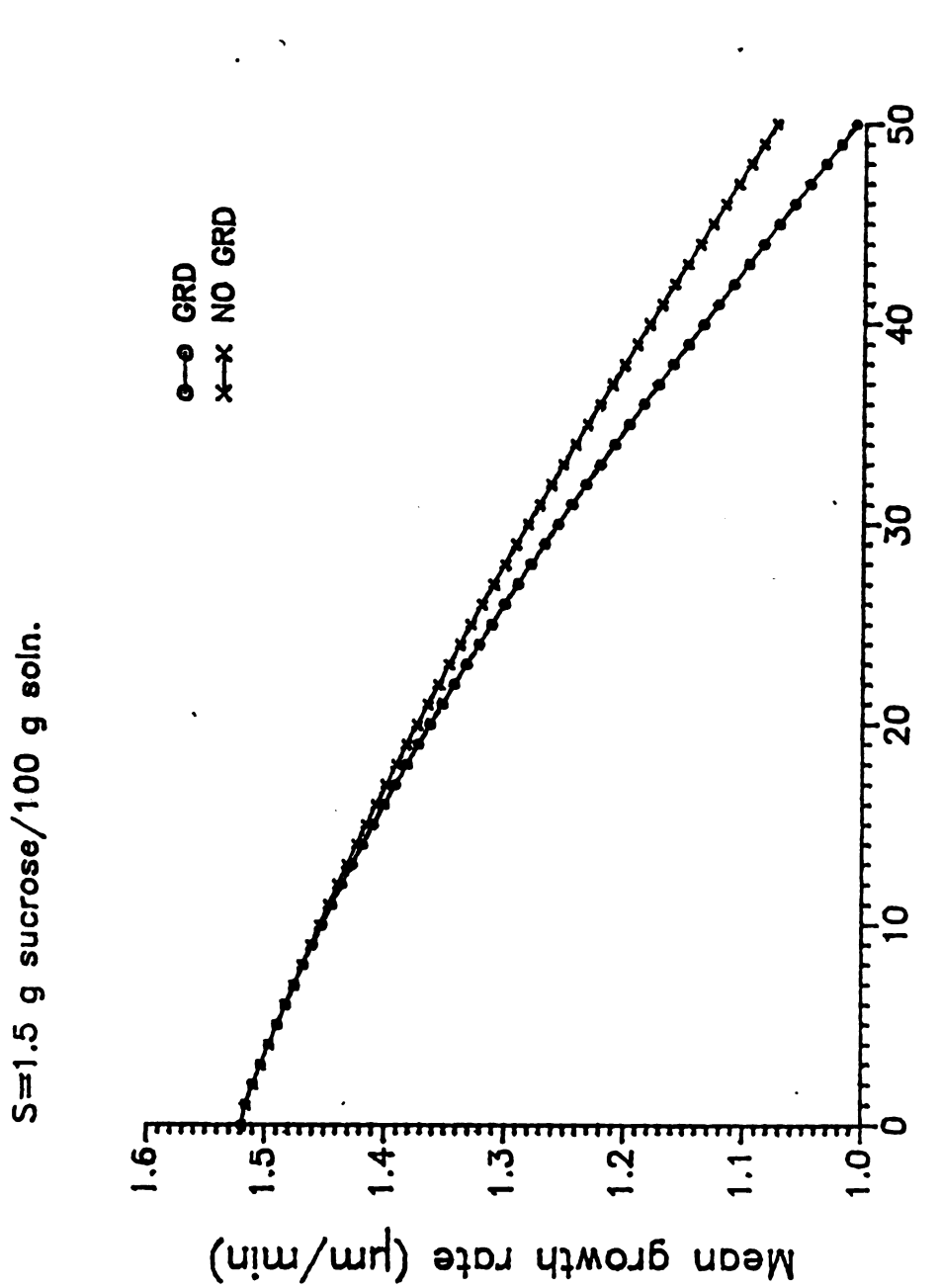

Figure 8. Mean growth rate versus time for both GRD and no GRD at a constant level of supersaturation of 1.5 g sucrose/100 g soln in Example 2.

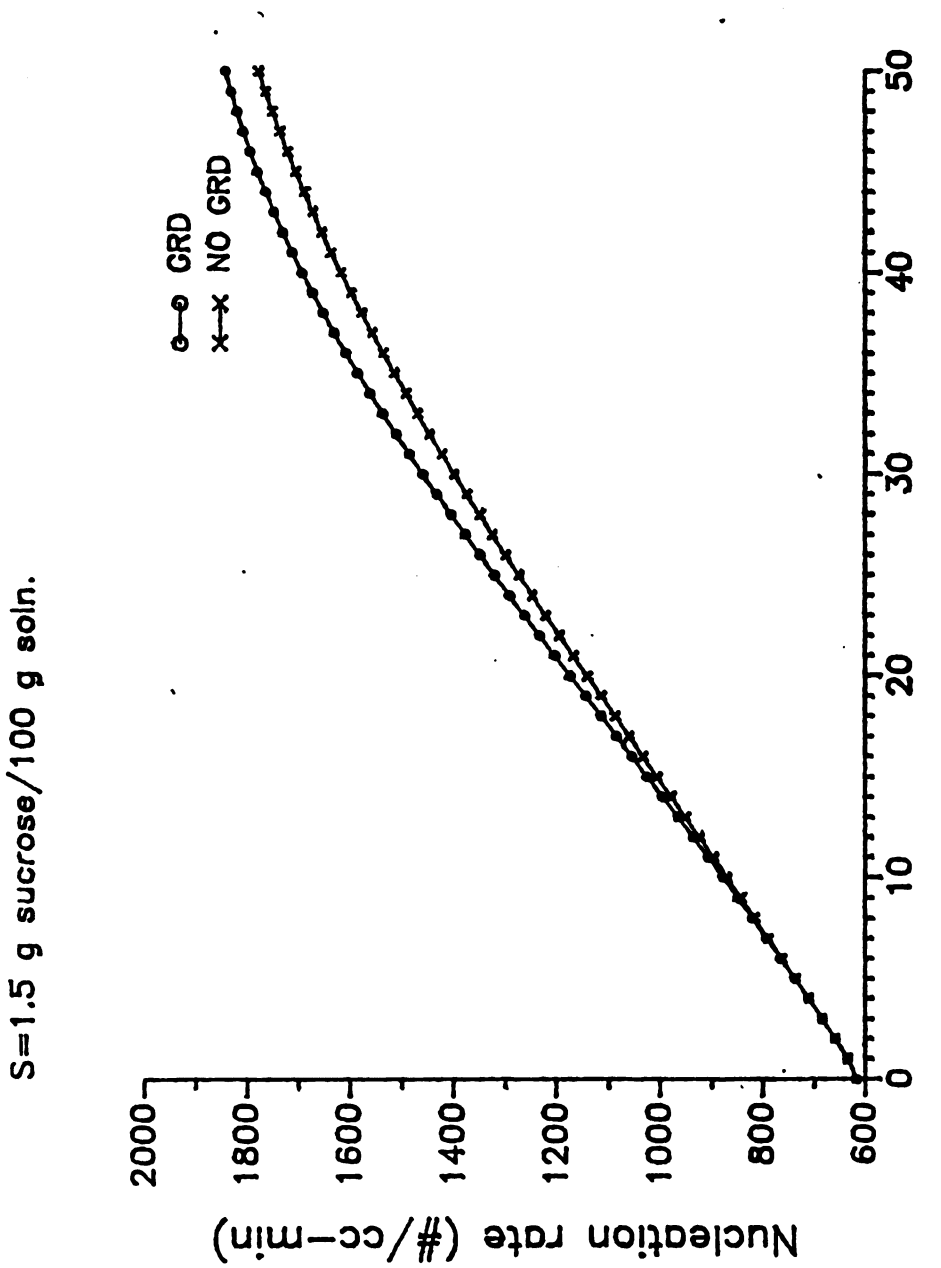

Figure 9. Nucleation rate versus time for both GRD and no GRD at a constant level of supersaturation of 1.5 g sucrose/100 g soln in Example 2.

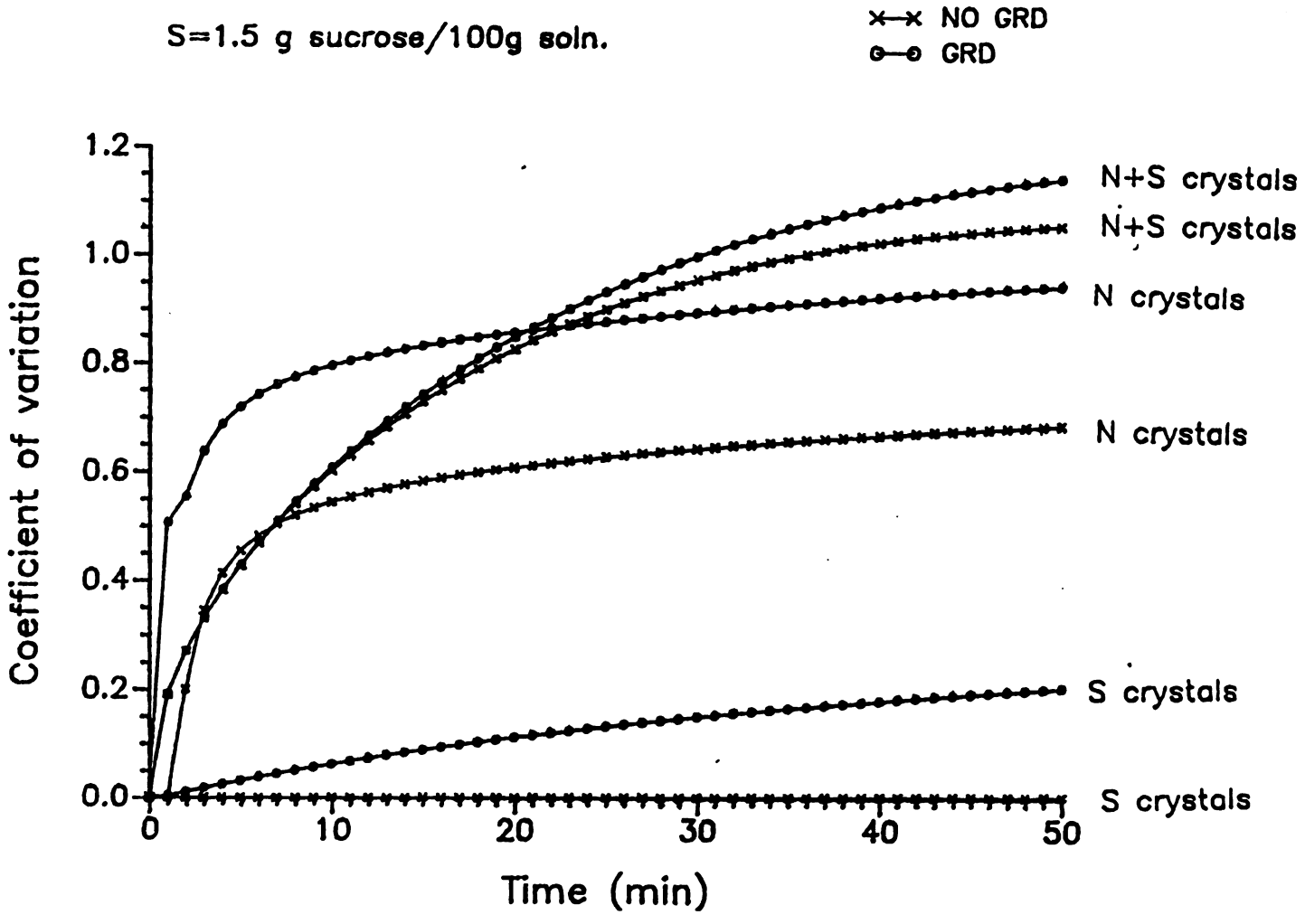

Figure 10. C.V. on a number basis for N, S, and N+S crystals versus time for both GRD and no GRD at a constant level of supersaturation of 1.5 g sucrose/100 g soln in Example 2.

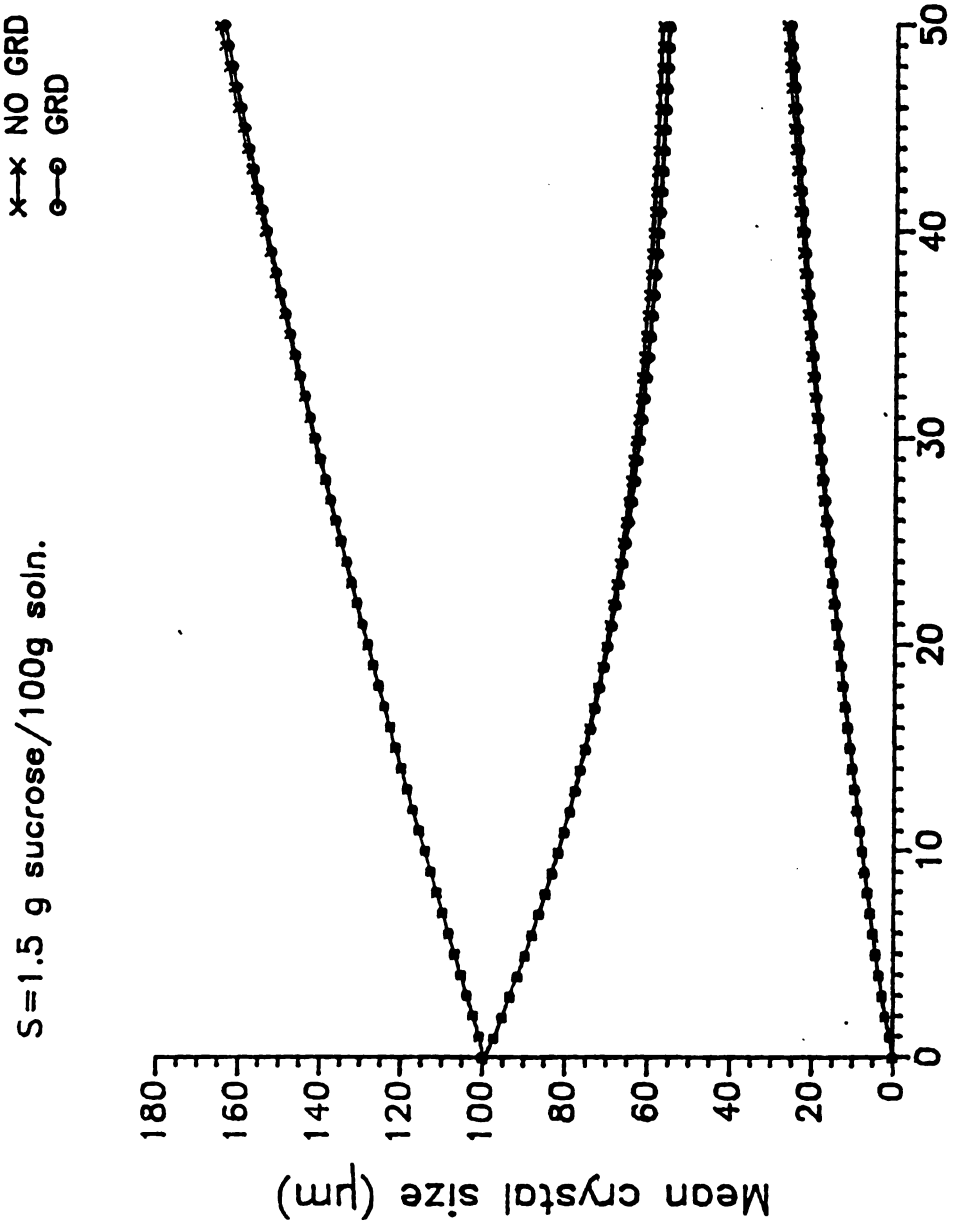

Figure 11. Mean crystal size on a number basis for N, S, and N+S crystals versus time for both GRD and no GRD at a constant level of supersaturation of 1.5 g sucrose/100 g soln in Example 2.

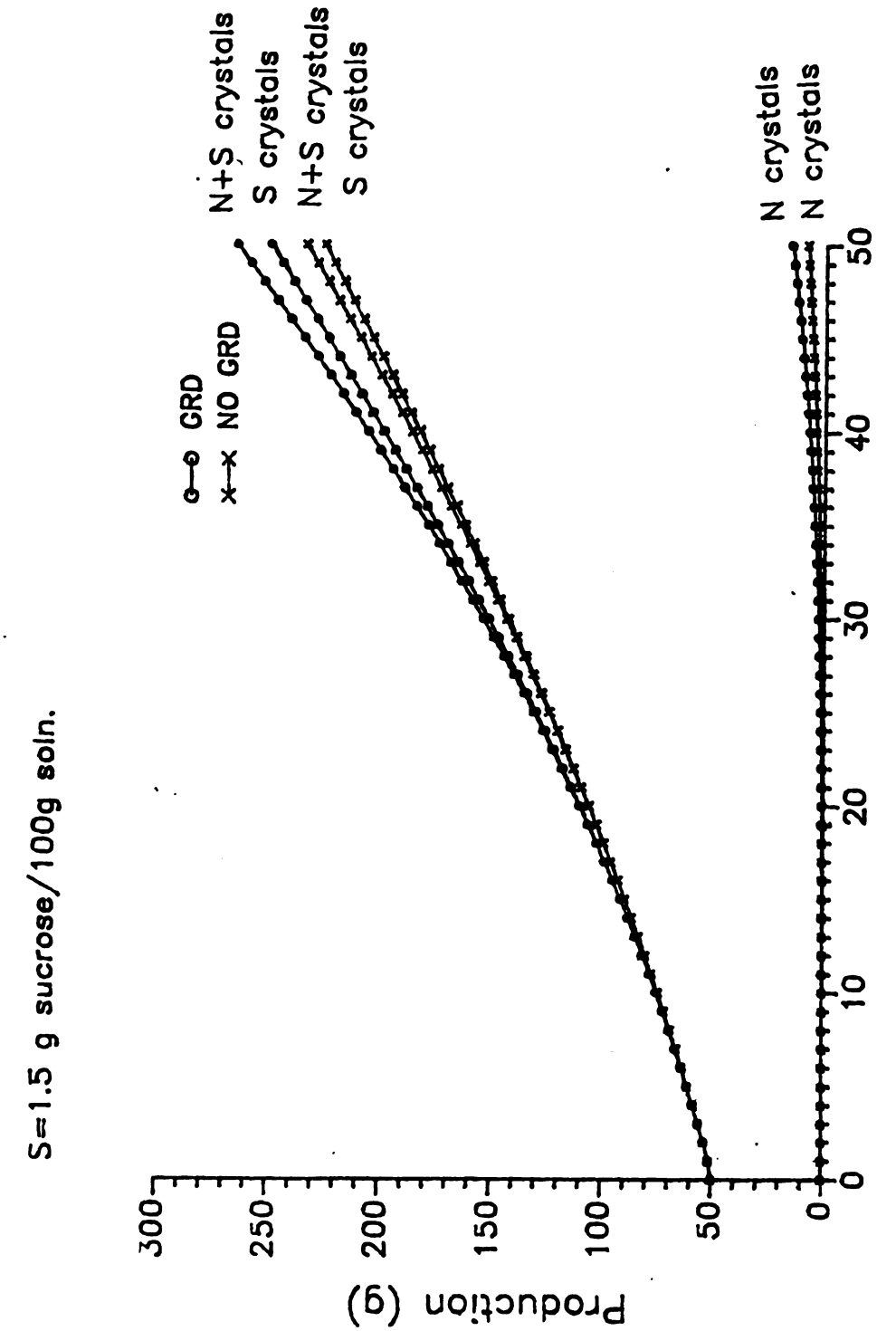

Figure 12. Production for N, S, and N+S crystals versus time for both GRD and no GRD at a constant level of supersaturation of 1.5 g sucrose/100 g soln in Example 2.

limited applicability of nucleation, growth rate, and growth rate dispersion kinetics. The effects of GRD on these product performances are also expected to be more significant during a longer time period as in Example 1.

4.6 Conclusions

In a seeded batch crystallizer with nucleation, the following conclusions can be drawn for the cases studied.

1. In general, smaller mean crystal sizes on a number basis are produced in the case of GRD than those in the case of no GRD for S, N, and S+N crystals.
2. The production tends to be larger in the case of GRD than those in the case of no GRD for S, N, and S+N crystals.
3. Coefficient of variation on a number basis in the case of GRD is always greater than that in the case of no GRD for S, N, and S+N crystals. The presence of GRD will result in a wider CSD for S, N, and S+N crystals.

4.7 Nomenclature

A = frequency factor, μm/min

a,b = correlation constants

$B^0(t)$ = nucleation rate at time t, nuclei/cm^3-min

C(t) = solute concentration at t, g solute/100 g soln

C*(t) = saturated solute concentration at t, g solute/100 g soln

C.V. = coefficient of variation

E_G = activation energy, cal/g-mole

$f_G(t;g)$ = probability density function for growth rate at t

$f_{L_{N_o}}(t;\ell_{N_o})$ = probability density function for birth size of N crystals at t

$f_{L_{s_o}}(0;\ell_{s_o})$ = probability density function for initial size of S crystals at t=0

$\bar{G}(T)$ = mean linear growth rate at T, μm/min

$g(t)$ = individual linear growth rate at t, μm/min

I = nucleation rate order w.r.t. M_T

J = nucleation rate order w.r.t. S

k_N = nucleation rate parameter

k_V = volume shape factor

$\ell_{N_o}(t)$ = birth size of N crystals generated at t, μm

$\ell_{s_o}(0)$ = initial size of S crystals initially charged into crystallizer t=0

$M_G(t;j)$ = the normalized jth moment of growth rate distribution about the origin at t

$M'_{L_N}(T;j)$ = the jth moment of all the N crystals, generated from 0 to T, about the origin at T

$M_{L_N}(T;j)$ = the normalized jth moment of all the n crystals, generated from 0 to T, about the origin at T

$M_{L_{N_o}}(t;j)$ = the normalized jth moment of all the N crystals, generated at t, about the origin

$M'_{L_s}(T;j)$ = the jth moment of all the S crystals, charged into crystallizer at t=0, about the origin at T

$M_{L_s}(T;j)$ = the normalized jth moment of all the S crystals, charged

into crystallizer at t=0, about the origin at T

$M_{L_{s_o}}(0;j)$ = the normalized jth moment of all the S crystals, charged into crystallizer at t=0, about the origin at t=0

$M_{L_{N+S}}(T;j)$ = the normalized jth moment of all the N+S crystals in the crystallizer about the origin at T

M_T = suspension density for N and S crystals at t, g/cm^3

m = crystal growth rate order

$Num_{N+S}(t)$ = number of N+S crystals per unit volume at t

$N_N(t)$ = number density of N crystals at t, #/cm-cm^3

$N_S(t)$ = number density of S crystals at t, #/cm-cm^3

R = ideal gas constant, 1.987 cal/g-mole ^oK

S(t) = supersaturation (=c(t) - c* (t)) gm solute/100 gm soln

TEMP = temperature, ^oK

V(t) = free liquor volume, cm^3

V_T = crystallizer volume, cm^3

W_S = seed loading, g

$W_2(o)$ = initial solute in the crystallizer, g

$W_2(t)$ = solute in the crystallizer at t, g

Greek Letters

$\alpha(t)$, B(t) = parameters in Gamma distribution at t

ρ = crystal density, g/cm^3

$\sigma_G^2(t)$ = variance of growth rate distribution at t, $\mu m^2/min^2$

4.8 Literature Cited

Bates, F.J., Polariemtry, Saccharimetry and the Sugars, U.S.Government Printing Off., Washington, DC (1942).

Berglund, K.A.; deJong, E.J., accepted for publication by AIChE Journal

(1988).

Berglund, K.A.; Larson, M.A., "Growth and Growth Dispersion of Contact Nuclei," paper presented at 2nd World Cong. Chem. Eng., Montreal (1981).

Berglund, K.A.; Larson, M.A., AIChE J., 1984, 30(2), 280.

Berglund, K.A.; Kaufman, E.L.; Larson, M.A., AIChE J., 1983, 29(5), 867.

Berglund, K.A., "Growth and Size Distribution Kinetics for Sucrose Crystals in the Sucrose-Water System," M.S. Thesis, Colorado State U., Fort Collins, Colorado (1980).

Berglund, K.A.; Murphy, V.G., Ind. Eng. Chem. Fundam., 1986, 25, 174.

Garside, J.; Ristic, R.I., J. Cryst. Growth, 1983, 61, 215.

Hartel, R.W., "A Kinetic Study of the Nucleation and Growth of Sucrose Crystals in a Continuous Cooling Crystallizer," Ph.D. Dissertation, Colorado State U., Fort Collins, Colorado (1980)

Jones, A.G.; Mullin, J.W., Chem. Eng. Sci., 1974, 29, 105.

Lakatos, B.; Varga, E; Halasz, S; Blickle, T,"Simulation of Batch Crystallizer," Industrial Crystallization 84, edited by S.J. Jancic and E.J. deJong, Elsevier Science Publishers B.B., Amsterdam, 1984 - Printed in The Netherlands, p185.

Larson, M.A.; White, E.T.; Ramanarayanan, K.A., Berglund, K.A., AIChE J., 1985, 31(1), 90.

Mathis-Lilley, J.J.; Berglund, K.A., AIChE J. 1985, 31(5), 865.

Melikhov, I.V.; Berliner, L.B., Chem. Eng. Sci., 1981, 36, 1021.

Ramanarayanan, K.A., "Production and Growth of Contact Nuclei," Ph.D. Dissertation, Iowa State U., Ames, Iowa (1982).

Ramanarayanan, K.A.; Athreya, K; Larson, M.A., AIChE Sym. Ser., 1984, 80(240), 76.

Randolph, A.D.; White, E.T., Chem. Eng. Sci., 1977, 32, 1067.

Randolph, A.D.; Tan, C.S., Ind. Eng. Chem. Process Des., 1978, 17(2), 189.

Shanks, B.H.; Berglund, K.A., AIChE J., 1985, 31(1), 152.

Shiau, L.D.; Berglund, K.A., AIChE J., 1987, 33(6), 1028.

Shiau, L.D.; Berglund, K.A., Ind. Eng. Chem. Res., 1987, 26, 2515.

Zumstein, R.C.; Rousseau R.W., AIChE J., 1987, 33(1), 121.

CHAPTER 5

RECOVERY OF NUCLEATION AND GROWTH RATES FROM A BATCH FRUCTOSE CRYSTALLIZER*

5.1 Abstract

A method for determining nucleation and growth rates from a batch crystallizer in the presence of growth rate dispersion during constant nucleation and growth is presented, The analysis is based on the assumption that individual crystals have inherent constant growth rates, but the growth rate may vary from crystal to crystal, resulting in a distribution of growth rates. Even a limited knowledge of only the mean and variance of the crystal size distribution permits an approximation of the mean and variance of the growth rate distribution. Batch fructose experiments were analyzed to recover the growth and nucleation rates from the size distribution data through this analysis.

5.2 Introduction

The phenomenon of growth rate dispersion (GRD) is a significant factor in the establishment of the crystal size distribution (CSD) in crystallizers. Two methods of modeling GRD have been presented in the literature. The first, in which it is assumed that the growth rate of an individual crystal flucturates in the course of time is referred to as the random fluctuation (RF) model (Randolph and White, 1977). In the second, based on the contact nucleation studies of Berglund and

* a paper submitted to AIChE Journal

Larson (1981), Ramanarayanan (1982), and Berglund et al. (1983), it is assumed that individual crystals haven inherent, constant growth rates, but different crystals have different inherent growth rates. This model will be referred to as the constant crystal growth (CCG) model.

The phenomenon of RF was only observed in a very few studies for very long time periods up to 15 days (Garside, 1985). However, the CCG model was found to be applicable in a number of systems for periods of a few hours (Garside, 1985; Berglund, 1986; Shiau and Berglund,1987 ; Chu et al.,1988) through the photomicroscopic technique developed by Garside and Larson (1978). Berglund (1986) concluded that GRD is a widespread phenomenon in contact nuclei of soluble materials and the CCG model applies in both inorganic and organic aqueous systems as well as those systems with large and small metastability.

Recent modeling studies have been performed based on these results. The statistical-mathematical model presented by Ramanarayanan et al. (1984) and Zumstein and Rousseau (1987) can be used to recover growth kinetics from the resulting CSD in a batch crystallizer. The limitation is that the model only allows the calculations for the case of a seeded crystallizer with no subsequent nucleation. Those seeds could be charged into the crystallizer (Berglund and Murphy, 1986) or be generated by dropping a rod on a well-faced parent crystal (Blem and Ramanarayanan, 1987).

Recently Shiau and Berglund (1988) developed a model based on the CCG model to relate the resulting CSD for both seeds and nuclei from a seeded batch crystallizer with non-negligible nucleation to the seed size distribution, the initial size distribution of subsequently generated nuclei and the growth rate distribution. The model allows recovery of the growth and nucleation rates from batch crystallizer

data where nuclei are generated by contact nucleation. The objective of this paper is to demonstrate the application of the model to recover growth and nucleation rates from batch crystallization experiments with pure and glucose-containing aqueous fructose solutions. The results will be compared with the unstirred solution studies from photomicroscopic experiments (Shiau and Berglund, 1987; Chu et al., 1988).

5.3 Determining Growth and Nucleation Rates in Presence of Growth Rate Dispersion

In order for the model presented by Shiau and Berglund (1988) for a batch crystallizer to be applicable, it is imperative that contact nuclei of fructose follow the CCG model. The photomicroscopic studies by Shiau and Berglund (1987) and Chu et al. (1988) have confirmed that fructose crystals formed by contact nucleation follows the constant crystal growth (CCG) model for the pure fructose solution and for the fructose solution in presence of glucose.

For nuclei generated in a seeded batch crystallizer, Shiau and Berglund (1988) have developed

$$M_L(T;j) = \frac{1}{\int_0^T B^o(t)dt} \cdot \int_0^T \left\{ B^o(t) \cdot \sum_{r=0}^{j} \binom{j}{r} \cdot M_{L_o}(t;j-r) \cdot \left[\int_t^T M_G(\theta;r)^{\frac{1}{r}} d\theta \right]^r \right\} dt \qquad (1)$$

Here, $M_L(T;j)$ is the normalized jth moment of all the nuclei about the origin of CSD at T, $M_{L_o}(t;j-r)$ is the normalized (j-r)th moment of the

nuclei generated at t about the origin of CSD, and $M_G(\theta;r)$ is the normalized rth moment of growth rates about the origin of GRD at time θ, where

$$M_L(T;j) = \int_0^\infty \ell^j \cdot f_L(T;\ell)d\ell \tag{2}$$

$$M_{L_o}(t;j-r) = \int_0^\infty \ell_o^{j-r} \cdot f_{L_o}(t;\ell_o)d\ell_o \tag{3}$$

$$M_G(\theta;r) = \int_0^\infty g^r \cdot f_G(\theta;g)dg \tag{4}$$

$f_L(T;\ell)$ and $f_{L_o}(t;\ell_o)$ represent the normalized CSD of nuclei at time T and the normalized birth size distribution of nuclei generated at time t, respectively. $f_G(\theta;g)$ represents the normalized distribution of growth rates for the nuclei at time θ.

In the case of constant nucleation and growth condition, the Equation 1 reduces to

$$M_L(j) = \sum_{r=0}^{j} \binom{j}{r} \cdot M_{L_o}(j-r) \cdot M_G(r) \cdot \frac{1}{r+1} \cdot T^r \tag{5}$$

Here, $M_L(T;j)$, $M_{L_o}(t;j)$ and $M_G(\theta,j)$ are replaced with $M_L(j)$, $M_{L_o}(j)$ and $M_G(j)$ since these functions are no longer time-dependent.

A variety of birth size distribtutions of nuclei for constant nucleation and growth will be discussed in the following.

Case 1: Nuclei are born at zero size.

Thus, Equation 5 reduces to

$$M_L(j) = \frac{1}{j+1} \cdot M_G(j) \cdot T^j \tag{6}$$

For j=1 and j=2

$$M_L(1) = \frac{1}{2} \cdot M_G(1) \cdot T \tag{7}$$

and

$$M_L(2) = \frac{1}{3} \cdot M_G(2) \cdot T^2 \tag{8}$$

knowing that $M_G(1) = \bar{G}$ (9)

and

$$M_G(2) = \bar{G}^2 + \sigma_G^2 \tag{10}$$

yields $M_L(1) = \bar{L}$ (11)

and

$$M_L(2) = \bar{L}^2 + \sigma_L^2 \tag{12}$$

Equations 7 and 8 can be written as

$$\bar{L} = \frac{1}{2} \cdot \bar{G} \cdot T \tag{13}$$

$$\bar{L}^2 + \sigma_L^2 = \frac{1}{3} \cdot T^2 \cdot (\bar{G} + \sigma_G^2) \tag{14}$$

Therefore, a plot of $\bar{L}$ versus $\frac{T}{2}$ passes through the origin with a slope of $\bar{G}$. Furthermore, a plot of $\bar{L} + \sigma_L^2$ versus $\frac{T^2}{3}$ passes through the origin with a slope of $\bar{G} + \sigma_G^2$. Therefore, $\bar{G}$ and σ_G^2 can be determined from the CSD data.

For a batch crystallizer without agglomeration and particle breakage, the total number of crystals generated can be represented as

$$N = \int_0^T B^o(t)\, dt \tag{15}$$

at constant nucleation and growth conditions,

$$B^o = \frac{dN}{dT} \tag{16}$$

The nucleation rate can simply be evaluated from the rate of change of the total number of crystals.

Case 2: Nuclei are born at zero size and the smallest measurable size is Lmin.

In practical situations any kind of particle size analyzer has its smallest measurable size. Thus, nuclei have to grow up to Lmin to be measurable.

$$t_o = \frac{Lmin}{\bar{G}} \tag{17}$$

Here, $\bar{G}$ is the mean growth rate and t_o is the average time required for nuclei to grow into the smallest measureable size.

Starting with Equation 1 and taking t_o into consideration, Equation 1 can be modified for simplicity as

$$M_L'(j) \approx \frac{1}{\int_0^{T-t_o} B^o(t)dt} \cdot \int_o^{T-t_o} \left\{ B^o(t) \cdot \left[\int_t^T M_G(j)^{\frac{1}{j}} d\theta \right]^j \right\} dt$$

$$= \frac{1}{j+1} \cdot M_G(j) \cdot \frac{T^{j+1} - t_o^{j+1}}{T - t_o} \tag{18}$$

Here $M_L'(j)$ stands for the normalized jth moment of all the nuclei with sizes greater than Lmin about the origin of CSD at T.

For j=1 and j=2,

$$M_L'(1) = \frac{1}{2} \cdot M_G(1) \cdot (T+t_o) \tag{19}$$

and

$$M_L'(2) = \frac{1}{3} \cdot M_G(2) \cdot (T^2+T \cdot t_o+t_o^2) \tag{20}$$

Substituting Equations 9,10,11,12,and 15, Equations 17 and 18 can be written as

$$\bar{L}' = \frac{Lmin}{2} + \frac{\bar{G} \cdot T}{2} \tag{21}$$

$$\bar{L}'^2 + \sigma_{L'}^2 = \frac{(T^2+T \cdot t_o+t_o^2)}{3} (\bar{G}^2+\sigma_G^2) \tag{22}$$

Here, $\bar{L}'$ and $\sigma_{L'}^2$ are the mean size and the variance of nuclei distribution with sizes greater than Lmin at T.

Therefore, a plot of $\bar{L}' - \frac{Lmin}{2}$ versus $\frac{T}{2}$ passes through the origin with a slope of $\bar{G}$. Once $\bar{G}$ is determined, t_o can be calculated from Equation 17. Then, a plot of $\bar{L}'^2 + \sigma_{L'}^2$ versus $\frac{T^2+T \cdot t_o+t_o^2}{3}$ passes through the origin with a slope of $\bar{G} + \sigma_G^2$. As in case 1, the growth parameters can be estimated from the CSD data.

The smallest particle capable of accurate detection by the size analysis technique is Lmin, and thus total crystal counts give only N', the number of crystals with size greater than Lmin.

$$N' \approx \int_0^{T-\frac{Lmin}{G}} B^o_{eff}(t)\, dt \tag{23}$$

In constant nucleation and growth condition,

$$N' \approx B^o_{eff} \cdot \left(T - \frac{Lmin}{G} \right) \tag{24}$$

Therefore,
$$B^o_{eff} \approx \frac{dN'}{dT} \tag{25}$$

The nucleation rate can thus be approximately evaluated from the rate of change of the total number of crystals greater than Lmin. This gives an effective nucleation rate which is analogous to the one reported in linear extraplolation of data from contiuuous crystallizers (Hartel et al., 1980; Kuijvenhoven and deJong, 1982).

Case 3: Nuclei are born with an initial size distribution, and all are greater than Lmin.

Under the above assumption, Equation 1 reduces to

$$M_L(j) = \sum_{r=0}^{j} \binom{j}{r} \cdot M_{L_o}(j-r) \cdot M_G(r) \cdot \frac{1}{r+1} \cdot T^r \tag{26}$$

For j=1 and j=2

$$M_L(1) = M_{L_o}(1) + \frac{1}{2} \cdot M_G(1) \cdot T \tag{27}$$

and

$$M_L(2) = M_{L_o}(2) + M_{L_o}(1) \cdot M_G(1) \cdot T + \frac{1}{3} \cdot M_G(2) \cdot T^2 \tag{28}$$

Substituting Equations 9,10,11 and 12, and knowing

$$M_{L_o}(1) = \bar{L}_o \tag{29}$$

$$M_{L_o}(2) = \bar{L}_o^2 + \sigma_{L_o}^2 \tag{30}$$

Equations 31 and 32 can be written as

$$\bar{L} = \bar{L}_o + \frac{1}{2} \cdot \bar{G} \cdot T \tag{31}$$

$$\bar{L}^2 + \sigma_L^2 = \bar{L}_o^2 + \sigma_{L_o}^2 + \bar{L}_o \cdot \bar{G} \cdot T + \frac{1}{3} \cdot T^2 \cdot (\bar{G} + \sigma_G^2) \tag{32}$$

Therefore, a plot of $\bar{L}$ versus $\frac{T}{2}$ has a slope of $\bar{G}$ and an intercept of $\bar{L}_o$. A plot of $\bar{L}^2 + \sigma_L^2 - \bar{L}_o^2 - \bar{L}_o \cdot \bar{G} \cdot T$ versus $\frac{T^2}{3}$ has a slope of $\bar{G}^2 + \sigma_G^2$ and an intercept of $\sigma_{L_o}^2$.

Since all nuclei are born with sizes greater Lmin, the total particle counts give N , all the particles present. Therefore,

$$B^o = \frac{dN}{dT} \tag{33}$$

<u>Case 4</u>: Nuclei are born with an initial size distribution, and $\bar{L}_o$ is smaller than Lmin. (In the case that $\bar{L}_o$ is greater than Lmin, it will be treated as the same as case 3 for simplicity.) Therefore,

$$t_o = \frac{\text{Lmin} - \bar{L}o}{\bar{G}} \tag{34}$$

Here, $\bar{G}$ is the mean growth rate, $\bar{L}_o$ is the mean birth size of nuclei and t_o is the average time required for nuclei of size $\bar{L}_o$ to grow into the smallest measureable size.

Starting with Equation 1 and taking t_o into consideration, the model equation can be approximately simplified as

$$M_L'(j) \approx \frac{1}{\int_0^{T-t_o} B^o(t)dt} \cdot \int_t^{T-t_o} \left[B^o(t) \cdot \sum_{r=0}^{j} \binom{j}{r} \cdot M_{L_o}(j-r) \cdot \left[\int_t^T M_G(r)^{\frac{1}{r}} d\theta \right]^r \right] dt$$

$$- \sum_{r=0}^{j} \binom{j}{r} \cdot M_{L_o}(j-r) \cdot M_G(r) \cdot \frac{1}{r+1} \cdot \frac{T^{r+1} - t_o^{r+1}}{T-t_o} \tag{35}$$

Here $M_L'(j)$ stands for the normalized jth moment of all the nuclei with sizes greater than Lmin about the origin of CSD at T.

For j=1 and j=2,

$$M_L'(1) = M_{L_o}(1) + \frac{1}{2} \cdot M_G(1) \cdot (T+t_o) \tag{36}$$

and

$$M_L'(2) = M_{L_o}(2) + M_{L_o}(1) \cdot M_G(1) \cdot (T+t_o) + \frac{1}{3} \cdot M_G(2) \cdot (T^2+T \cdot t_o+t_o^2) \tag{37}$$

Substituting Equations 9,10,11,12,24,25 and 28, Equations 30 and 31 can be written as

$$\bar{L}' = \frac{Lmin + \bar{L}_o}{2} + \frac{\bar{G} \cdot T}{2} \tag{38}$$

$$\bar{L}'^2 + \sigma_{L'}^2 = \bar{L}_o^2 + \sigma_{L_o}^2 + \bar{L}_o \cdot \bar{G} \cdot (T + t_o) + \frac{(T^2 + T \cdot t_o + t_o^2)}{3} \cdot (\bar{G}^2 + \sigma_G^2) \quad (39)$$

Therefore, a plot of $\bar{L}' - \frac{Lmin}{2}$ versus $\frac{T}{2}$ has a slope of $\bar{G}$ and an intercept of $\frac{L_o}{2}$. Once $\bar{G}$ is determined, t_o can be calculated from Equation 34. Then, a plot of $\bar{L}'^2 + \sigma_{L'}^2 - \bar{L}_o^2 - \bar{L}_o \cdot \bar{G} \cdot (T + t_o)$ versus $\frac{T^2 + T \cdot t_o + t_o^2}{3}$ has a slope of $\bar{G} + \sigma_G^2$ and an intercept of $\sigma_{L_o}^2$.

In this case, the total crystal counts give only N', the number of crystals with size greater than Lmin.

$$N' \approx \int_0^{T - \frac{Lmin - \bar{L}_o}{\bar{G}}} B^o_{eff}(t)\, dt \quad (40)$$

In the case of constant growth and nucleation condition,

$$N' \approx B^o_{eff} \cdot \left(T - \frac{Lmin - \bar{L}_o}{\bar{G}} \right) \quad (41)$$

Therefore,

$$B^o_{eff} \approx \frac{dN'}{dT} \quad (42)$$

The effective nucleation rate can thus be evaluated from the rate of change of the total number of crystals grater than Lmin.

5.4 Experimental Procedure

A series of batch experiments were performed in a 1.0-liter agitated, baffled vessel. The crystallizer was immersed in a constant-temperature bath and all runs were carried out isothermally. Initial

supersaturation was achieved by slow cooling of a solution saturated at an elevated temperature. When the working temperature was attained, 10 grams of presized (200-500μm) and cured seeds were charged into the crystallizer. Seed size was chosen such that growing seed crystals would at least an order of magnitude larger than nuclei. The current study concentrated on the analysis of the nuclei generated only. The seeds were cured by keeping them in a small amount (about 50 ml) of solution saturated at the working temperature prior to the experiments to prevent secondary nucleation by initial breeding. The beaker containing the seeds and solution was preheated 5^{o}C above the saturation temperature of the solution for about 20 minutes. The seeds dissolved slightly since the solution was undersaturated at this condition. The solution containing seeds was cooled to the working temperature and charged into the crystallizer at the start of the run. The impeller speed was kept at 480 r.p.m., which was observed adequate to keep the seeds uniformly dispersed in the solution. Small volume samples of the solution were removed from the crystallizer to determine the particle counts and the CSD of the nuclei through image analysis at regular intervals during the course of the run. Sample measurements were taken within 10-20 hours depending on the supersaturation and impurity ratio so as not to change the supersaturation drastically. The experimental conditions are given in Table 1.

5.5 Data Analysis

Hartel (1980) analyzed the CSD of aqueous sucrose solution with an Coulter counter with an appropriate electrolyte. Attempts failed in developing a proper electrolyte to determine the CSD from fructose

solutions. The generation of bubbles, which could be counted as particles in Coulter Counter, could not be avoided during the handling of the sample due to the extremely high viscosity of the aqueous fructose solution.

A cell (shown in Figure 1) was found to be appropriate in analyzing the data with an image analyzer. Pictures were taken of the crystals contained in the solution chamber. The volume of the solution taken in a picture was estimated by the area of the picture multiplied by the thickness of the solution chamber (about 500 μm). Therefore, the number of nuclei per unit volume and the mean and variance of the CSD of the nuclei were determined. The raw data obtained from each experiment consisted of a series of photographs at various times. The negatives of the photographs were projected to enlarge them for measurement. An image analyzer was used to determine the area of each crystal in the enlargement. The characteristic size was taken as the equivalent circular diameter, which could be transformed to the geometric mean size by multiplying by $\sqrt{\pi}/2$.

The smallest measurable size for the image analyzer under 100x magnification was taken as 5μm. Nuclei were considered born at near zero size, so the analysis in case 2 was applied to determine the growth kinetics and nucleation rate for each experimental condition.

5.6 Results and Discussion

Growth Kinetics

Figure 2 shows an example of $\bar{L}' - \frac{L_{min}}{2}$ plotted versus $\frac{T}{2}$ with the slope equal to $\bar{G}$ and Figure 3 shows an example of $\bar{L}'^2 + \sigma_{L'}^2$ plotted

versus $\frac{T^2+T\cdot t_o+t_o^2}{3}$ with the slope equal to $\bar{G} + \sigma_G^2$ for pure fructose solution at 3°C supercooling at 40°C. It is evident, and confirmed by high correlation coefficients, that linear relations exist in these two figures as derived from the analysis in case 2.

The effects of glucose on growth kinetics of fructose crystals were also examined. Glucose was added to pure fructose solution at various impurity/water ratios (I/W). Plots similar to figure 2 and 3 were made for the fructose solutions at various levels of impurity and degrees of supercooling at 40°C. $\bar{G}$ and σ_G^2 were determined at each experimental conditions from those plots.

Figure 4 shows the comparison of the mean growth rates obtained from the batch crystallization experiments for different levels of impurity at 40° with the results determined from the photomicroscopic studies for pure fructose solutions (Shiau and Berglund, 1987) and glucose-containing fructose solutions (Chu et al., 1988). As seen in the figure, they are in good agreement. This agreement between such different experiments is probably due to the high viscosity of the fructose solutions such that the stirring provided by the impeller in the batch crystallizer does not affect its volume diffusion limitation during the process of crystallization. (In fact, those small nuclei might essentially flow around the crystallizer with the solution, i.e. the relative motion between nuclei and solution may be negligible.)

The solubility data were taken from circular C440 of the National Bureau of Standards (Bates, 1943). Since the effects of glucose on fructose solubility are not clear, the same definition for

Table 1. Range of experimental variables for the batch fructose experiments.

Operating temperature (^{o}C)	40
Stirrer speed (r.p.m.)	480
Relative supersaturation	0.003 ~ 0.042
Impurity ratio, glucose/water (g/g)	0 ~ 0.9
Seeding charge (g)	10
Seed size (μm)	200 - 500
Run time (hr)	10 - 20

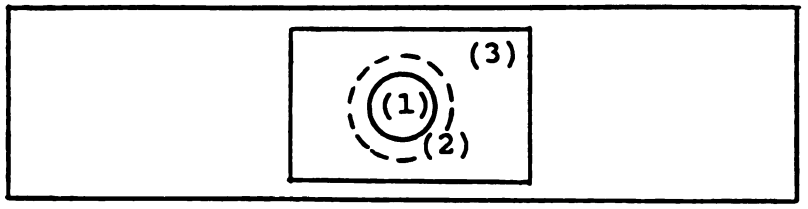

Top View

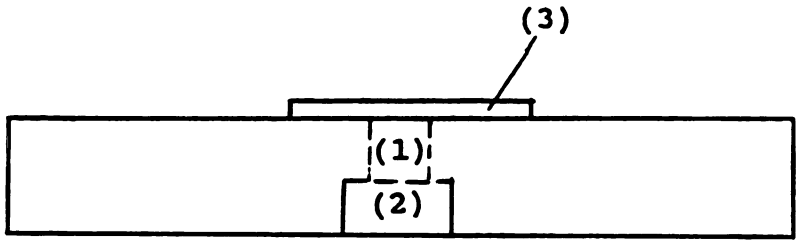

Side View

Figure 1. Schematic diagram of the cell
(1) chamber containing solution
(2) fixed transparent glass
(3) movable cover glass

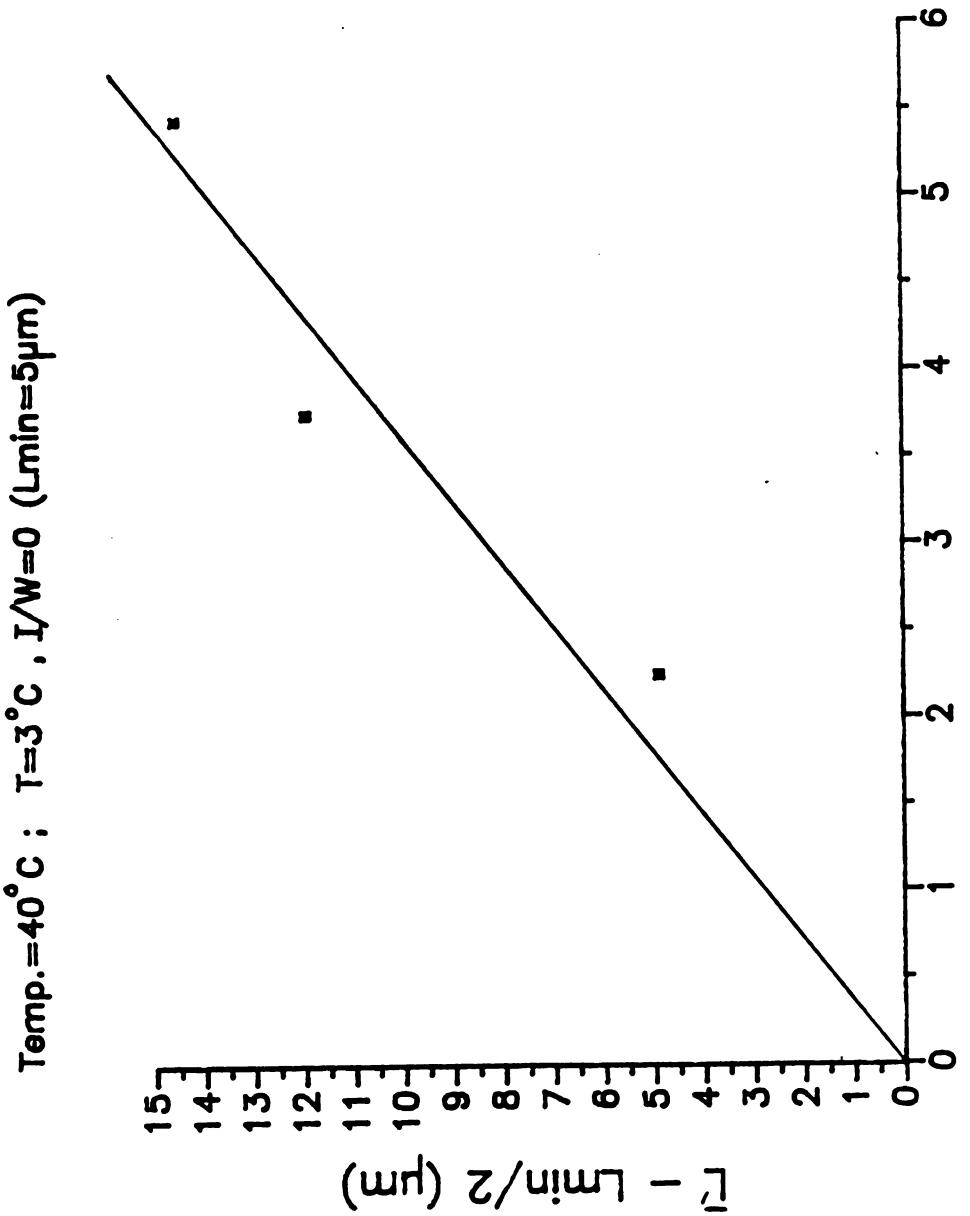

Figure 2. An Example of $\bar{L}'$ - Lmin/2 vs. T/2 data for contact nuclei formed during the batch crystallization.

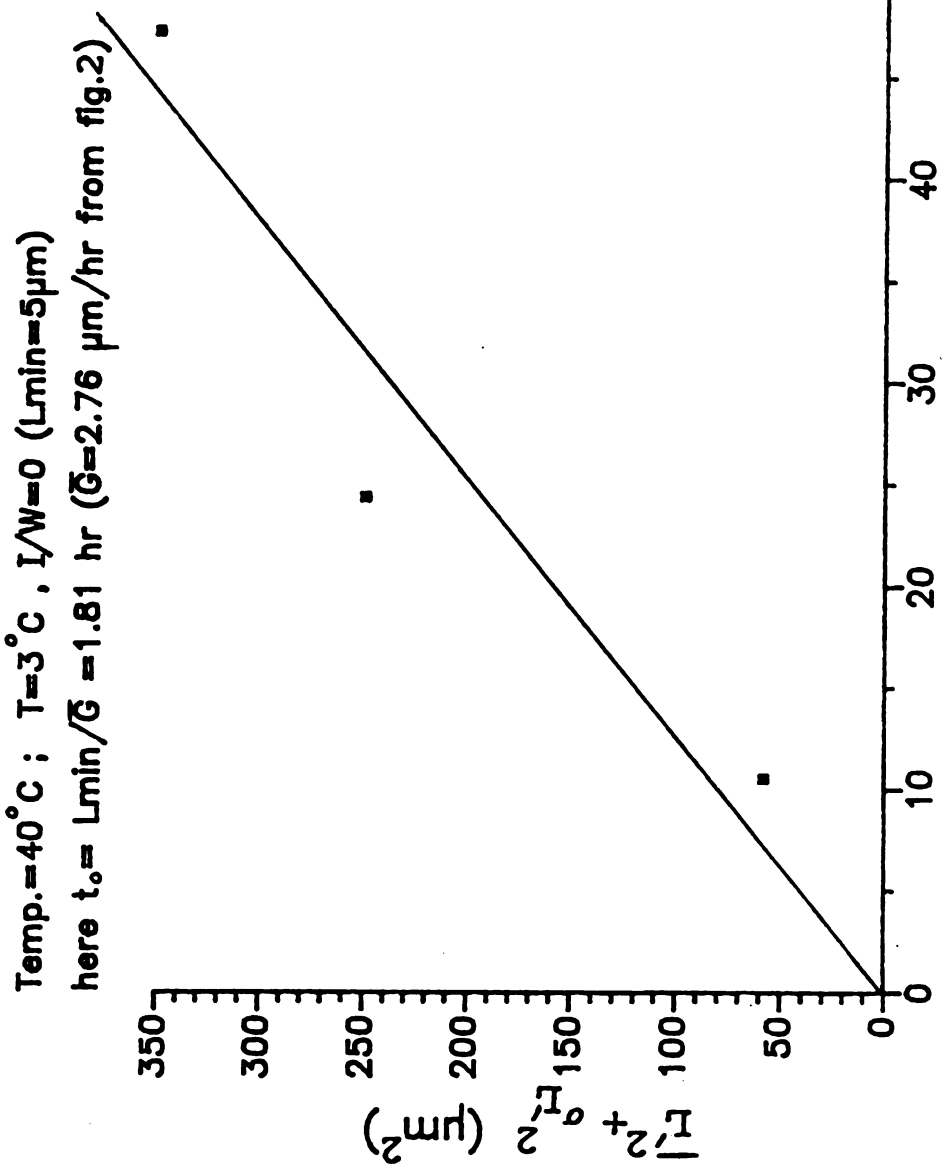

Figure 3. An Example of $\bar{L}'^2 + \sigma_{L'}^2$ vs. $(T^2+T\cdot t_o+t_o^2)/3$ data for contact nuclei formed during the batch crystallization.

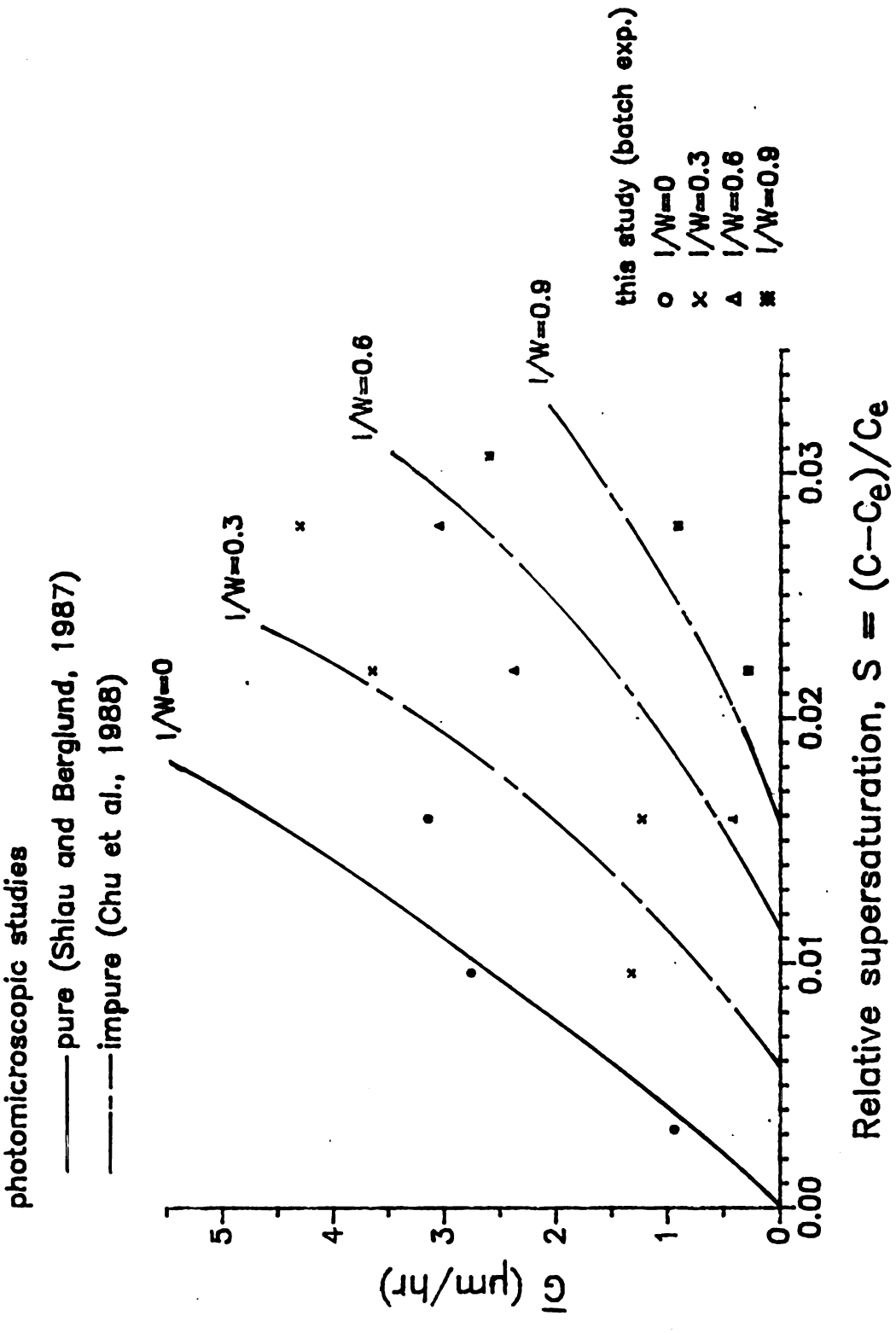

Figure 4. Comparison of the mean growth rates obtained from the batch experiments with the results from the photomicroscopic studies.

relative supersaturation is used in the fructose solution with glucose, i.e. , as if the presence of glucose does not affect solubility of fructose in water. However, it was observed that nuclei could be generated and start to grow only when S reached a critical value at each condition, and that critical value of S increased as I/W was increased. This phenomenon indicates an increase of solubility at increase of I/W, which is consistent with the results from the photomicroscopic studies (Chu et al.,1988).

The variances of growth rates were plotted against mean growth rates for each experimental condition for comparison with the results obtained from the photomicroscopic studies from pure fructose solutions (Shiau and Berglund, 1987) and glucose-containing fructose solutions (Chu et al., 1988) in Figure 5. The data from the batch experiments were comparable but quite widely scattered compared to the results from the photomicroscopic studies. The scatter is probably due to the limited nuclei data used for analysis in these batch experiments. The variances of growth rate distributions in the photomicroscopic studies were determined from the growth rate distributions of the nuclei generated by contact nucleation through sliding a parent crystal against a glass plate. However, the variances in the batch experiments were predicted from the change of the means and variances of the nuclei generated constantly by contact nucleation through the stirring of the impeller in the solutions; therefore, a sufficicient amount of nuclei data is critical to represent the true mean and variance of the sizes of the nuclei generated constantly in the solutions.

Unlike photomicroscopic experiments, in which the contacting is accomplished by sliding a parent crystal against cover glass without measuring the energy of contacting, the contacting of crystals is

caused by the impeller in the seeded solutions during the batch crystallization experiments. Since the energy of contact can be estimated from the stirring rate of the impeller in batch crystallization experiments, this could allow the effects of contact energy on mean growth rates and variances of growth rate distributions to be studied.

Nucleation

Fructose is most often crystallized from aqueous solutions as anhydrous crystals (cubic crystals). However, it has been reported that spherulitic aggregates of fine needles (hemihydrates) frequently crystallize from concentrated solution under some conditions (Young et al., 1952). The difficulties in handling these needle crystals render them unacceptable. The present studies showed the possible existence of three nucleation regions for various impurity ratios and relative supersaturations at 40°C as in Figure 6. It indicated that no nucleation occurred in section I. Anhydrous crystals could be generated and start to grow only when S reached its critical value at each value of I/W. These critical values of S increased as I/W was increased (section II). It was also observed that fructose hemihydrates crystallized from highly concentrated solutions as shown in section III. It was found that once hemihydrates formed, they dominated so that the nucleation and growth of anhydrous crystals drastically decreased. No attempts were made in these experiments to measure the nucleation and growth rate of hemihydrates.

Figure 7 shows the relationship between effevtive nucleation rate and mean growth rate for anhydrous fructose at 40°C. The effective

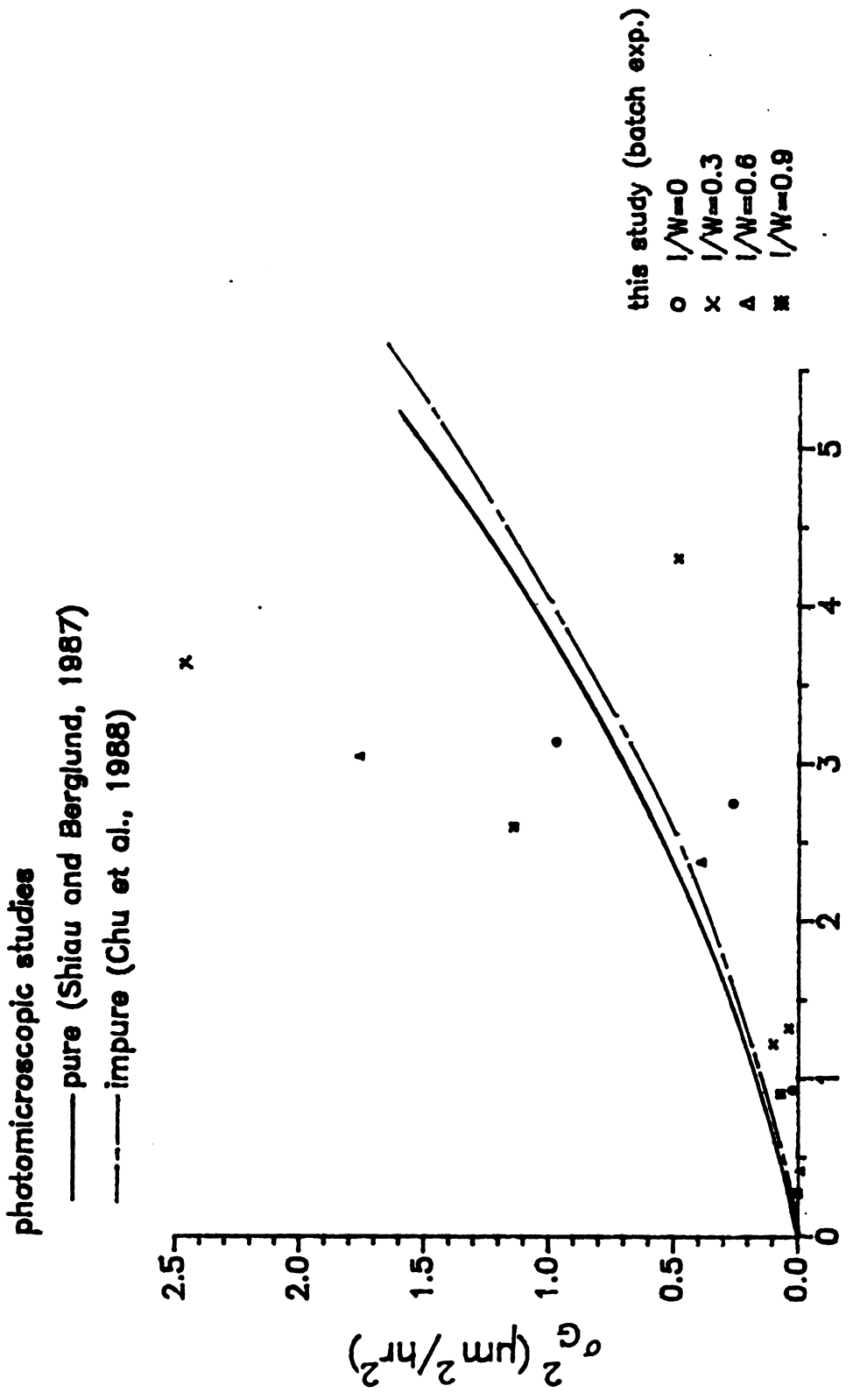

Figure 5. Comparison of the variances of growth rate distribution obtained from the batch experiments with the results from the photomicroscopic studies.

0.9

0.6

1/W

0.3

0.0

0.

Fi

Section I (△) : no nucleation occurred
Section II (o) : nucleation of anhydrous fructose occurred
Section III (x) : nucleation of fructose hemihydrates occurred and dominated

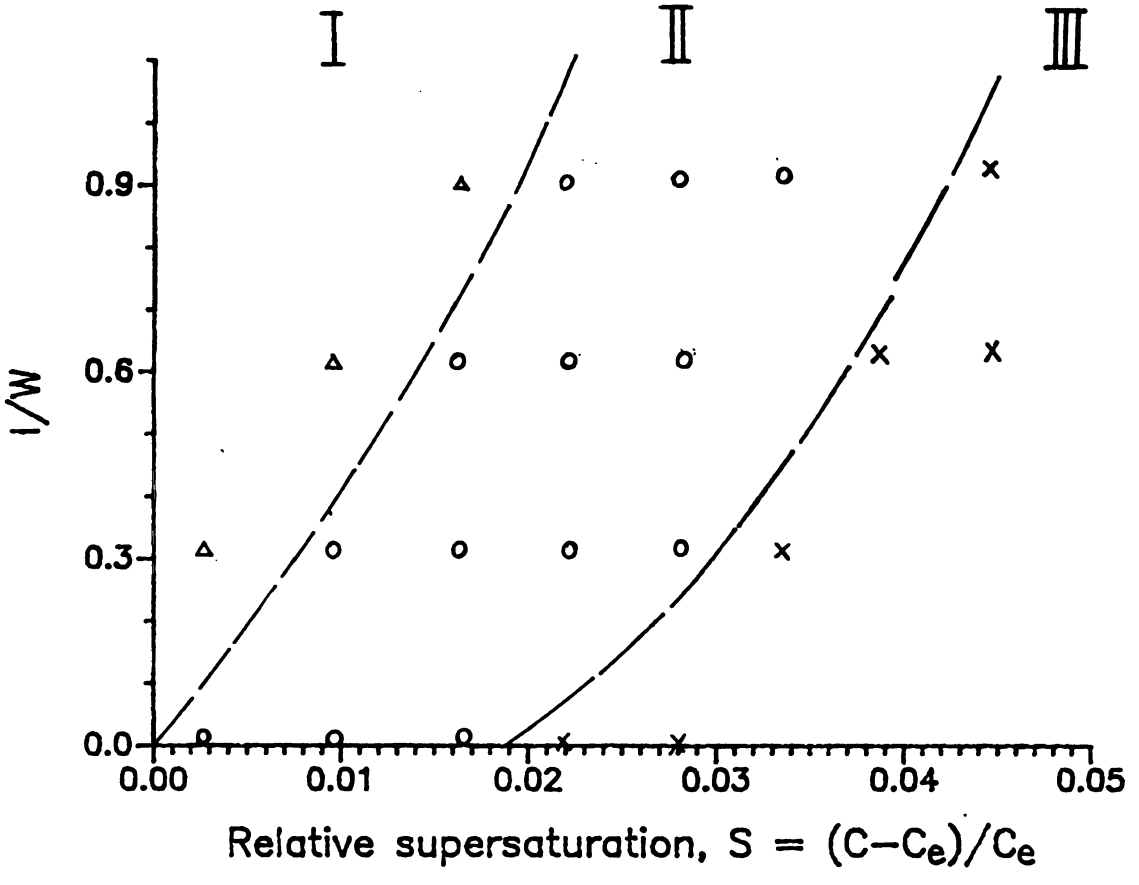

Figure 6. The existence of three nucleation regions for various impurity ratios and relative supersaturations in the batch experiments.

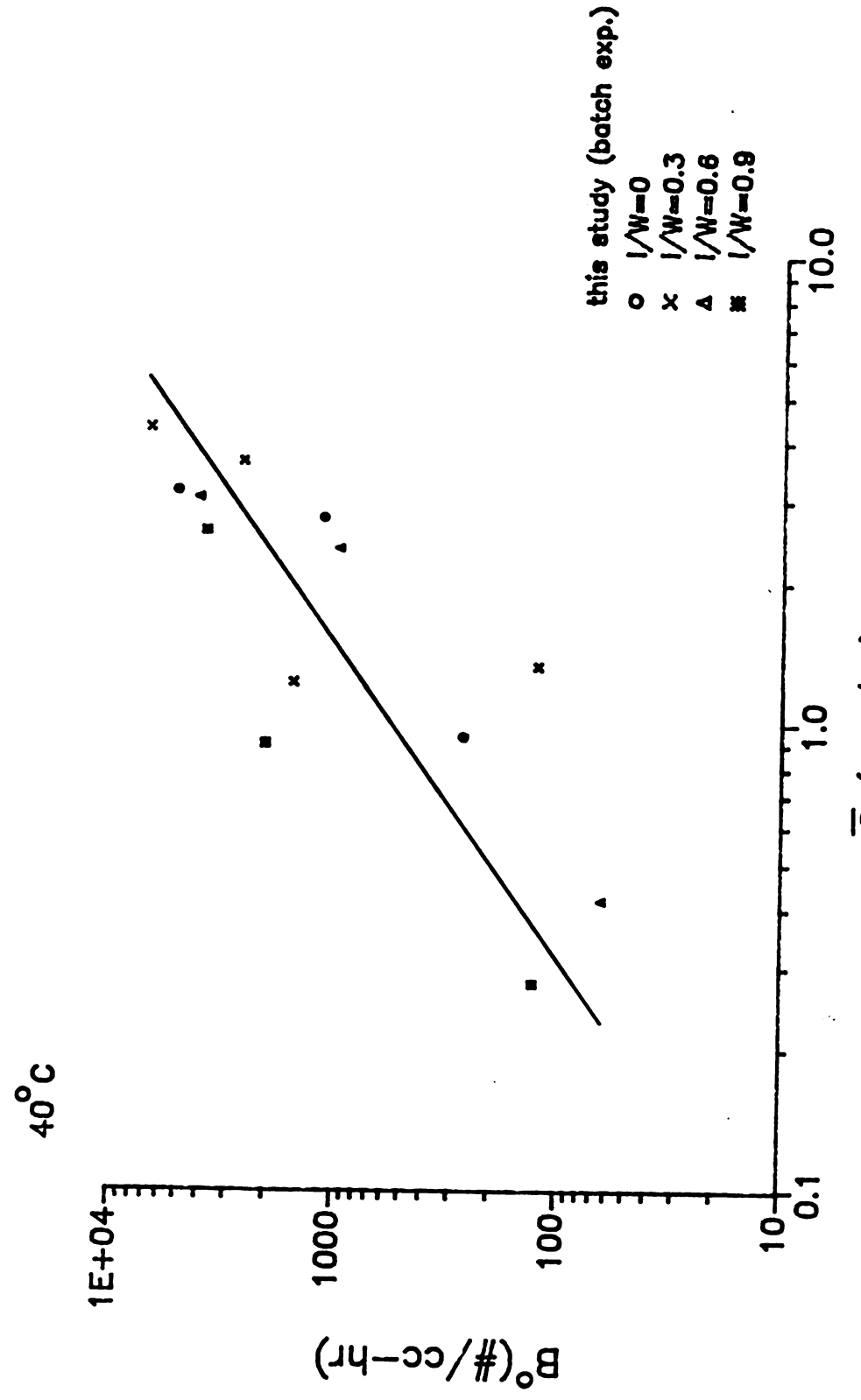

Figure 7. Nucleation rate of anhydrous fructose versus mean growth rate for the batch experiments.

nucleation rate was determined by Equation 25. Since the major effect of glucose on fructose crystal growth is the increase of solubility as seen in the present batch studies and the photomicroscopic studies (Chu et al., 1988), it would be reasonable to predict the similar phenomenon on the nucleation. The effective nucleation rate was correlated by an empirical power law expression with the mean growth rate

$$B^{o} = 5.0 \times 10^{2} \bar{G}^{1.5} \tag{43}$$

5.7 Conclusions

This analysis based on the model presented by Shiau and Berglund (1988) provides a simple method of recovering growth and nucleation rates from the resulting CSD of nuclei during a seeded batch crystallizer in the presence of GRD. The growth rates recovered from stirred batch fructose experiments through this analysis are in good agreement with the unstirred solution studies through the photomicroscopic technique (Shiau and Berglund, 1987 and Chu et al., 1988). The present studies show the possible existence of three nucleation regions for various impurity ratios and relative supersaturations at 40°: no nucleation in low supersaturated solution, nucleation of anhydrous crystals in moderately supersaturated solution, and formation of hemihydrates in highly supersaturated solution.

5.8 Nomenclature

$B^{o}(t)$ = nucleation rate at time t, nuclei/cm^3-hr

B^{o}_{eff} (t) = nucleation rate at t, nuclei/cm^3-hr

C = solute concentration, g solute/100 g soln

C* = saturated solute concentration, g solute/100 g soln

$f_G(t;g)$ = probability density function for growth rate at t

$f_L(t;\ell)$ = probability density function for birth size of crystals at t

$f_{L_o}(0;\ell_o)$ = probability density function for birth size of crystals at t=0

$\bar{G}$ = mean linear growth rate, μm/hr

$g(t)$ = individual linear growth rate at t, μm/hr

Lmin = smallest measurable size

$\bar{L}$ = mean of the crystal size distribution, μm

$\bar{L}'$ = mean of the crystal size distribution with size greater than Lmin, μm

$\bar{L}_o$ = mean of the birthl size distribution, μm

$\ell(t)$ = crystal size at t, μm

$\ell_o(t)$ = birth size of crystals, μm

$M_G(t;j)$ = the normalized jth moment of growth rate distribution about the origin at t

$M_L(T;j)$ = the normalized jth moment of all the crystals, generated from 0 to T, about the origin

$M_{L_o}(t;j)$ = the normalized jth moment of all the crystals, generated at t about the origin

$M_G(j)$ = the normalized jth moment of growth rate distribution about the origin

$M_{L'}(j)$ = the normalized jth moment of all the crystals greater than Lmin, generated from 0 to T, about the origin

$M_{L_o}(j)$ = the normalized jth moment of the birth size distribution about the origin

S = relative supersaturation, = (C - C*)/C*

T = time, hr

t = time, hr

t_o = the average time required for nuclei to grow into the smallest measureable size

Greek Letters

σ_G^2 = variance of growth rate distribution, $\mu m^2/hr^2$

σ_L^2 = variance of crystal size distribution, μm^2

$\sigma_{L'}^2$ = variance of crystal size distribution with sizes greater than Lmin, μm^2

$\sigma_{L_o}^2$ = variance of birth size distribution, μm^2

5.9 Literature Cited

Bates, F.J., Polariemtry, Saccharimetry and the Sugars, U.S. Government Printing Off., Washington, DC (1942).

Berglund, K.A.; Larsonn, M.A., "Growth and Growth Dispersion of Contact Nuclei," paper presented at 2nd World Cong. Chem. Eng., Montreal (1981).

Berglund, K.A., et al., AIChE J., 1983, 29(5), 867.

Berglund, K.A., Chem. Eng. Commun., 1986, 41, 357.

Berglund, K.A.; Murphy, V.G., Ind. Eng. Chem. Fundam., 1986, 25, 174.

Blem, K.E.; Ramanarayanan, K.A., AIChE J., 1987, 33(4), 677.

Chu , Y.D. et al., in preparation for publication

Garside, J., Chem. Eng. Sci., 1985, 40(1), 3.

Garside, J.; Larson, M.A., J. Cryst. Growth, 1978, 43, 694.

Hartel, R.W., "A Kinetic Study of the Nucleation and growth of Sucrose Crystals in a Continuous Cooling Crystallizer," Ph.D. Dissertation, Colorado State U., Fort Collins, Colorado (1980).

Young, F.E. et al., J. Phys. Chem., 1952, 56, 738.

Ramanarayanan, K.A., "Production and Growth of Contact Nuclei," Ph.D. Dissertation, Iowa State U., Ames, Iowa (1982).

Ramanarayanan, K.A. et al., AIChE Sym. Ser., 1984, 80(240), 76.

Randolph, A.D.; White, E.T., Chem. Eng. Sci., 1977, 32, 1067.

Shiau, L.D.; Berglund, K.A., AIChE J., 1987, 33(6), 1028.

Shiau, L.D.; Berglund, K.A., submitted for publication.

Zumstein, R.C.; Rousseau R.W., AIChE J., 1987, 33(1), 121.

CHAPTER 6

A MODEL FOR A CASCADE CRYSTALLIZER IN THE PRESENCE OF GROWTH RATE DISPERSION*

6.1 Abstract

A model is developed based on the population balance to relate the resulting crystal size distribution (CSD) from a cascade of mixed suspension, mixed product removal (MSMPR) crystallizers to the growth rate distributions of each stage. This model employs the constant crystal growth (CCG) model, in which it is assumed that an individual crystal has an inherent, constant growth rate, but different crystals might have different inherent growth rates. An explicit recursion formula between the first three moments of the resulting crystal size distribution and the first three moments of growth rate distributions of each state is presented for a N-stage MSMPR crystallizer. A computer program has been developed to predict the CSD from a three-stage MSMPR crystallizer with continuous seeding into the first stage and growth in the subsequent stages. The model is solved simultaneously with the mass balance by using power law growth kinetics. The CSD in each stage is assumed as a gamma distribution to compute the mean crystal size, production rate, and coefficient of variance.

6.2 Introduction

The control of the crystal size distribution (CSD) is a very

---

* a paper published in Ind. Eng. Chem. Res., 1987, 26(12), 2512.

important consideration in most crystallization processes. A possible method for control of the CSD is the use of cascade crystallizers to approximate a plug flow residence time distribution. It is the purpose of this work to develop a new cascade model to include growth rate dispersion (GRD).

Randolph and Larson (1962) analytically solved the transient and steady-state size distributions for continuous multistage mixed suspension, mixed product removal (MSMPR) crystallizers in the absence of GRD. Subsequently, Larson and Wolff (1971) used the population balance to determine the effects of operating conditions on the CSD obtained from staged crystallization systems. By use of power law models for nucleation and growth kinetics, the size distribution of the product of any stage can be represented in terms of the residence time in each stage, the amount crystallized in each stage, and the number of stages.

White and Wright (1971) and Berglund and Murphy (1986) have shown that GRD is an extremely important phenomena affecting the CSD. Using the results of batch sucrose crystallization, they show conclusively that crystals of the same size can grow at different rates in identical environments. Two methods of modeling GRD have resulted from these experimental studies. Randolph and White (1977) developed a model on the assumption that the growth rate of an individual crystal fluctuates in the course of time, which will be denoted as the random fluctuation (RF) model. A second model, based on the contact nucleation studies of Berglund et al. (1983), Berglund and Larson (1981), and Ramanarayanan (1982), has been developed with the assumption that individual crystals have different inherent growth rates. This model will be referred to as the constant crystal growth (CCG) model.

Randolph and White (1977) modeled the CSD for a multistage MSMPR crystallizer including GRD based on the RF model. In these studies, a growth rate diffusivity term was added to the general population balance to represent the fluctuation of growth rate. In a subsequent study, Randolph and Tan (1978) employed the RF model to predict the CSD form a multistage classified recycle crystallization process. The population and mass balance equations were solved simultaneously by using power law kinetics for nucleation and growth rates. Once again, the GRD was modeled by using a growth rate diffusivity term in the general population balance.

Berglund and Larson (1984) used a probability transform technique with the CCG model to develop a computer solution for the CSD in a single-stage MSMPR crystallized with GRD. Larson et al. (1985) modeled a single-stage MSMPR crystallizer starting with the ideal MSMPR equations and then accounting for the variation of the growth rate among crystals based on the CCG model. An explicit relationship between the moments of the size distribution and the moments of the growth rate distribution was developed.

The purpose of this paper is to relate the resulting CSD of a multistage MSMPR crystallizer based on the CCG model. The same approach as used in a single-stage MSMPR crystallizer by Larson et al. (1985) is extended to a multistage MSMPR crystallizer. An analogous but more complex relationship between the moments of the size distribution and the moments of the growth rate distribution is presented.

A computer program has been developed to predict CSD from a three-stage cascade continuously seeded in the first stage and growth in the first, second and third stages. The population balance is solved

simu

The

crys

(198

6.3

MSMP

Sing

deve

rate

and

B.C.

(B.C

grow

simultaneously with the mass balance for power law growth kinetics. The data used to model the cascade are taken from the batch sucrose crystallization studies of Berglund (1980) and Berglund and Murphy (1986).

6.3 Model

The following assumptions are made in developing this multistage MSMPR crystallizer model.

1. The CCG model is assumed applicable.
2. The growth rate is independent of crystal size.
3. The crystals are born close to zero size, and the product size is much larger than the size at which they were born.
4. The growth rate distributions are independent of stages.

Single-Stage MSMRP Crystallizer. Randolph and Larson (1971) have developed the population balance for the crystals growing with a growth rate of g_{1i} as

$$V_1 g_{1i} dn_{1i}/dL = -Q_1 n_{1i} \tag{1}$$

and

B.C. $\quad n_{1i}(0) = n_{1i}^{o}$

(B.C. = boundary condition) so the population density of crystals growing with a growth rate g_{1i} is

$$n_{1i} = n_{1i}^{0} \exp\left(\frac{-1}{g_{1i}\tau_1}\right) \tag{2}$$

The use of the additional subscripts will become clear as the model is extended to a cascade. Starting with this form, Larson et al. (1985) developed the relationship between the moments of CSD and the moments of growth rate distribution for a single-state MSMPR crystallizer,

$$\int_0^\infty L^k f_{L_1}(L)dL = k!\tau_1^k \int_0^\infty g_1^k f_{G_1}(g_1)dg_1 \tag{3}$$

or in moment notation,

$$M_L(1,k) = k!\tau_1^k M_G(1,k) \tag{4}$$

where in general

$$M_L(1,k) = \int_0^\infty L^k f_{L_1}(L)dL \tag{5}$$

$$M_G(1,k) = \int_0^\infty g_1^k f_{G_1}(g_1)dg_1 \tag{6}$$

Two-Stage MSMPR Crystallizer Cascade. Since the effluent crystals from the first stage are the seeds to the second stage, the population balance on the second state takes the form

wher

and

B.C.

If t

grow

n_{2ij}

Sinc

of t

each

$n_2(L$

$$V_2 g_{2j}\, dn_{2ij}/dL = Q_1 n_{1i} - Q_2 n_{2ij} \tag{7}$$

where

$$n_{1i}(L) = n_{1i}^{o} e^{-L/(g_{1i} r_1)} \tag{8}$$

and

B.C. $\qquad n_{2ij}(0) = n_{2ij}^{o}$

If the above equations are solved, the population density of crystals growing with w growth rate g_{2j} in the second stage is given by

$$n_{2ij}(L) = \frac{n_{1i}^{o}(Q_1/Q_2)}{1 - \dfrac{g_{2j} r_2}{g_{1i} r_1}} \left[e^{-L/(g_{1i} r_1)} - e^{-L/(g_{2j} r_2)}\right] + n_{2ij}^{o} e^{-L/(g_{2j} r_2)} \tag{9}$$

Since g_{1i} and g_{2j} are random variables independent of size L, the CSD of the product is merely the double summation of the distribution of each g_{1i} and g_{2j}

$$n_2(L) = \sum_{i=0}^{\infty} \sum_{j=0}^{\infty} n_{2ij}(L) =$$

∞
Σ
i=

f_G

cr

f_G

ha

re

gr

is

n_2(

whe

rep

in

f_{L_2}

$$\sum_{i=0}^{\infty}\sum_{j=0}^{\infty} \frac{n_{1i}^{o}(Q_1/Q_2)}{1 - \frac{g_{2j}r_2}{g_{1i}r_1}} [e^{-L/(g_{1i}r_1)} - e^{-L/(g_{2j}r_2)}] + n_{2ij}^{o} e^{-L/(g_{2j}r_2)} \tag{10}$$

$f_{G_1}(g_1)$ and $f_{G_2}(g_2)$ represent the distribution of growth rates for crystals in the first and second stages, respectively, such that $f_{G_1}(g_1)\, f_{G_2}(g_2)\, dg_1\, dg_2$ is the fraction of the total number of crystals having growth rates of g_1 and g_2 in the first and second stages, respectively. Thus, the number of crystals of size L with all possible growth rates of g_1 and g_2 in the first and second stages, respectively, is

$$n_2(L) = \int_0^{\infty}\int_0^{\infty} \left(\frac{B_1^{o} r_1 (Q_1/Q_2)}{1 - \frac{g_{2i}r_2}{g_{1i}r_1}} [e^{-L/(g_1 r_1)} - e^{-L/(g_2 r_2)}] + B_2^{o} r_2 e^{-L/(g_2 r_2)} \right) f_{G_1}(g_1)\, f_{G_2}(g_2)\, dg_1\, dg_2 \tag{11}$$

where the subscripts i and j have been dropped due to integration replacing summation. Thus, the fraction of the total crystals of size L in the second-stage MSMPR crystallizer is

$$f_{L_2}(L) = \frac{n_2(L)}{B_1^{o} r_1 (Q_1/Q_2) + B_2^{o} r_2} = \frac{1}{B_1^{o} r_1 (Q_1/Q_2) + B_2^{o} r_2} \times$$

wher

the

tota

Eq.1

the

and

expr

$$\int_0^\infty$$

$$\int_0^\infty \int_0^\infty \left[\frac{B_1^{\circ} r_1 (Q_1/Q_2)}{1 - \frac{g_{2i} r_2}{g_{1i} r_1}} \left[e^{-L/(g_1 r_1)} - e^{-L/(g_2 r_2)} \right] + B_2^{\circ} r_2 e^{-L/(g_2 r_2)} \right] f_{G_1}(g_1)\, f_{G_2}(g_2)\, dg_1\, dg_2 \tag{12}$$

where $B_1^{\circ} r_1 (Q_1/Q_2) + B_2^{\circ} r_2$ is the number of crystals per unit volume in the second-stage crystallizer. $f_{L_2}(L)\, dL$ equals the fraction of the total number of crystals in the size range from L to L + dL. From Eq.12, the CSD $f_{L_2}(L)$ can be obtained by simple integration, knowing the growth rate distributions $f_{G_1}(g_1)$ and $f_{G_2}(g_2)$.

Multipling both size of eq 12 by L^k, integrating between 0 and ∞, and assuming that g_1, g_2, and L are independent, the following expression for the moments is obtained

$$\int_0^\infty L^k f_{L_2}(L)\, dL = \int_0^\infty \int_0^\infty \int_0^\infty \frac{n_2(L)}{B_1^{\circ} r_1 (Q_1/Q_2) + B_2^{\circ} r_2} \times L^k f_{G_1}(g_1)\, f_{G_2}(g_2)\, dg_1\, dg_2$$

$$= \frac{1}{B_1^{\circ} r_1 (Q_1/Q_2) + B_2^{\circ} r_2} \times$$

$$\int_0^\infty \int_0^\infty \int_0^\infty \left[\frac{B_1^{\circ} \tau_1 (Q_1/Q_2)}{1 - \frac{g_{2i} \tau_2}{g_{1i} \tau_1}} \left[e^{-L/(g_1 \tau_1)} - e^{-L/(g_2 \tau_2)} \right] + \right.$$

$$\left. B_2^{\circ} \tau_2 e^{-L/(g_2 \tau_2)} \right] L^k f_{G_1}(g_1) f_{G_2}(g_2) \, dg_1 \, dg_2 \qquad (13)$$

There is no simple recursion formula relating the moments of CSD of the second stage to the moments of growth rate distributions of the first and second stages in this case. However, by integration for k = 1, (i.e., the first moment of the CSD in the second stage),

$$M_L(2,1) = \frac{B_1^{\circ} \tau_1 (Q_1/Q_2)}{B_1^{\circ} \tau_1 (Q_1/Q_2) + B_2^{\circ} \tau_2} \left[\tau_1 M_G(1,1) + \tau_2 M_G(2,1) \right] +$$

$$\frac{B_1^{\circ} \tau_1 (Q_1/Q_2)}{B_1^{\circ} \tau_1 (Q_1/Q_2) + B_2^{\circ} \tau_2} \left[\tau_2 M_G(2,1) \right] \qquad (14)$$

For k=2,

$$M_L(2,2) = \frac{2!\, B_1^{\circ} \tau_1 (Q_1/Q_2)}{B_1^{\circ} \tau_1 (Q_1/Q_2) + B_2^{\circ} \tau_2} \left[\tau_1^2 M_G(1,2) + \tau_1 \tau_2 M_G(1,1) + \right.$$

$$\left. \tau_2^2 M_G(2,2) \right] + \frac{2!\, B_2^{\circ} \tau_2}{B_1^{\circ} \tau_1 (Q_1/Q_2) + B_2^{\circ} \tau_2} \left[\tau_2^2 M_G(2,2) \right] \qquad (15)$$

and for k = 3

$M_L(2$

whe

Thre

crys

popu

whe

n_{2i}

and

$$M_L(2,3) = \frac{3!\, B_1^{\circ} \tau_1 (Q_1/Q_2)}{B_1^{\circ} \tau_1 (Q_1/Q_2) + B_2^{\circ} \tau_2} \left[\tau_1^3 M_G(1,3) + \right.$$

$$\tau_1^2 \tau_2 M_G(1,2) M_G(2,1) + \tau_1 \tau_2^2 M_G(1,1) M_G(2,2) +$$

$$\left. \tau_2^3 M_G(2,3)\right] + \frac{3!\, B_2^{\circ} \tau_2}{B_1^{\circ} \tau_1 (Q_1/Q_2) + B_2^{\circ} \tau_2} \left[\tau_2^3 M_G(2,3)\right] \qquad (16)$$

where

$$M_L(2,k) = \int_0^{\infty} L^k f_{L_2}(L)\, dL \qquad (17)$$

$$M_G(2,k) = \int_0^{\infty} g_2^k f_{G_2}(g_2)\, dg_2 \qquad (18)$$

Three-Stage MSMPR Crystallizer Cascade. Similarly, since the effluent crystals from the second stage are the seeds to the third stage, the population balance on the third stage takes the form

$$V_3 g_{3k}\, dn_{3ijk}/dL = Q_2 n_{2ij} - Q_3 n_{3ijk} \qquad (19)$$

where

$$n_{2ij}(L) = \frac{n_{1i}^{\circ}(Q_1/Q_2)}{1 - \frac{g_{2j}\tau_2}{g_{1i}\tau_1}} \left[e^{-L/(g_{1i}\tau_1)} - e^{-L/(g_{2j}\tau_2)}\right] + n_{2ij}^{\circ} e^{-L/(g_{2j}\tau_2)} \qquad (20)$$

and

B.C. $\quad n_{3ijk}(0) = n_{3ijk}^{o}$

If the above equations are solved, the population density of crystals with a growth rate g_{1i} in the first stage, a growth rate g_{2j} in the second stage, and a growth rate g_{3k} in the third stage is given by

$$n_{3ijk}(L) = \frac{n_{1i}^{o}(Q_1/Q_3)}{\left(1 - \frac{g_{2j}\tau_2}{g_{1i}\tau_1}\right)\left(1 - \frac{g_{3k}\tau_3}{g_{1i}\tau_1}\right)}\left[e^{-L/(g_{1i}\tau_1)} - e^{-L/(g_{3k}\tau_3)}\right] -$$

$$\frac{n_{1i}^{o}(Q_1/Q_3)}{\left(1 - \frac{g_{2j}\tau_2}{g_{1i}\tau_1}\right)\left(1 - \frac{g_{3k}\tau_3}{g_{2j}\tau_2}\right)}\left[e^{-L/(g_{2j}\tau_2)} - e^{-L/(g_{3k}\tau_3)}\right] +$$

$$\frac{n_{2ij}^{o}(Q_2/Q_3)}{1 - \frac{g_{3k}\tau_3}{g_{2j}\tau_2}}\left[e^{-L/(g_{2j}\tau_2)} - e^{-L/(g_{3k}\tau_3)}\right] + n_{3ijk}^{o}e^{-L/(g_{3k}\tau_3)} \qquad (21)$$

By a similar approach as for the two-stage case, the moments of CSD of the third stage can be related to the moments of GRD, of the first, second, and third stages as follows:

$$M_L(3,1) = \frac{B_1^{o}\tau_1(Q_1/Q_3)}{B_1^{o}\tau_1(Q_1/Q_3) + B_2^{o}\tau_2(Q_2/Q_3) + B_3^{o}\tau_3} \times$$

$$[\tau_1 M_G(1,1) + \tau_2 M_G(2,1) + \tau_3 M_G(3,1)] +$$

$$\frac{B_2^{o}\tau_2(Q_1/Q_3)}{B_1^{o}\tau_1(Q_1/Q_3) + B_2^{o}\tau_2(Q_2/Q_3) + B_3^{o}\tau_3} \times$$

$$[r_2 M_G(2,1) + r_3 M_G(3,1)] +$$

$$\frac{B_3^{\circ} r_3}{B_1^{\circ} r_1 (Q_1/Q_3) + B_2^{\circ} r_2 (Q_2/Q_3) + B_3^{\circ} r_3} \times [r_3 M_G(3,1)]$$

(22)

$$M_L(3,2) = \frac{2!\, B_1^{\circ} r_1 (Q_1/Q_3)}{B_1^{\circ} r_1 (Q_1/Q_3) + B_2^{\circ} r_2 (Q_2/Q_3) + B_3^{\circ} r_3} \times$$

$$[r_1^2 M_G(1,2) + r_2^2 M_G(2,2) + r_3^3 M_G(3,2) +$$

$$r_1 r_2 M_G(1,1) M_G(2,1) + r_1 r_3 M_G(1,1) M_G(3,1) +$$

$$r_2 r_3 M_G(2,1) M_G(3,1)] +$$

$$\frac{2!\, B_2^{\circ} r_2 (Q_2/Q_3)}{B_1^{\circ} r_1 (Q_1/Q_3) + B_2^{\circ} r_2 (Q_2/Q_3) + B_3^{\circ} r_3} \times$$

$$[r_2^2 M_G(2,2) + r_3^2 M_G(3,2) + r_2 r_3 M_G(2,1) M_G(3,1)] +$$

$$\frac{2!\, B_3^{\circ} r_3}{B_1^{\circ} r_1 (Q_1/Q_3) + B_2^{\circ} r_2 (Q_2/Q_3) + B_3^{\circ} r_3} \times [r_3^2 M_G(3,2)]$$

(23)

$$M_L(3,3) = \frac{3!\, B_1^{\circ} r_1 (Q_1/Q_3)}{B_1^{\circ} r_1 (Q_1/Q_3) + B_2^{\circ} r_2 (Q_2/Q_3) + B_3^{\circ} r_3} \times$$

$$[r_1^3 M_G(1,3) + r_2^3 M_G(2,3) + r_3^3 M_G(3,3) +$$

$$r_1^2 r_2 M_G(1,2) M_G(2,1) + r_1 r_2^2 M_G(1,1) M_G(2,2) +$$

$$\tau_1^2\tau_3 M_G(1,2)M_G(3,1) + \tau_1\tau_3^2 M_G(1,1)M_G(3,2) +$$

$$\tau_2^2\tau_3 M_G(2,2)M_G(3,1) + \tau_2\tau_3^2 M_G(2,1)M_G(3,2) +$$

$$\tau_1\tau_2\tau_3\, M_G(1,1)M_G(2,1)M_G(3,1)] +$$

$$\frac{3!\, B_2^{\circ}\tau_2(Q_2/Q_3)}{B_1^{\circ}\tau_1(Q_1/Q_3) + B_2^{\circ}\tau_2(Q_2/Q_3) + B_3^{\circ}\tau_3} \times$$

$$[\tau_2^3 M_G(2,3) + \tau_3^3 M_G(3,3) + \tau_2^2\tau_3\, M_G(2,2)M_G(3,1) +$$

$$\tau_2\tau_3^2 M_G(2,1)M_G(3,2)] +$$

$$\frac{3!\, B_3^{\circ}\tau_3}{B_1^{\circ}\tau_1(Q_1/Q_3) + B_2^{\circ}\tau_2(Q_2/Q_3) + B_3^{\circ}\tau_3} \times [\tau_3^3 M_G(3,3)] \tag{24}$$

where in general

$$M_L(3,k) = \int_0^{\infty} L^k f_{L_3}(L)\,dL \tag{25}$$

$$M_G(3,k) = \int_0^{\infty} g_3^k f_{G_3}(g_3)\,dg_3 \tag{26}$$

In summary, the recursion formula is for an N-stage MSMPR crystallizer.

$$M_L(N,1) = \sum_{k=1}^{N}\left[\frac{B_k^{\circ}\tau_k(Q_k/Q_N^{\circ})}{\sum_{i=1}^{N} B_i^{\circ}\tau_i(Q_i/Q_N)}\left[\sum_{i=k}^{N}\tau_i M_G(i,1)\right]\right] \tag{27}$$

$$M_L(N,2) = \sum_{k=1}^{N}\left[\frac{2!\, B_k^{\circ}\tau_k(Q_k/Q_N^{\circ})}{\sum_{i=1}^{N} B_i^{\circ}\tau_i(Q_i/Q_N)} \times\right.$$

$$\left[\sum_{i-k}^{N} \sum_{j>i}^{N} \tau_i \tau_j M_G(i,1) M_G(j,1) + \sum_{i-k}^{N} \tau_i^2 M_G(i,2) \right] \qquad (28)$$

$$M_L(N,3) - \sum_{k-1}^{N} \left(\frac{3!\, B_k^{\circ} \tau_k (Q_k/Q_N)^{\circ}}{\sum_{i=1}^{N} B_i^{\circ} \tau_i (Q_i/Q_N)} \right) x$$

$$\left[\sum_{i-k}^{N} \sum_{(j \neq 1)}^{N} \tau_i^2 \tau_j M_G(i,2) M_G(j,1) + \sum_{i-k}^{N} \tau_i^3 M_G(i,3) + \right.$$

$$\left. \sum_{i-k}^{N} \sum_{j>k}^{N} \sum_{\ell>j}^{N} \tau_i \tau_j \tau_\ell M_G(i,1) M_G(j,1) M_G(\ell,1) \right] \qquad (29)$$

6.4 Application of the Model

In the case of considering GRD based on the above model for a cascade of multistage MSMPR crystallizers, the CSD modeling equations describing the process of Figure 1 can be summarized as follows:

Population Balance (Moment Form):

It has been stated in the recursion formula, Eq. 27, 28, and 29.

Mass Balance on Solute:

Randolph and Tan (1978) showed the mass balance equation without considering GRD as

For jth stage

$$Q_{j-1}\, C_{j-1} - Q_j\, C_j + V_j \rho\, k_A\, (G_j/2) \int_0^{\infty} n_j\, L^2\, dL$$

Here, considering GRD and normalizing CSD,

$$Q_{j-1}\, C_{j-1} - Q_j\, C_j + 1/2\, V_{j\rho}\, k_A\, M_G(j,1)\, M_L(J,2)\, Num(j)$$

Growth Kinetics:

Berglund and Murphy (1986) and Shiau and Berglund (1987) measured the man growth kinetics and the variance of growth rate distribution for sucrose and fructose, respectively. In both cases, the mean growth rate has a Arrhenius form and the variance of growth rate distribution can be represented as a power law expression as

$$\bar{G}_j = A\, e^{-E_G/(RT)} C_j^{\,m}$$

$$\sigma_{G_j}^{\,2} = a\, \bar{G}_j^{\,b}$$

In terms of the moment from, we have

$$M_G(j,1) = \bar{G}_j = A\, e^{-E_G/(RT)} C_j^{\,m}$$

and

$$M_G(j,2) = \bar{G}_j^{\,2} + \sigma_{G_j}^{\,2} = \bar{G}_j^{\,2} + a\, \bar{G}_j^{\,b}$$

When the model coupled with the mass balance equation is applied, the third moment of growth rate distribution needs to be estimated from the knowledge of the first and second moments. In most cases, the growth rate distribution can be fit to a gamma distribution, allowing the two parameters α_j and β_j for the gamma distribution to be calculated from the mean and variance; thus,

$$\beta_j = \sigma_{G_j}^{\,2} / \bar{G}_j$$

$$\alpha_j = \bar{G}_j / \beta_j$$

The third moment then may be written

$$M_G(j,3) = \alpha_j\ (\alpha_j+1)\ (\alpha_j+2)\ \beta_j^3$$

Slurry Density:

$$M_{T_j} = \rho\ k_V\ M_L(j,3)\ Num(j)$$

Nucleation Kinetics:

$$B_j^o = k_{N_j} M_{T_j}^{\ I}\ C_j^{\ J}$$

Free Liquor Volume:

$$V_j = \frac{V_{T_j}}{1 + k_V\ M_L(j,3)\ Num(j)}$$

Number of Nuclei per Unit Volume in Each Stage:

$$Num(1) = B_1^o \tau_1$$

$$Num(2) = B_1^o \tau_1 (Q_1/Q_2) + B_2^o \tau_2$$

$$Num(3) = B_1^o \tau_1 (Q_1/Q_3) + B_2^o \tau_2 (Q_2/Q_3) + B_3^o \tau_3$$

$$Num(j) = \sum_{i=1}^{j} B_i^o \tau_i (Q_i/Q_j)$$

In general, the above set of equations will contain more unknowns, and it is necessary to fix some variable to obtain a solution. A particular useful selection of variables for a sucrose cooling crystallizer is to choose G_j and V_{Tj} as independent variables and treat Q_j, T_j, C_j, τ_j, and M_T, as dependent variables.

6.5 Example Calculations

A computer program was developed to predict the CSD for continuously seeded three-staged MSMPR sucrose cooling crystallizers without nucleation by simultaneous solution of the population and mass balances. The algorithm is shown in Figure 2. The conditions employed in the example are listed in Table 1.

Case One. The reactor volume in each stage is held equal at 5000 cm^3. Supersaturation in each stage is the same, ranging from S =0.8 to 1.8 g of sucrose/100 g of solution. (This is the range that was studied by Berglund (1980) and Berglund and Murphy (1986) to model mean growth rate kinetics and the variance of growth rate distribution in the case of growth with no nucleation.)

Figures 3 and 4 show that both the mean crystal size on a number basis and the production rate increase as supersaturation is increased. However, the mean crystal size on a number basis is always smaller in the presence of GRD (Figure 3).

On the other hand, GRD has the opposite result on the production rate as shown in Figure 4. Figure 5 shows that CV on a number basis increases as supersaturation in increased in each case and the CV on a number basis is much larger in the presence of GRD.

Case Two. Supersaturation in each stage is held the same at S = 1.0 g of sucrose/100 g of solution. The reactor volume in each stage is held equal, ranging from 3000 to 7000 cm^3.

Figures 6 and 7 shown that mean crystal size on a number basis and production rate increase as volume is increased in both cases of GRD and no GRD. However, it is clear from Figure 6 that in the case of GRD

Table 1. Conditions employed in the example of a three-stage crystallizer cascade for sucrose.

Parameters	Quantity
sucrose crystal density, gm/cc	1.588
feed concentration, gm sucrose/100 gm soln	75.5
feed flowrate, cc/min	202.43
number of crystals per unit volume in stage I, #/cc	10^5
saturated sucrose concentration at a given temperature T, where C* is in gm sucrose/100 gm soln and T is in ^oC	$C^*=62.77+0.1706T+0.000344T^2$
the mean growth rate kinetics, where $\bar{G}$ is in $\mu m/min$ and T is in ^oK	$\bar{G} = 7.99 \times 10^6 \exp\left(\frac{-13600}{RT}\right) \cdot C$
the variance of growth rate distribution where $\bar{G}$ is in $\mu m/min$ and σ_G^2 is $\mu m^2/min^2$	$\sigma_G^2 = 0.286\bar{G}^{1.74}$

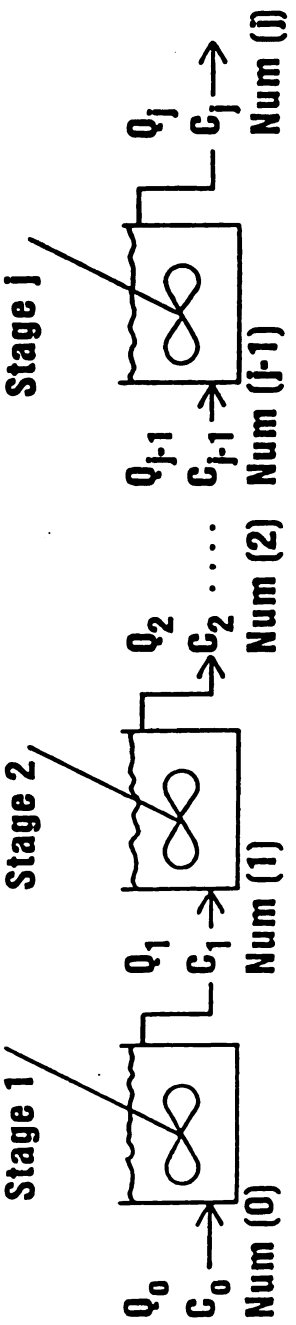

Figure 1. Schematic of continuous mutlistage crystallizer.

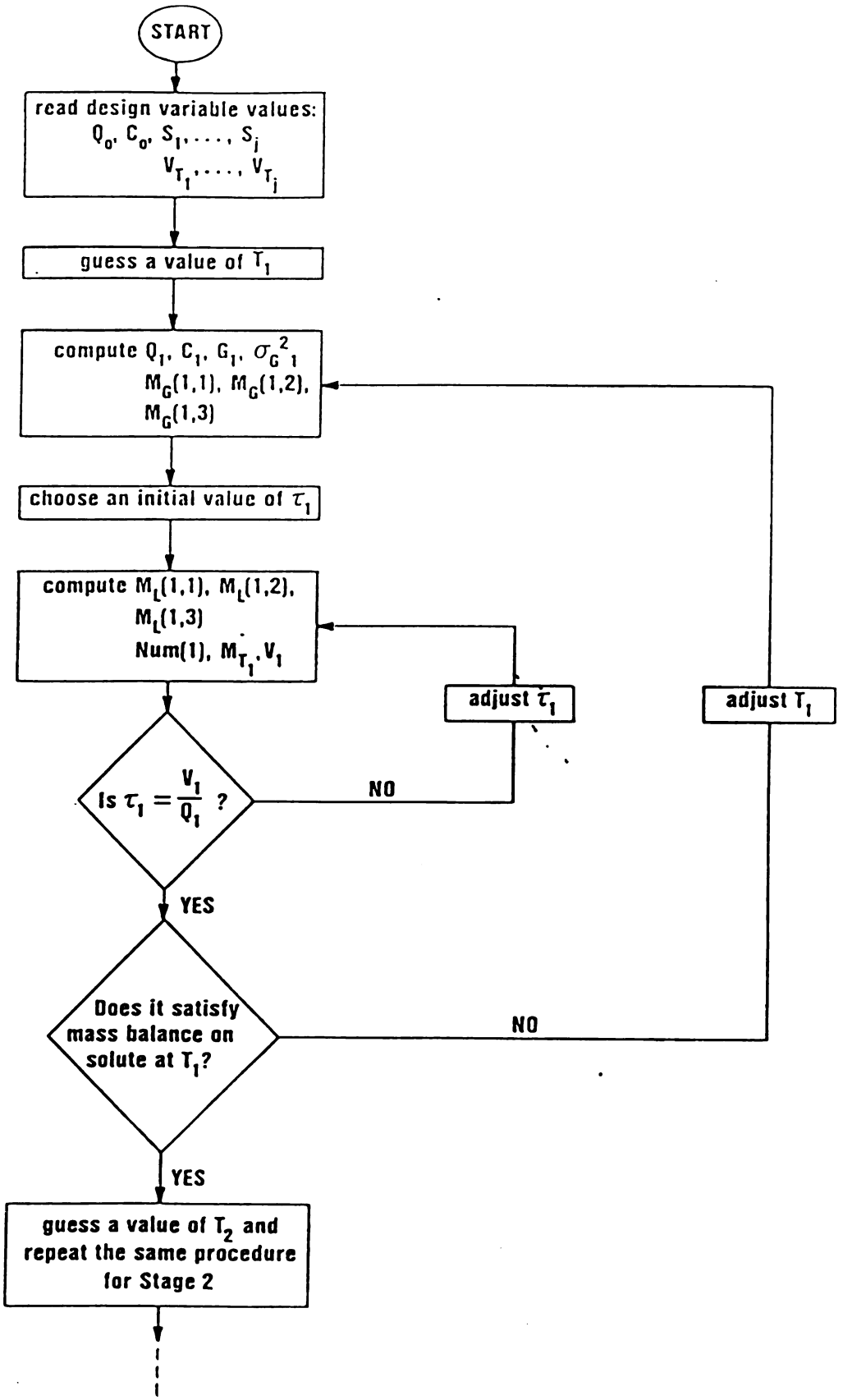

Figure 2. Algorithm used in the computer program for continuously seeded multistage crystallizer without nucleation.

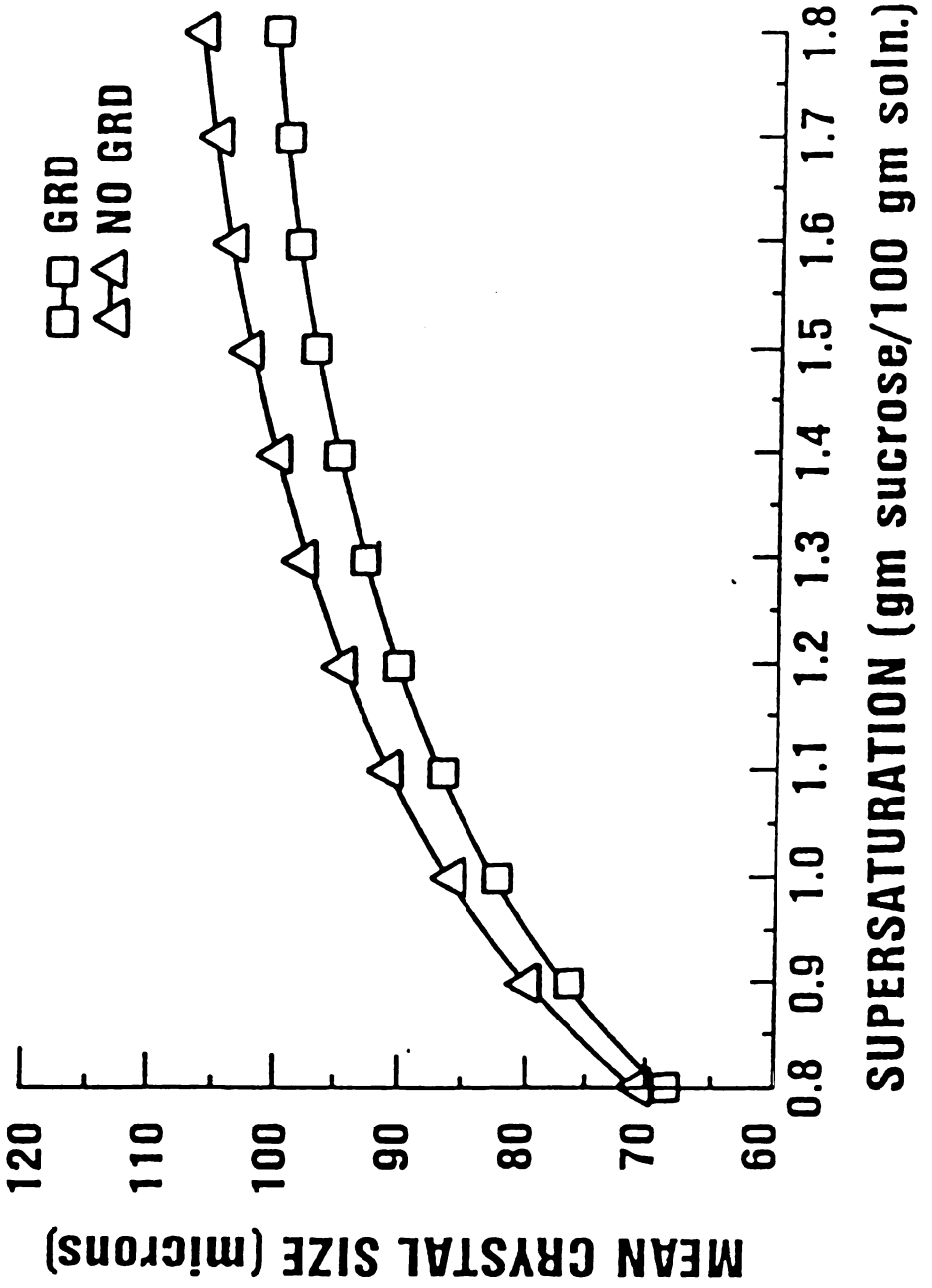

Figure 3. Mean crystal size on a number basis versus supersaturation for both GRD and no GRD.

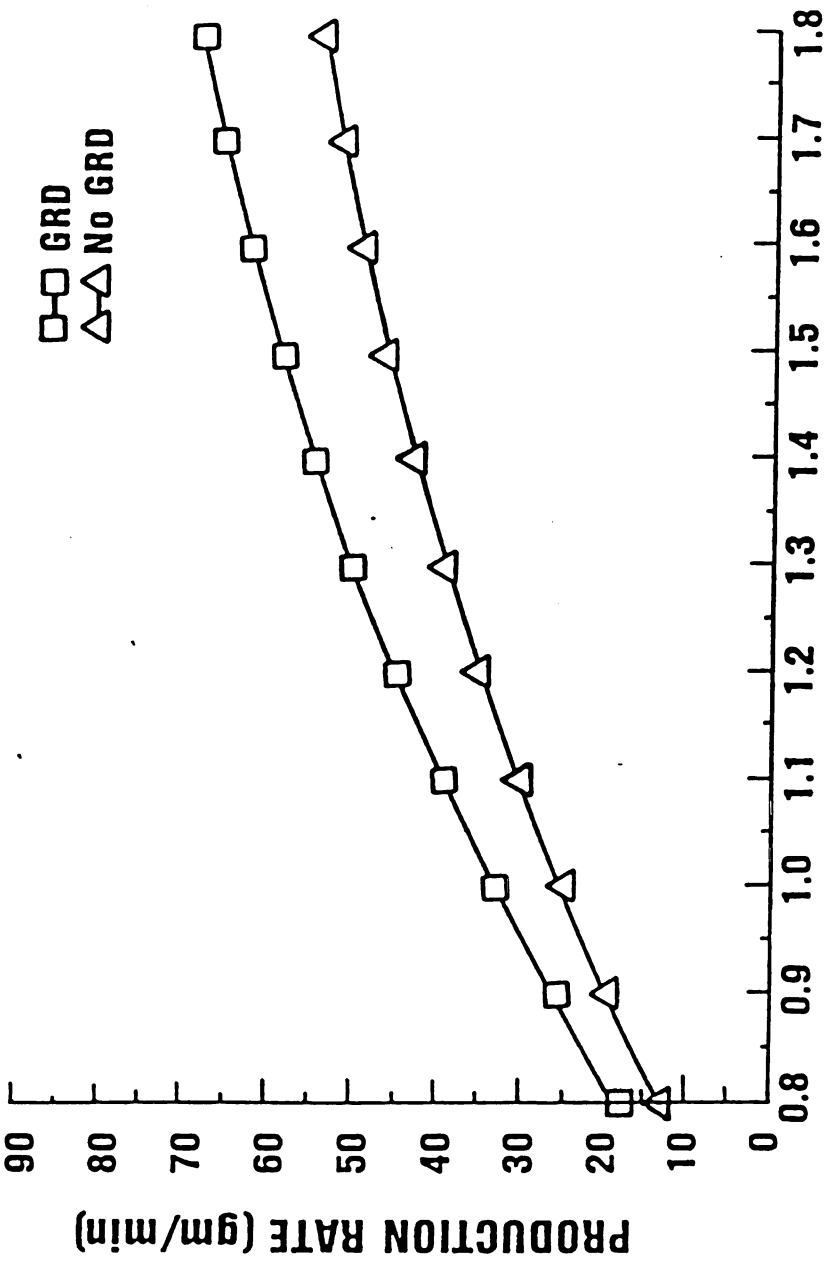

Figure 4. Production rate versus supersaturation for both GRD and no GRD.

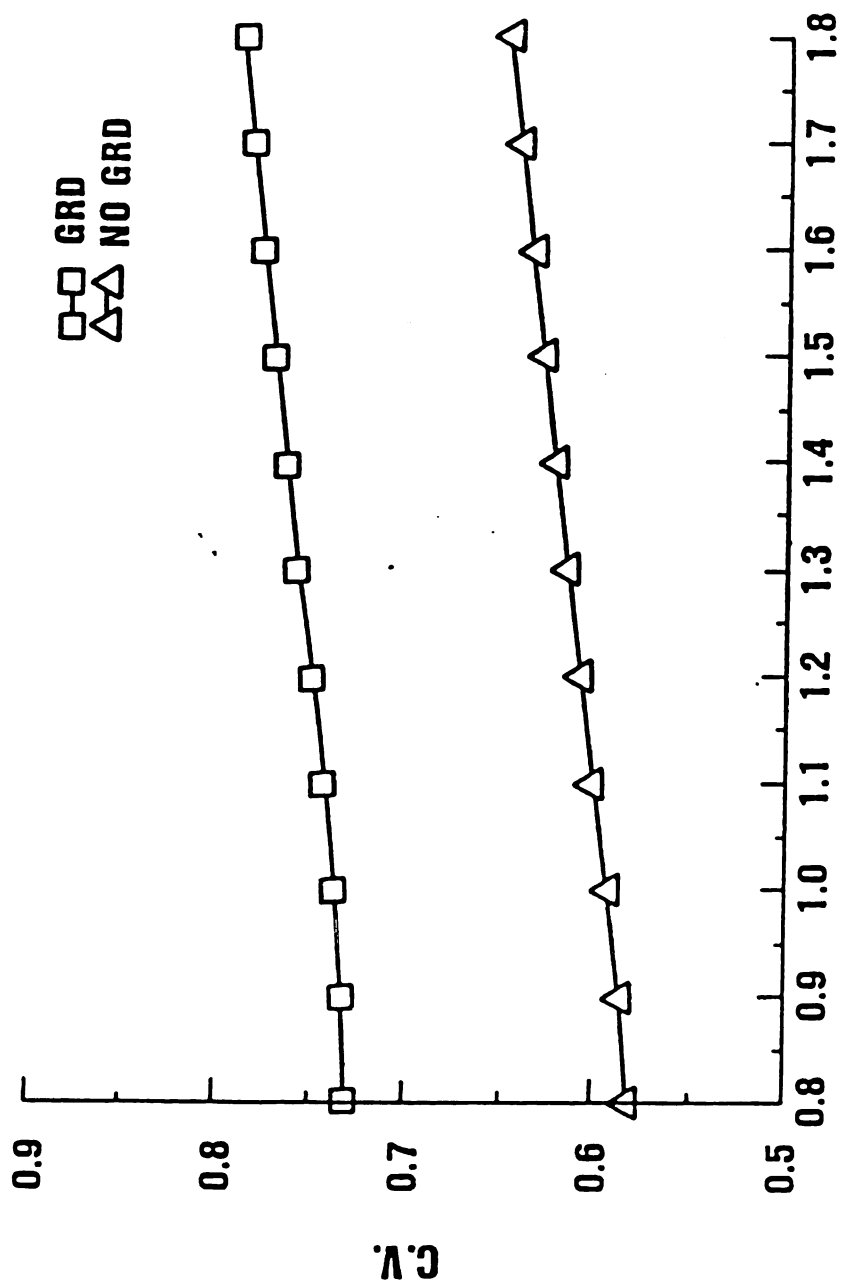

Figure 5. C.V. on a number basis versus supersaturation for both GRD and no GRD.

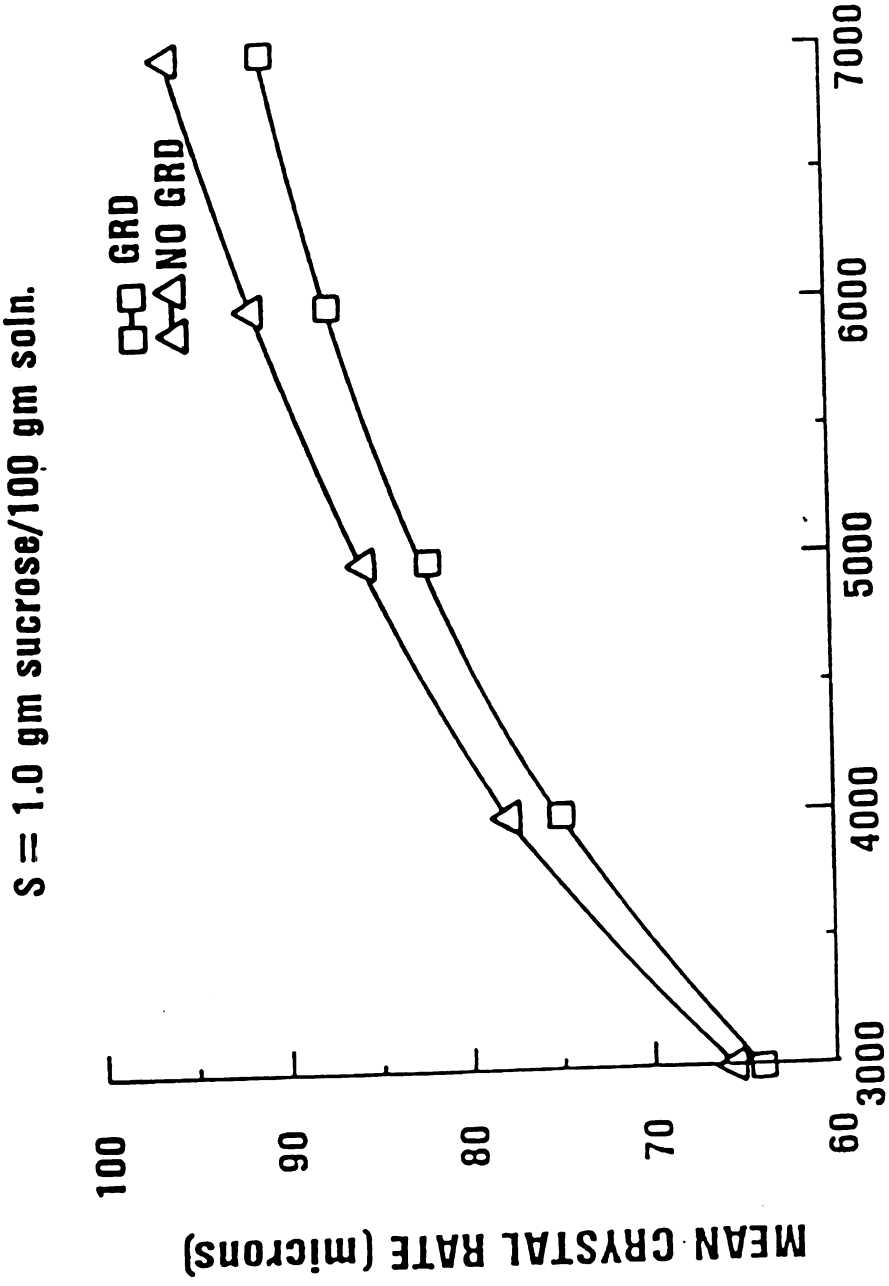

Figure 6. Mean crystal size on a number basis versus volume for both GRD and no GRD at the supersaturation of 1.0 g sucrose/100 g soln.

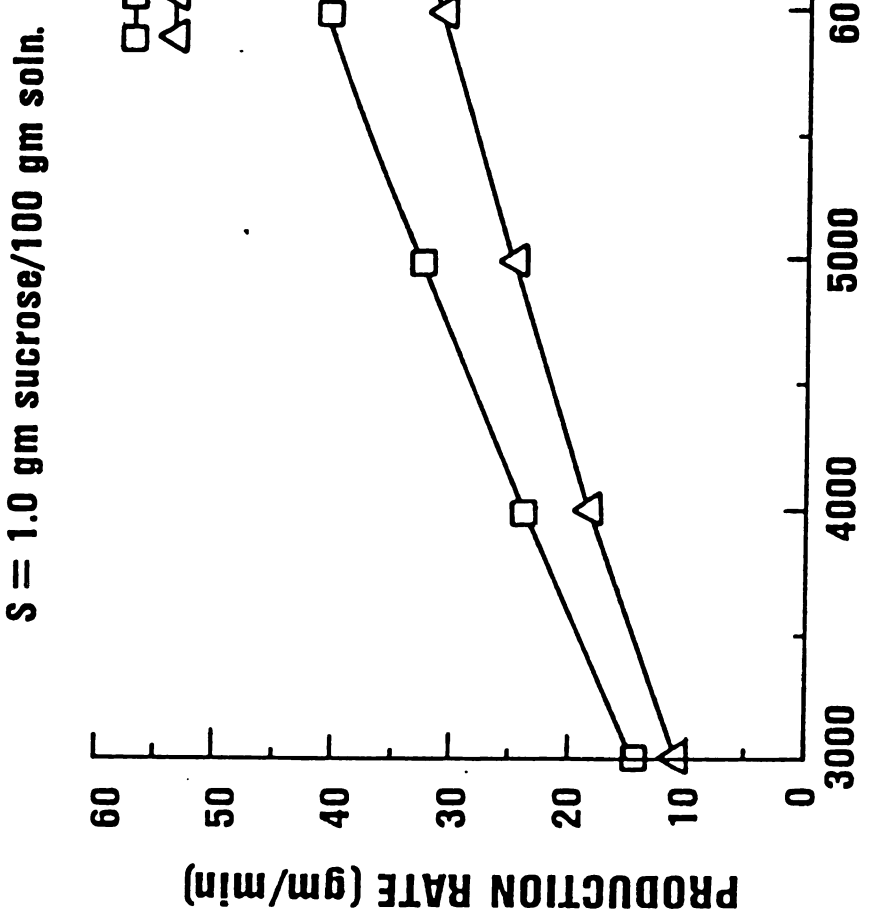

Figure 7. Production rate versus volume for both GRD and no GRD at the supersaturation of 1.0 g sucrose/100 g soln.

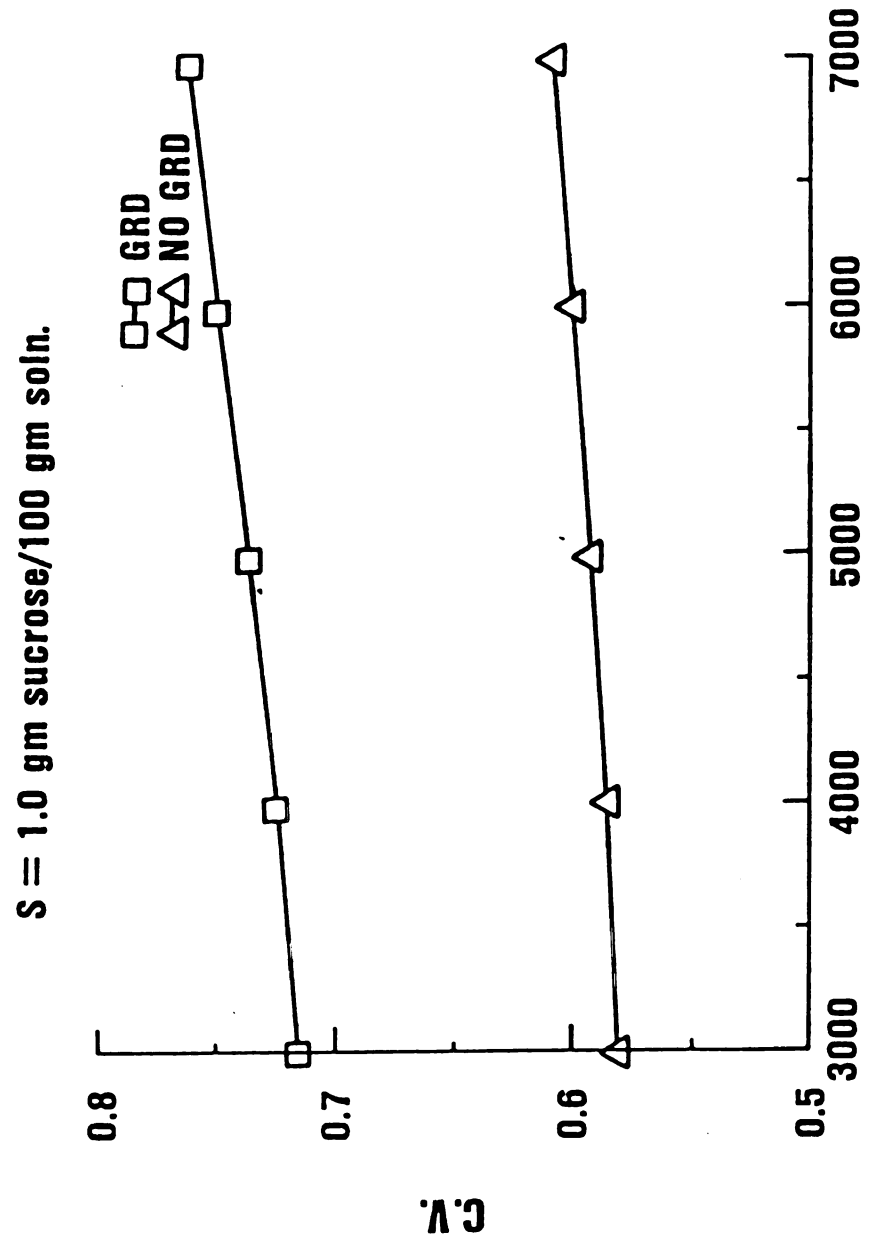

Figure 8. C.V. on a number basis versus volume for both GRD and no GRD at the supersaturation of 1.0 g sucrose/100 g soln.

the mean crystal size on a number basis is smaller than that in the case of no GRD. On the other hand, production rate shows the opposite result as shown in Figure 7. Figure 8 shows that the CV on a number basis increases as volume is increased in each of the cases and the CV on a number basis is much larger in the presence of GRD.

Case Three. The supersaturation is held constant at S = 1.0 g of sucrose/100 g of solution. The effects of staging are compared by holding the total system volume constant at 15000 cm^3, that is, $V_{T_1} = V_{T_2} = V_{T_3} = 5000\ cm^3$ for a three-stage system.

Figure 9 shows that the mean crystal size on a number basis increases as the number of stages is increased and the mean crystal size on a number basis is smaller in the presence of GRD. Figure 10 shown that the production rate decreases as the number of stages is increased in the presence of GRD, while the opposite phenomena was observed in the case of no GRD> However, the production rate in the presence of GRD is always larger than that in the case of no GRD. Figure 11 shows that the CV on a number basis decreases as the number of stages is increased in both cases.

A check of the consistency of the solution can be made by observing that the CV on a number basis is 1 for a single-stage ideal MSMPR crystallizer as predicted by Randolph and Larson (1971).

6.6 Conclusions

In a continuously seeded single-stage or multistage cooling crystallizer without nucleation choosing S_j, T_j, C_j, τ_j, and N_{T_j} as

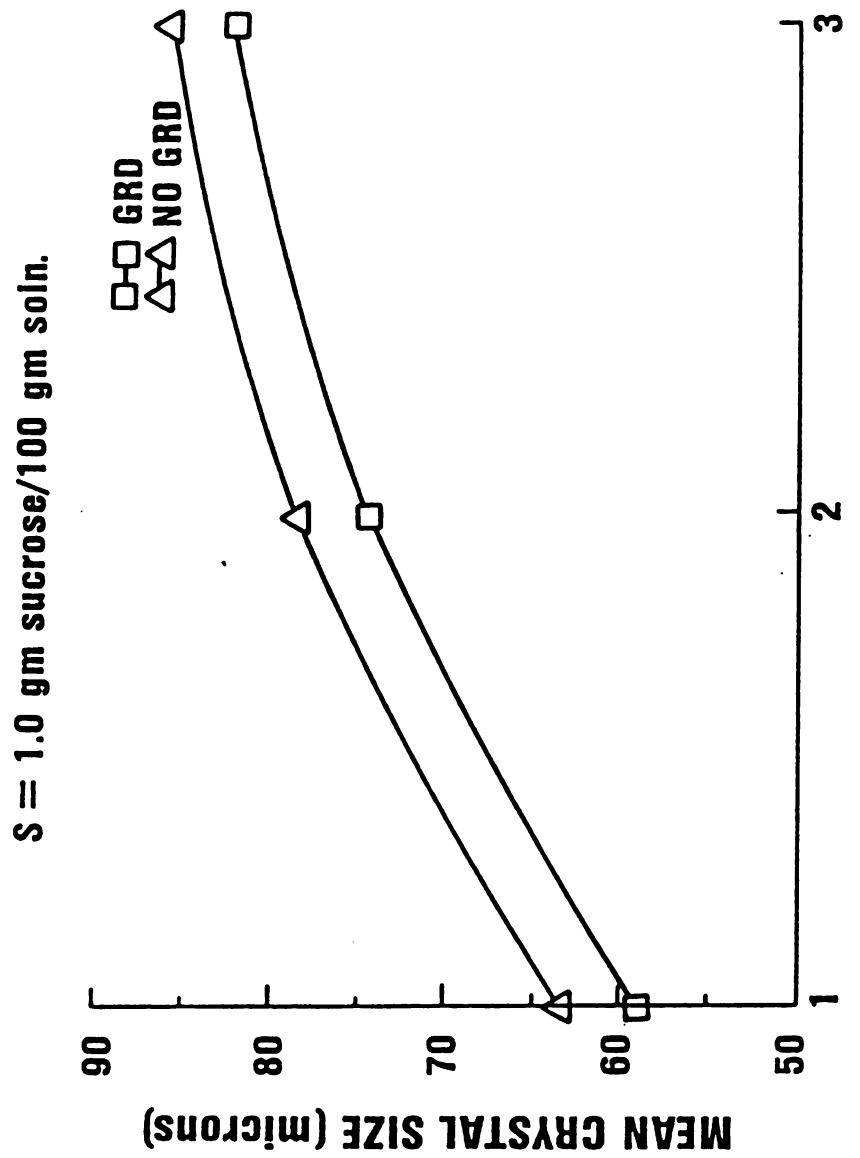

Figure 9. Mean crystal size on a number basis versus number of stages for both GRD and no GRD at the supersaturation of 1.0 g sucrose/100 g soln.

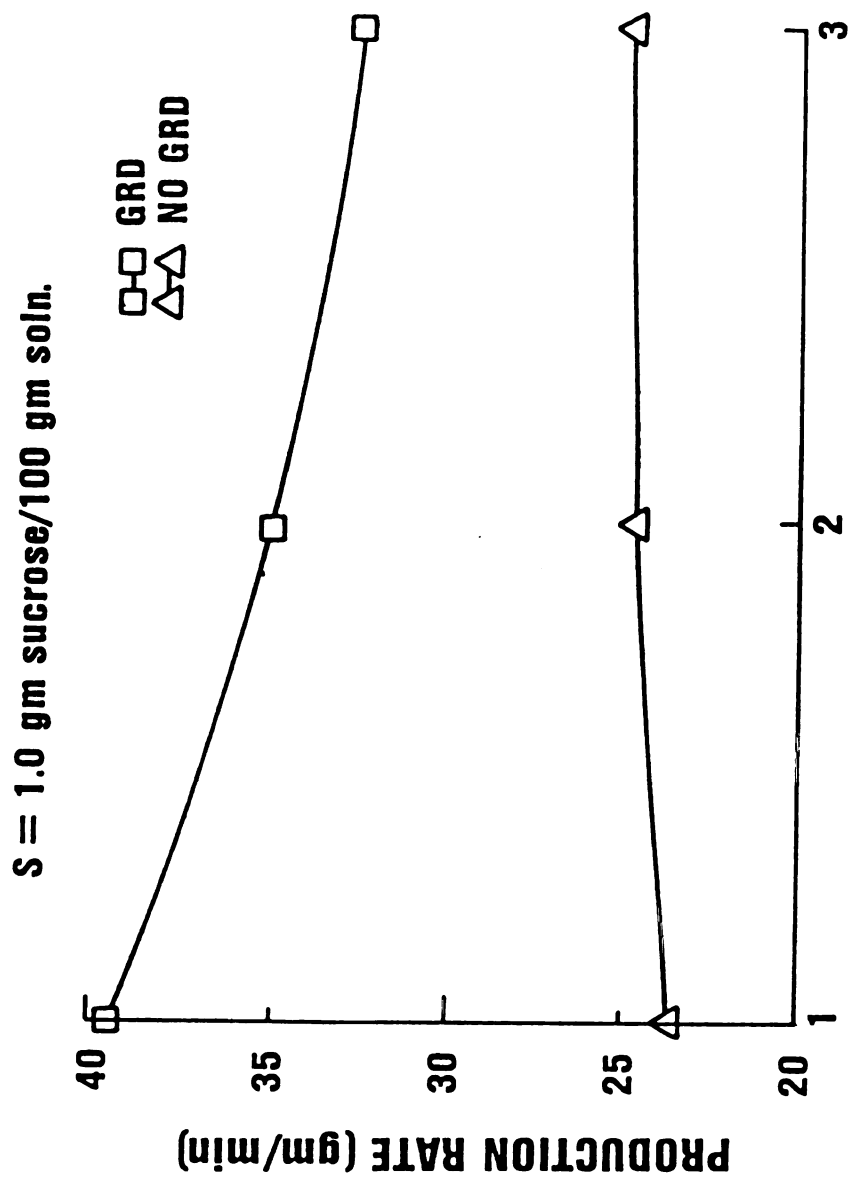

Figure 10. Production rate versus number of stages for both GRD and no GRD at the supersaturation of 1.0 g sucrose/100 g soln.

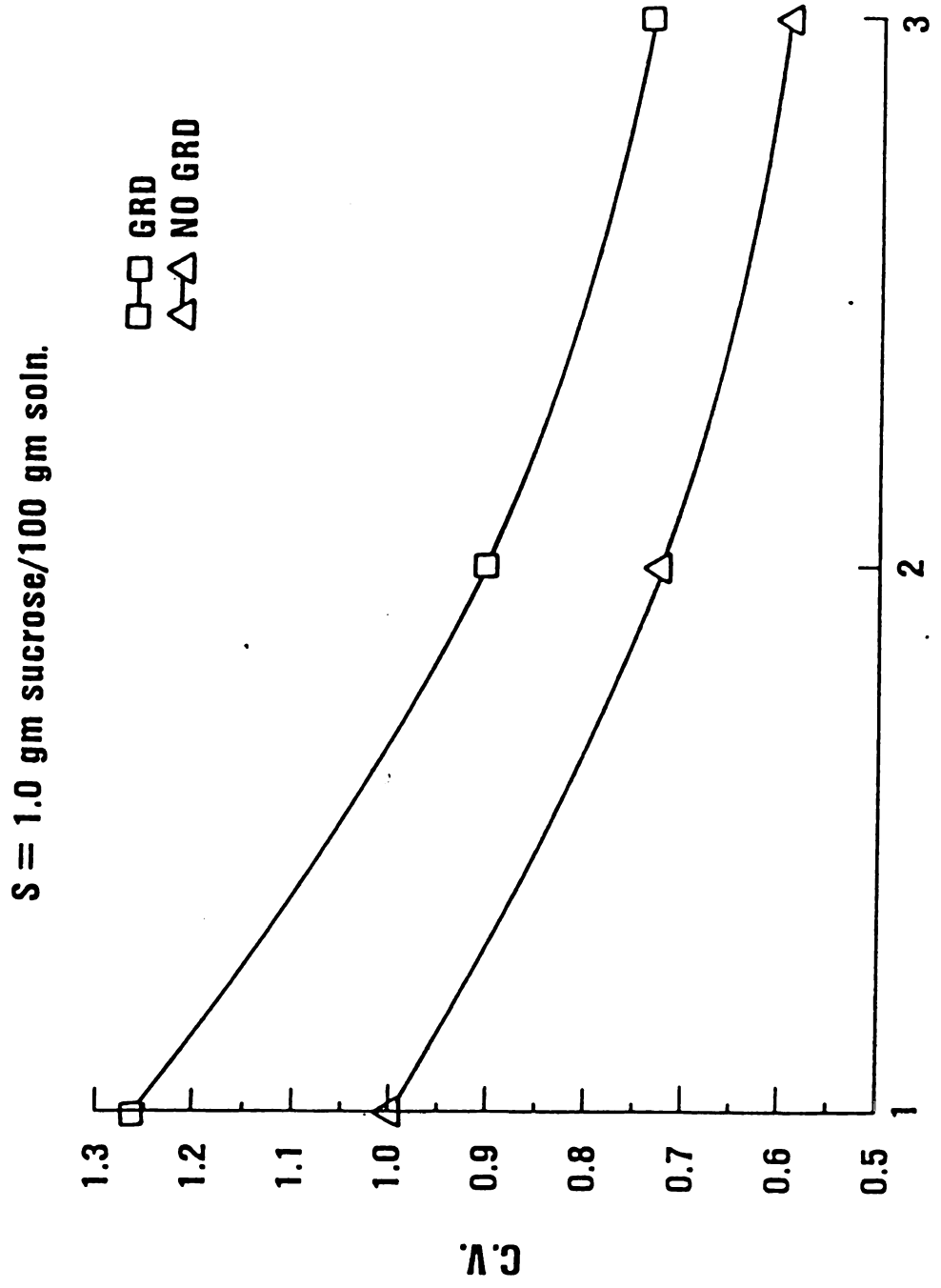

Figure 11. C.V. on a number basis versus number of stages for both GRD and no GRD at the supersaturation of 1.0 g sucrose/100 g soln.

dependent variables, the following conclusions can be drawn.

1. In general, a smaller mean crystal size on a number basis is produced in the case of GRD than that in the case of no GRD for both a single-stage and multistage MSMPR crystallizer. (Under the above design condition, the mean crystal size is determined mainly by the mean growth rate, which is a function of temperature on [S_j is a specified design variable]. Since GRD would result in a greater solute consumption, the operating temperature in the case of GRD is lower than that in the case of no GRD, so the mean crystal size in the case of GRD is smaller than that in the case of no GRD.)

2. The production rate tends to be larger in the case of GRD than that in the case of no GRD for both a single-stage and a multistage MSMPR crystallizer. (Since GRD would result in a greater solute consumption, the production rate in the case of GRD is larger than that in the case of no GRD.)

3. Staging increases the mean crystal size on a number basis for both GRD and no GRD

4. Staging decreases the production rate in the case of GRD; however, it increases the production slowly in the case of no GRD.

6.7 Nomenclature

A = frequency factor, μm/min

a, b = correlation constants

B° = nucleation rate, nuclei/(cm^3·min)

C = solute concentration, g/cm^3

C_o = inlet solute concentration g/cm^3

C^* - saturated solute concentration, g/cm^3

CV - coefficient of variation

E_G -activation energy, cal/g-mol

$f_G(g)$ - probability density function for growth rate

$f_L(L)$ - probability density function for crystal size

$\bar{G}$ - mean linear growth rate, $\mu m/min$

g - individual linear growth rat, $\mu m/min$

I - nucleation rate order with respect to M_T

J - nucleation rate order with respect to C

k_N - nucleation rate parameter

k_A - surface shape factor

k_v - volume shape factor

L - particle size, μm

$M_G(j,i)$ - the ith moment of growth rate distribution in the jth unit

$M_L(j,i)$ - the ith moment of crystal size distribution in the jth unit

M_T - suspension density, g/cm^3

m - crystal growth rate order

Num(j) - number of crystals per unit volume in the jth unit

n - number density of crystals, $\#/cm\text{-}cm^3$

n^o- number density of nuclei, $\#/cm\text{-}cm^3$

Q_o - free liquor feed rate, cm^3/min

Q - free liquor flow rate, cm^3/min

R - ideal gas constant, 1.987 cal/(g-mol K)

S = supersaturation, g of solute/100 g of solution

T = temperatre, K

V = free liquor volume

V_T = crystallizer volume

Greek Symbols

α, β = parameters in gamma distribution

ρ = crystal density, g/cm^3

τ = residence time, min

σ_G^2 = variance of growth rate distribution, $\mu m^2/min^2$

Subscript

j = in the jth unit

6.8 Literature Cited

Berglund, K.A. "Growth and Size Distribution Kinetics for Sucrose Crystals in the Sucrose-Water System", M.S. Thesis, Colorado State University, Ft. Collins, 1980.

Berglund, K.A.; Larson, M.A. "Growth and Growth Dispersion of Contact Nuclei", paper presented at 2nd World Congress Chemical Engineering, Montreal, 1981.

Berglund, K.A.; Larson, M.A., AIChE J., 1984, 30(2), 280.

Berglund, K.A.; Murphy, V.G., Ind. Eng. Chem. Fundam., 1986, 25, 174.

Berglund, K.A.; Kaufman, E.L.; Larson, M.A., AIChE J., 1983, 29(5), 867.

Larson, M.A.; White, E.T.; Ramanarayanan, K.A.; Berglund, K. A., AIChE J., 1985, 31(1), 90.

Larson, M.A.; Wolff, P.R., Chem. Eng. Prog. Symp.Ser., 1971, 67(110), 97.

Ramanarayanan, K.A., "Production and Growth of Contact Nuclei", Ph.D. Dissertation, Iowa State University, Ames, 1982.

Randolph, A.D.; Larson, M.A., AIChE J., 1962, 8(5), 639.

Randolph, A.D.; Larson, M.A.,"Theory of Particulate Processes", Academic Press, New York (1971).

Randolph, A.D.; Tan, C.S., Ind. Eng. Chem. Process Des. Dev., 1978, 17(2), 189.

Randolph, A.D.; White, E.T., Chem. Eng. Sci., 1977, 32, 1067.

Shiau, L.D.; Berglund, K.A., AIChE J., 1987, 33(6), 1028.

White, E.T.; Wright, P.G., Chem. Eng. Prog. Symp. Ser., 1971, 67(110), 81.

CHAPTER 7

SUMMARY

7.1 Concusions

From photomicroscopic experiments (Ch.3):

1. The photomicroscopic studies show that contact nuclei of fructose follow the CCG model in both pure fructose solution and fructose solution with glucose.

2. The mean and variance of the growth rate distribution were correlated in a power law. It was found that the variance of growth rate distribution increases as the mean growth rate is increased for both pure and impure solutions.

3. The presence of glucose greatly reduces the mean growth rate of fructose crystals. However, the correlation between the mean and variance of growth distribution has no significant change.

From modeling growth rate dispersion in a batch crystallizer (Ch.4):

1. A model has been developed to relate the resulting CSD from a seeded batch crystallizer with variable supersaturation during nucleation to the seed size distribution, the initial size distribution of subsequently generated nuclei, and the growth rate distribution based on the CCG assumption.

2. The model has been solved with a mass balance constraint to generate the resulting CSD for both an isothermal batch sucrose crysallizer and a constant level of supersaturation batch sucrose crystallizer. In general, smaller mean crystal sizes, larger

production rates, and larger coefficients of variation are produced in the case of GRD than those in the case of no GRD.

From batch crystallization experiments (Ch.5):

1. An analysis suggested based on the model developed in Ch.4 provides a simple method of recovering growth and nucleation rates from the resulting CSD of nuclei in a seeded batch crystallizer in presence of GRD.

2. The means and variances of growth rate distributions determined from the batch crystallization experiments of fructose through this analysis were in fairly good agreement with the results from the photomicroscopic studies.

3. The studies show the possible existence of three nucleation regions for various impurity ratios and relative supersaturation at $40^{o}C$: no nucleation in low supersaturated solution, nucleation of anhydrous crystals in moderately supersaturated solution, and formation of hemihydrates in highly supersaturated solution.

From modeling growth rate dispersion in a cascade of MSMPR crystallizers (Ch.6):

1. A model has been developed to relate the resulting CSD from a cascade of MSMPR crystallizers to the growth rate distributions of each stage based on the CCG assumption.

2. The model has been solved simultaneously with the mass balance to predict the CSD from a three-stage MSMPR sucrose crysallizer with continuous seeding into the first stage and growth in the subsequent stages. In general, smaller mean crystal sizes, larger production

rates, and larger coefficients of variation are produced in the case of GRD than those in the case of no GRD.

7.2 Proposals for Future Research

1. Hussmann et al. (1985) and Elankovan and Berglund (1987) suggested that the laser Raman microprobe can be an important tool in the study of contact nucleation. The technique should be used to determine if possibly structural differences of individual crystals are the causes of growth rate dispersion. In addition, the source of contact nuclei may be determined by comparing the nuclei spectra to the parent crystal spectra.

2. A Coulter counter should be used to determine the CSD from the fructose solutions in batch crystallization experiments through introducing a proper electrolyte. It would allow recovery of growth kinetics (mean and variance of growth rate diatribution) and nucleation rate from the CSD based on a larger amount of crystals.

3. Since the energy of contact can be controlled from the stirring rate of the impeller in batch crystallization experiments, the effects of contact energy on the growth behavior of nuclei (mean and variance of growth rate diatribution) generated should be examined.

4. Since a continuous process would always be of great interest, a cascade of single-stage or multi-stage crystallizers should be investigated to study growth and nucleation rates. The method of analysis is developed in Ch.6.

7.3 Literature Cited

Hussmann, G.A. et al., Applied Spectroscopy, 1985, 39(3), 560.

Elankovan, P.; Berglund, K.A., AIChE J., 1987, 33(11), 1844.

APPENDIX A: RAW DATA: INITIAL SIZES, GROWTH RATES, AND CORRELATION COEFFICIENTS FOR REGRESSION OF SIZE VERSUS TIME FOR CRYSTALS IN FRUCTOSE SOLUTION FROM THE PHOTOMICROSCOPIC EXPERIMENTS

Run 1, T=30°C; ΔT=1°C

Crystal no.	Size, μm, at various times			
	1.0hr	4.0hr	6.5hr	9.25hr
1	2.45	3.67	5.02	6.87
2	3.24	3.94	4.87	5.02
3	4.56	5.42	6.01	7.14
4	2.76	3.87	5.43	7.02
5	3.52	4.56	6.02	7.52
6	1.43	2.57	3.82	4.56
7	2.57	3.86	4.97	5.41
8	0.89	1.53	2.43	3.91
9	0.72	1.84	2.32	3.22
10	1.87	2.42	3.05	4.31
11	2.87	3.96	4.52	5.55
12	3.55	4.31	5.00	6.13
13	3.68	4.97	6.09	6.51
14	2.76	4.61	6.25	9.36
15	2.72	3.96	6.87	10.51
16	2.84	4.05	6.01	8.42

Crystal no.	Slope -growth rate μm/hr	intercept -initial size μm	Correlation coefficient
1	0.54	1.73	0.9932
2	0.23	3.08	0.9683
3	0.31	4.15	0.9944
4	0.52	2.05	0.9939
5	0.49	2.85	0.9938
6	0.39	1.07	0.9943
7	0.35	2.37	0.9819
8	0.36	0.30	0.9787
9	0.29	0.50	0.9937
10	0.29	1.40	0.9757
11	0.32	2.58	0.9961
12	0.32	3.14	0.9945
13	0.34	3.48	0.9818
14	0.83	1.41	0.9830
15	0.96	1.04	0.9735
16	0.68	1.79	0.9858

mean growth rate, μm/hr = 0.45

variance of growth rates, $\mu m^2/hr^2$ = 0.058

Run 2, T=30°C; ΔT=3°C

Crystal no.	Size, μm, at various times 0.5hr	2.0hr	5.2hr	8.5hr
1	2.82	7.90	12.30	19.46
2	0.75	7.82	14.13	22.31
3	1.21	3.57	5.89	9.21
4	1.45	4.83	6.92	10.57
5	0.93	5.88	9.42	15.21
6	0.53	7.91	11.22	20.10
7	0.47	8.23	11.89	19.73
8	3.21	10.81	13.72	20.17
9	2.86	9.75	11.24	17.62
10	1.92	8.74	10.92	16.78
11	4.21	9.32	19.92	28.26
12	1.39	3.18	5.16	8.47

Crystal no.	Slope -growth rate μm/hr	intercept -initial size μm	Correlation coefficient
1	1.97	2.66	0.9908
2	2.55	0.91	0.9892
3	0.95	1.11	0.9931
4	1.05	1.68	0.9801
5	1.67	1.12	0.9850
6	2.22	0.94	0.9733
7	2.19	1.22	0.9714
8	1.90	4.29	0.9594
9	1.61	3.83	0.9469
10	1.65	2.92	0.9545
11	3.03	3.20	0.9975
12	0.85	1.11	0.9943

mean growth rate, μm/hr = 1.80

variance of growth rates, $\mu m^2/hr^2$ = 0.42

Run 3, T=30°C; ΔT=5°C

Crystal no.	Size, μm, at various times 0.5hr	1.6hr	3.5hr	5.4hr
1	1.87	5.50	12.21	18.91
2	1.97	4.96	11.76	17.98
3	2.86	5.27	11.86	16.23
4	2.21	6.89	13.21	21.32
5	0.85	4.72	11.63	19.61
6	3.24	7.61	14.98	23.22
7	3.07	6.01	11.32	16.27
8	1.63	5.09	10.26	14.98
9	1.27	4.96	9.81	13.87
10	2.61	6.93	12.74	20.02
11	3.72	8.43	15.72	26.31

Crystal no.	Slope -growth rate μm/hr	intercept -initial size μm	Correlation coefficient
1	3.49	2.87	0.9999
2	3.32	4.73	0.9992
3	2.76	2.21	0.9854
4	3.83	0.37	0.9987
5	3.81	-1.30	0.9992
6	4.06	1.10	0.9997
7	2.70	1.73	0.9999
8	2.71	1.13	0.9927
9	2.54	0.48	0.9961
10	3.49	0.98	0.9986
11	4.54	1.06	0.9962

mean growth rate, μm/hr = 3.40

variance of growth rates, $\mu m^2/hr^2$ = 0.46

Run 4, T=30°C; ΔT=7°C

Crystal no.	Size, μm, at various times 0.4hr	1.5hr	2.5hr	3.4hr
1	4.51	10.62	16.31	22.12
2	3.72	9.97	13.29	17.92
3	0.97	8.72	13.93	16.89
4	1.34	6.64	12.81	18.22
5	2.87	7.97	12.73	18.44
6	4.52	8.01	12.07	15.62
7	3.97	7.86	11.22	16.93
8	2.53	7.12	12.93	17.17
9	3.72	6.70	10.20	13.96
10	2.53	5.64	8.91	11.72
11	5.62	10.17	16.31	21.14
12	4.71	8.11	12.91	15.62
13	6.01	11.32	17.02	23.51
14	4.31	10.87	16.69	19.71
15	4.13	8.71	13.53	16.72
16	5.71	10.86	16.73	21.46
17	6.72	14.01	21.40	26.98

Crystal no.	Slope -growth rate μm/hr	intercept -initial size μm	Correlation coefficient
1	5.84	2.00	0.9994
2	4.60	2.26	0.9905
3	4.97	0.99	0.9837
4	4.93	0.25	0.9835
5	5.13	0.50	0.9972
6	3.73	2.79	0.9984
7	4.20	1.81	0.9878
8	4.97	0.25	0.9980
9	4.19	1.13	0.9715
10	3.82	1.15	0.9450
11	5.26	3.10	0.9969
12	3.75	3.02	0.9957
13	5.80	3.16	0.9960
14	5.23	2.70	0.9936
15	4.26	2.46	0.9987
16	5.31	3.34	0.9990
17	6.82	3.98	0.9995

mean growth rate, μm/hr = 4.87

variance of growth rates, $\mu m^2/hr^2$ = 0.69

Run 5, T=40°C; ΔT=1°C

Crystal no.	Size, μm, at various times 1.0hr	3.0hr	5.0hr	7.0hr	9.0hr
1	2.31	3.01	3.89	4.56	5.37
2	4.61	8.08	13.21	17.28	21.58
3	5.58	7.87	10.47	12.91	15.36
4	5.43	6.19	7.12	7.84	8.46
5	5.51	6.46	7.48	8.89	9.76
6	6.92	7.03	7.54	8.04	9.08
7	7.26	10.01		14.27	16.02
8	8.64	10.07	11.46	12.68	14.01
9	10.80	12.31		14.73	16.23
10	8.64	10.22		13.70	14.04
11	14.04	15.22	16.44	17.48	18.14

Crystal no.	Slope -growth rate μm/hr	intercept -initial size μm	Correlation coefficient
1	0.38	1.91	0.9993
2	2.11	2.60	1.0000
3	1.23	4.29	0.9998
4	0.39	5.08	0.9977
5	0.55	4.89	0.9974
6	0.27	6.39	0.9572
7	1.09	6.44	0.9973
8	0.67	8.03	0.9996
9	0.66	10.20	0.9990
10	0.71	8.08	0.9849
11	0.63	13.65	0.9944

mean growth rate, μm/hr = 0.75

variance of growth rates, $\mu m^2/hr^2$ = 0.31

Run 6, T=40°C; ΔT=3°C

Crystal no.	Size, μm, at various times 1.0hr	2.0hr	3.0hr	5.0hr	7.0hr
1	3.66	5.81	8.47	12.91	17.28
2	5.18	6.87	10.83	16.32	21.63
3	4.23		6.68	9.27	11.74
4	5.47	7.18	9.54	13.49	17.94
5	6.47	10.19	13.55	20.52	27.51
6	6.42	9.43	12.24	17.43	23.01
7	7.94	9.08	12.45	16.04	20.45
8	7.53	8.17	11.31	14.23	17.69
9	7.19		13.02	15.34	19.76
10	9.64		14.93	19.42	24.31
11	11.07	14.53	18.11	24.51	31.24
12	10.44		12.63	15.72	17.54

Crystal no.	Slope -growth rate μm/hr	intercept -initial size μm	Correlation coefficient
1	2.28	1.41	0.9996
2	2.82	2.01	0.9975
3	1.26	2.96	1.0000
4	2.09	3.21	0.9994
5	3.49	3.07	0.9999
6	2.74	3.85	0.9997
7	2.13	5.54	0.9958
8	1.75	5.48	0.9925
9	2.00	5.82	0.9873
10	2.42	7.38	0.9995
11	3.35	7.84	0.9998
12	1.22	9.20	0.9955

mean growth rate, μm/hr = 2.29

variance of growth rates, $\mu m^2/hr^2$ = 0.52

Run 7, T=40°C; ΔT=5°C

Crystal no.	Size, μm, at various times 0.5hr	1.0hr	2.0hr	3.0hr
1	2.39	4.25	8.29	11.33
2	1.77	4.97	7.87	11.92
3	3.64	6.11	10.64	14.21
4	3.64	5.50	11.17	15.31
5	2.84	5.23	8.94	13.34
6	4.44	6.31	12.10	18.11
7	4.81	6.04	9.96	15.16
8	4.03	5.74	10.02	13.24
9	7.71	11.30	20.42	28.01
10	8.28	12.54	15.39	24.74
11	5.86	10.12	14.47	16.53
12		6.86	10.51	15.59

Crystal no.	Slope -growth rate μm/hr	intercept -initial size μm	Correlation coefficient
1	3.62	0.69	0.9980
2	3.85	0.37	0.9918
3	4.23	1.77	0.9977
4	4.80	1.10	0.9974
5	4.13	0.88	0.9992
6	5.56	1.21	0.9977
7	4.49	1.95	0.9732
8	3.75	2.16	0.9982
9	8.25	3.45	0.9991
10	6.14	5.26	0.9756
11	4.13	5.03	0.9651
12	4.36	2.26	0.9956

mean growth rate, $\mu m/hr$ = 4.78

variance of growth rates, $\mu m^2/hr^2$ = 1.77

Run 8, T=40°C; ΔT=7°C

Crystal no.	Size, μm, at various times 0.5hr	1.0hr	1.5hr	2.0hr
1	5.13	9.67	14.12	18.81
2	5.81	9.94	15.29	17.23
3	6.24	9.56	13.19	16.56
4	7.07	10.51	13.43	16.16
5	10.74	13.28	16.33	18.46
6	11.64	14.13	17.28	23.31
7	7.82	10.77	13.12	16.01
8	8.42	10.34	13.67	15.82
9	6.74	9.36	12.91	14.72
10	3.31	7.23		13.59
11	4.52	8.74		17.59
12	4.09	6.54	8.51	11.17

Crystal no.	Slope -growth rate $\mu m/hr$	intercept -initial size μm	Correlation coefficient
1	9.10	0.11	0.9999
2	7.92	2.17	0.9858
3	6.92	2.74	0.9998
4	6.04	4.24	0.9986
5	5.24	8.15	0.9979
6	7.63	7.05	0.9776
7	5.38	5.40	0.9991
8	5.11	5.68	0.9947
9	5.50	4.06	0.9932
10	6.78	0.13	0.9985
11	8.38	0.35	0.9985
12	4.64	1.78	0.9985

mean growth rate, $\mu m/hr$ = 6.55

variance of growth rates, $\mu m^2/hr^2$ = 2.25

Run 9, T=50°C; ΔT=3°C

Crystal no.	Size, μm, at various times 1.0hr	2.0hr	3.0hr	5.0hr	7.0hr
1	10.54		13.75	16.82	19.64
2	7.49		13.32	15.64	20.06
3	7.83	8.91	12.34	15.93	19.35
4	5.42	8.43	14.99		25.03
5	4.67	6.82	9.48	13.92	18.29
6	6.43		10.88	11.47	16.94
7	4.07	5.76	9.72	15.21	20.52
8	7.13		12.42	16.90	22.72
9	6.58	8.29	10.65	14.60	19.05
10	4.53	5.17	8.31	11.23	14.69
11	8.14		13.43	17.92	23.81
12	8.43	11.44	14.25	19.44	25.02
13	3.54	4.68	8.05	11.64	16.05
14	3.50	4.14	7.28	10.26	13.68
15	5.47	9.48	12.56	19.52	26.49
16	3.04	4.92	7.95		15.72
17	7.38	9.74	13.02		18.04
18	8.54		13.74	18.92	23.78
19	5.45	10.62	13.41	20.06	27.12
20	6.48	10.49	13.57	20.53	27.80

Crystal no.	Slope -growth rate μm/hr	intercept -initial size μm	Correlation coefficient
1	1.52	9.10	0.9996
2	2.00	6.12	0.9873
3	2.13	5.43	0.9958
4	3.25	2.91	0.9837
5	2.28	2.42	0.9996
6	1.56	7.06	0.8667
7	2.82	0.90	0.9975
8	2.56	4.54	0.9989
9	2.09	4.32	0.9994
10	1.75	2.48	0.9925
11	2.42	5.88	0.9995
12	2.74	5.86	0.9997
13	2.13	1.14	0.9958
14	1.77	1.45	0.9925
15	3.47	2.22	0.9997
16	2.12	1.02	0.9975
17	1.72	6.47	0.9776
18	2.55	6.07	0.9998
19	3.50	2.75	0.9974
20	3.48	3.23	0.9997

mean growth rate, μm/hr = 2.40

variance of growth rates, $\mu m^2/hr^2$ = 0.41

Run 10 ,T=50°C; ΔT=5°C

Crystal no.	Size, μm, at various times 0.5hr	1.0hr	2.0hr	3.0hr
1	7.96	12.22	16.57	18.63
2	4.13	5.84	10.12	13.34
3	4.80	6.03	9.95	15.15
4		8.86	12.52	17.58
5	5.43	9.05	13.42	18.06
6	3.72	7.24	9.51	12.22
7	3.86	8.12	12.47	14.53
8	2.87	6.12	10.97	13.82
9	3.02	7.96	9.52	13.97
10	5.01	9.96	13.42	16.02
11	2.04	6.46	10.02	13.59
12	2.47	5.06	7.34	9.58
13		8.94	14.01	19.52
14	4.82	7.54	12.43	15.02
15	1.46	4.32	6.03	9.23

Crystal no.	Slope -growth rate $\mu m/hr$	intercept -initial size μm	Correlation coefficient
1	4.13	5.03	0.9651
2	3.75	2.26	0.9982
3	4.49	1.94	0.9732
4	4.36	4.46	0.9956
5	4.91	3.51	0.9960
6	3.16	3.03	0.9739
7	4.13	3.03	0.9652
8	3.76	2.20	0.9699
9	3.91	2.27	0.9405
10	4.12	4.40	0.9600
11	4.37	0.93	0.9805
12	2.71	1.71	0.9842
13	5.29	3.58	0.9997
14	4.12	3.26	0.9882
15	2.88	0.58	0.9817

mean growth rate, $\mu m/hr$ = 4.03

variance of growth rates, $\mu m^2/hr^2$ = 0.56

Run 11, T=50°C; ΔT=7°C

Crystal no.	Size, μm, at various times 0.5hr	1.0hr	1.5hr	2.0hr
1	6.24	10.78	15.23	19.92
2	6.06	9.50	12.42	15.15
3	6.43	9.82	13.42	16.51
4	3.41	8.24		14.05
5	4.62	9.75		17.52
6	9.52	11.44	14.77	16.92
7	7.73	10.37	13.92	15.73
8	5.53	10.42	14.08	19.42
9	4.47	10.51	15.41	19.96
10	7.43	10.53	13.81	16.22
11	8.74	11.40	13.95	16.70
12	10.62	12.53	15.82	18.01
13	9.42	13.42	16.51	21.20

Crystal no.	Slope -growth rate μm/hr	intercept -initial size μm	Correlation coefficient
1	9.10	1.22	0.9999
2	6.04	3.23	0.9986
3	6.77	3.09	0.9996
4	6.91	0.51	0.9906
5	8.48	0.74	0.9974
6	5.12	6.78	0.9948
7	5.51	5.07	0.9933
8	9.07	1.03	0.9977
9	10.27	-0.26	0.9978
10	5.93	4.59	0.9980
11	5.53	5.07	0.9931
12	5.07	7.90	0.9963
13	7.69	5.53	0.9971

mean growth rate, μm/hr = 7.02

variance of growth rates, $\mu m^2/hr^2$ = 3.28

Run 12, T=50°C; ΔT=9°C

Crystal no.	Size, μm, at various times 0.5hr	1.0hr	1.5hr	2.0hr
1	7.93	13.42	18.05	24.03
2	8.71	13.59	19.41	25.22
3	9.41	14.06	20.51	26.43
4	13.62	20.43	27.53	33.66
5	10.42	18.41		32.40
6	5.63	10.76		16.43
7	8.31	12.30	15.42	20.09
8	6.43	11.65	15.06	19.43
9	10.30	14.57	17.99	23.54
10	6.46	10.50	14.43	17.99
11	7.07	12.47	17.04	21.90
12	9.32	13.34	16.49	21.53
13	9.39	12.34		20.66
14	10.02	17.93	25.93	33.80

Crystal no.	Slope -growth rate μm/hr	intercept -initial size μm	Correlation coefficient
1	10.59	2.63	0.9989
2	11.07	2.90	0.9991
3	11.50	3.23	0.9980
4	13.44	7.01	0.9996
5	14.56	3.43	0.9994
6	6.98	2.80	0.9870
7	7.71	4.40	0.9972
8	8.48	2.54	0.9969
9	8.63	5.82	0.9954
10	7.70	2.72	0.9996
11	9.81	2.36	0.9994
12	7.96	5.23	0.9960
13	7.63	5.23	0.9969
14	15.92	2.04	0.9999

mean growth rate, μm/hr = 10.14

variance of growth rates, $\mu m^2/hr^2$ = 7.67

APPENDIX B: RAW DATA: INITIAL SIZES, GROWTH RATES, AND CORRELATION COEFFICIENTS FOR REGRESSION OF SIZE VERSUS TIME FOR CRYSTALS IN GLUCOSE-CONTAINING FRUCTOSE SOLUTION FROM THE PHOTOMICROSCOPIC EXPERIMENTS

Run 13, T=40°C; ΔT=1°C; I/W=0.05

Crystal no.	Size, μm, at various times 1.0hr	4.0hr	6.5hr	9.25hr
1	2.82	4.16	7.08	12.50
2	1.86	2.95	3.51	4.54
3	3.87	4.43	5.04	6.31
4	1.48	2.62	3.88	4.60
5	4.52		6.73	8.42
6	3.87	4.98	6.54	8.13
7	5.56	6.42	7.02	8.13
8	1.85	4.08	6.09	7.93
9	2.84		6.43	8.12
10	2.71		6.25	9.41
11	3.88	4.87	6.42	7.97
12	3.57		6.42	7.01

Crystal no.	Slope -growth rate μm/hr	intercept -initial size μm	Correlation coefficient
1	0.97	1.24	0.9736
2	0.32	1.57	0.9962
3	0.29	3.40	0.9756
4	0.39	1.09	0.9944
5	0.46	3.97	0.9936
6	0.52	3.16	0.9940
7	0.31	5.14	0.9939
8	0.74	1.13	0.9994
9	0.64	2.21	0.9999
10	0.79	1.72	0.9876
11	0.51	3.17	0.9916
12	0.43	3.26	0.9852

mean growth rate, μm/hr = 0.53

variance of growth rates, $\mu m^2/hr^2$ = 0.047

Run 14, T=40°C; ΔT=3°C; I/W=0.05

Crystal no.	Size, μm, at various times 0.5hr	2.0hr	5.2hr	8.5hr
1	2.97	9.86	11.35	17.73
2	1.81	8.63	10.80	16.70
3	0.57	8.34	11.98	19.83
4	1.93	6.97	10.43	16.21
5	1.76	7.83	12.14	21.33
6	1.26	3.66	5.93	9.26
7	3.42	4.57	5.81	7.42
8	3.72	5.06	7.92	10.88
9	1.72		9.89	15.43
10	2.87	5.31	8.94	14.88
11	2.87	9.69	11.42	17.68
12	4.32	11.42	13.52	18.93
13	1.82	8.74	10.61	16.05

Crystal no.	Slope -growth rate μm/hr	intercept -initial size μm	Correlation coefficient
1	1.62	3.94	0.9468
2	1.66	2.81	0.9545
3	2.18	1.32	0.9713
4	1.68	2.12	0.9851
5	2.28	1.52	0.9862
6	0.94	1.16	0.9932
7	0.48	3.36	0.9945
8	0.89	3.27	1.0000
9	1.72	0.89	0.9999
10	1.46	2.08	0.9952
11	1.63	3.82	0.9507
12	1.61	5.53	0.9465
13	1.56	2.98	0.9454

mean growth rate, μm/hr = 1.56

variance of growth rates, $\mu m^2/hr^2$ = 0.20

Run 15, T=40°C; ΔT=5°C; I/W=0.05

Crystal no.	Size, μm, at various times 1.0hr	2.0hr	3.0hr	5.0hr	7.0hr
1	7.68	9.39	11.75	15.70	20.15
2	4.52	5.18	8.33	11.20	14.70
3	10.16		15.45	19.94	25.83
4	8.42		14.33	17.82	23.02
5	3.40	4.04	7.18	10.16	13.57
6	6.45	11.61	14.40	21.07	28.11
7	4.48	8.49	11.56	18.54	25.79
8	3.54		8.74	13.93	18.79
9	8.40	11.41	14.22	19.41	25.00
10	7.42	9.62	13.02	15.72	17.63
11	3.69	7.42	8.39	10.52	15.06
12	2.45	6.92	10.45	14.32	20.88
13	0.48	1.52	2.49		6.44
14	1.43	2.06	3.97		8.02
15	5.24	8.02	11.43	19.02	28.31

Crystal no.	Slope -growth rate μm/hr	intercept -initial size μm	Correlation coefficient
1	2.08	5.42	0.9995
2	1.76	2.47	0.9926
3	2.42	8.91	0.9996
4	2.36	6.44	0.9957
5	1.76	1.35	0.9926
6	3.51	3.74	0.9974
7	3.47	1.22	0.9997
8	2.55	1.06	0.9998
9	2.74	5.83	0.9997
10	1.70	6.56	0.9729
11	1.70	2.90	0.9778
12	2.90	0.56	0.9917
13	0.99	-0.49	0.9999
14	1.12	0.22	0.9939
15	3.86	0.51	0.9964

mean growth rate, μm/hr = 2.33

variance of growth rates, $\mu m^2/hr^2$ = 0.77

Run 16, T=40°C; ΔT=7°C; I/W=0.05

Crystal no.	Size, μm, at various times 0.5hr	1.5hr	3.4hr	5.0hr
1	4.21	10.82	21.43	30.52
2	7.64	12.82	22.73	37.54
3	5.89	11.42	20.62	25.60
4	6.24	13.62		27.82
5	7.25	14.52	21.52	29.62
6	4.31	12.53	24.82	34.11
7	3.79	13.45	22.79	35.91
8	3.72	9.69	21.42	29.50
9	4.53	15.72	24.83	38.82
10	3.94	16.83	25.77	39.59
11	3.25	8.01		22.98

Crystal no.	Slope -growth rate μm/hr	intercept -initial size μm	Correlation coefficient
1	5.79	1.68	0.9996
2	6.50	3.28	0.9890
3	4.15	5.61	0.9843
4	4.60	5.15	0.9916
5	4.75	5.87	0.9935
6	6.56	1.88	0.9980
7	6.79	1.32	0.9932
8	5.78	1.06	0.9990
9	7.18	2.31	0.9899
10	7.39	2.31	0.9859
11	4.36	1.25	0.9998

mean growth rate, μm/hr = 5.81

variance of growth rates, $\mu m^2/hr^2$ = 1.48

Run 17, T=40°C; ΔT=9°C; I/W=0.05

Crystal no.	Size, μm, at various times 0.5hr	1.0hr	1.5hr	2.0hr
1	8.72	12.89	16.73	19.92
2	8.93	11.88	14.24	17.10
3	5.53	9.75	14.73	17.72
4	7.33		13.99	17.78
5	6.04		12.54	16.44
6	4.12	8.66	13.11	17.80
7	5.70	9.83	15.19	17.13
8	4.53	8.94	12.71	17.50
9	7.63	9.06	11.82	17.44
10	6.09	9.71	12.56	18.91
11	4.87	8.99	11.34	14.59
12	8.71	13.45	18.93	23.02
13	7.49	11.02	14.01	16.78
14	3.72	6.93	8.92	11.31

Crystal no.	Slope -growth rate $\mu m/hr$	intercept -initial size μm	Correlation coefficient
1	7.49	5.21	0.9983
2	5.39	6.51	0.9990
3	8.31	1.55	0.9956
4	6.92	3.80	0.9995
5	6.87	2.51	0.9989
6	9.11	-0.90	0.9989
7	7.93	2.06	0.9857
8	8.54	0.25	0.9990
9	6.44	3.44	0.9591
10	8.26	1.49	0.9841
11	6.30	2.07	0.9945
12	9.68	3.93	0.9986
13	6.17	4.61	0.9984
14	4.95	1.53	0.9951

mean growth rate, $\mu m/hr$ = 7.32

variance of growth rates, $\mu m^2/hr^2$ = 1.94

Run 18, T=40°C; ΔT=1°C; I/W=0.3

Crystal no.	Size, μm, at various times 2.24hr	9.5hr	16.8hr	22.0hr
1	0.89	1.24	2.36	3.06
2	1.24	3.02	4.05	4.91
3	2.44	5.87	9.01	11.72
4	1.89	4.53		8.41
5	1.51	2.02	2.87	3.08
6	1.56	1.98		2.86
7	1.72	3.08	6.24	7.02
8	0.74	1.06	3.04	3.87
9	1.56	2.93	4.52	6.77
10	2.46	5.62	9.42	12.91
11	0.72	1.36	2.06	2.72
12	0.93	1.24	1.97	2.40
13	0.45	0.96	1.23	1.48

Crystal no.	Slope -growth rate μm/hr	intercept -initial size μm	Correlation coefficient
1	0.11	0.45	0.9781
2	0.18	1.01	0.9918
3	0.46	1.39	0.9995
4	0.33	1.26	0.9991
5	0.08	1.31	0.9888
6	0.06	1.39	0.9988
7	0.29	0.88	0.9832
8	0.17	0.03	0.9643
9	0.25	0.72	0.9817
10	0.52	0.97	0.9959
11	0.10	0.45	0.9970
12	0.07	0.66	0.9870
13	0.05	0.39	0.9901

mean growth rate, μm/hr = 0.21

variance of growth rates, $\mu m^2/hr^2$ = 0.026

Run 19, T=40°C; ΔT=3°C; I/W=0.3

Crystal no.	Size, μm, at various times 1.5hr	4.0hr	6.2hr	9.5hr
1	1.78	3.02	4.21	5.62
2	0.98	3.42	5.06	6.51
3	2.42	4.68	5.99	7.61
4	2.89	5.08	5.92	6.54
5	0.88	1.42	1.99	2.56
6	1.42	1.96	2.42	3.87
7	1.36	3.89	5.45	7.02
8	0.87	1.36	2.30	3.31
9	1.42	3.03	3.97	5.22
10	0.72	1.36		2.43
11	0.67	0.93	1.21	1.42
12	1.24	4.22	6.36	8.06

Crystal no.	Slope -growth rate μm/hr	intercept -initial size μm	Correlation coefficient
1	0.48	1.10	0.9988
2	0.69	0.36	0.9820
3	0.64	1.79	0.9882
4	0.44	2.78	0.9364
5	0.21	0.59	0.9967
6	0.30	0.81	0.9797
7	0.70	0.73	0.9833
8	0.32	0.29	0.9926
9	0.47	0.93	0.9908
10	0.21	0.45	0.9976
11	0.10	0.55	0.9898
12	0.85	0.47	0.9806

mean growth rate, μm/hr = 0.45

variance of growth rates, $\mu m^2/hr^2$ = 0.055

Run 20, T=40°C; ΔT=5°C; I/W=0.3

Crystal no.	Size, μm, at various times 0.5hr	2.0hr	5.2hr	8.5hr
1	3.87	10.70	12.41	18.68
2	1.75		9.92	15.46
3	1.06	3.45	5.74	9.46
4	3.77	9.82	14.31	24.89
5	1.56	9.33	12.99	20.82
6	0.83	5.87	9.32	15.11
7	4.72	6.05	8.93	11.87
8	2.88	5.32	8.95	14.89
9	2.34	7.06	16.82	25.71
10	1.87	8.62	17.13	27.02
11	0.87	3.21	4.96	8.02

Crystal no.	Slope -growth rate μm/hr	intercept -initial size μm	Correlation coefficient
1	1.64	4.82	0.9508
2	1.72	0.92	0.9999
3	0.94	1.36	0.9932
4	2.43	3.02	0.9731
5	2.17	2.33	0.9712
6	1.69	1.02	0.9851
7	0.89	4.27	0.9999
8	1.46	2.09	0.9952
9	2.93	1.13	0.9994
10	3.05	1.31	0.9966
11	0.84	0.88	0.9873

mean growth rate, μm/hr = 1.79

variance of growth rates, $\mu m^2/hr^2$ = 0.62

Run 21, T=40°C; ΔT=7°C; I/W=0.3

Crystal no.	Size, μm, at various times 0.4hr	1.67hr	4.2hr	6.5hr
1	2.71	6.42	9.52	16.03
2	1.45	8.62	10.72	19.45
3	1.93	9.43	15.06	18.71
4	3.72	8.72	14.32	19.72
5	2.71	7.42	14.62	25.70
6	3.82	9.41	14.88	26.66
7	1.62	5.43		12.51
8	2.42	5.63	10.22	16.01
9	4.72	8.71	11.46	19.05
10	3.21		12.44	19.81
11	2.73		17.72	26.41
12	3.74	10.25	20.52	30.64
13	4.86	12.71	22.43	35.01
14	0.89		9.84	16.66
15	2.71	5.71	12.42	19.02

Crystal no.	Slope -growth rate μm/hr	intercept -initial size μm	Correlation coefficient
1	2.05	2.12	0.9861
2	2.63	1.68	0.9610
3	2.60	2.99	0.9634
4	2.54	3.19	0.9941
5	3.66	0.92	0.9933
6	3.54	2.38	0.9850
7	1.70	1.67	0.9883
8	2.17	1.64	0.9976
9	2.18	4.03	0.9778
10	2.69	1.86	0.9971
11	3.89	1.23	0.9999
12	4.35	2.41	0.9994
13	4.80	3.38	0.9966
14	2.56	-0.35	0.9980
15	2.68	1.41	0.9994

mean growth rate, μm/hr = 2.94

variance of growth rates, $\mu m^2/hr^2$ = 0.80

Run 22, T=40°C; ΔT=9°C; I/W=0.3

Crystal no.	Size, μm, at various times 0.4hr	1.5hr	3.2hr	5.25hr
1	3.45	9.42	17.63	24.50
2	1.86	9.43	16.93	23.71
3	2.74	11.31	19.26	27.02
4	2.64	13.62	20.72	29.52
5	3.65	14.64	21.02	30.64
6	4.04	15.72	23.62	34.51
7	3.71	16.72	24.06	35.22
8	1.89	8.46	15.72	20.88
9	2.41	9.56	17.02	22.91
10	2.41	8.55		20.19
11	2.70	11.42	19.99	28.12
12	4.66	16.79	23.51	35.20

Crystal no.	Slope -growth rate μm/hr	intercept -initial size μm	Correlation coefficient
1	4.34	2.53	0.9942
2	4.41	1.58	0.9881
3	4.87	2.48	0.9882
4	5.26	3.01	0.9798
5	5.25	3.90	0.9810
6	5.99	3.98	0.9857
7	6.12	4.09	0.9797
8	3.86	1.74	0.9836
9	4.15	2.23	0.9854
10	3.52	1.99	0.9917
11	5.04	2.07	0.9920
12	5.92	4.69	0.9830

mean growth rate, μm/hr = 4.93

variance of growth rates, $\mu m^2/hr^2$ = 0.74

Run 23, T=40°C; ΔT=11°C; I/W=0.3

Crystal no.	Size, μm, at various times 0.5hr	1.0hr	1.5hr	2.0hr
1	2.86	6.99	9.35	12.59
2	7.61	10.50		15.72
3	6.08	9.72	12.54	18.93
4	4.63	9.05	12.82	18.49
5	4.70	8.84	14.20	16.13
6	7.59	11.13	14.10	16.88
7	3.74	6.95	8.94	11.33
8	2.64	7.53	9.06	13.07
9	4.68	10.72	11.56	15.02
10	5.42	7.22		11.72
11	3.51	8.04	9.51	14.01
12	6.46	12.21	16.71	20.59
13	5.68	10.72	13.94	19.02

Crystal no.	Slope -growth rate μm/hr	intercept -initial size μm	Correlation coefficient
1	6.31	0.08	0.9946
2	5.38	5.00	0.9997
3	8.25	1.48	0.9841
4	8.53	0.35	0.9990
5	7.93	3.06	0.9856
6	6.18	4.70	0.9985
7	4.95	1.52	0.9951
8	6.56	-0.13	0.9828
9	6.37	2.53	0.9565
10	4.23	3.17	0.9986
11	6.59	0.53	0.9834
12	9.38	2.27	0.9960
13	8.65	1.53	0.9964

mean growth rate, μm/hr = 6.88

variance of growth rates, $\mu m^2/hr^2$ = 2.42

Run 24 T=40°C; ΔT=5°C; I/W=0.6

Crystal no.	Size, μm, at various times			
	2.24r	9.5hr	16.8hr	22.0hr
1	1.73	2.37	3.07	3.73
2	0.72	1.04	3.02	3.85
3	1.67	3.04	4.63	6.88
4	1.79	4.23		7.94
5	1.62	4.72	6.42	9.73
6	0.99	1.24	3.24	4.06
7	2.42	5.02		9.66
8	3.42	4.51	5.96	7.02
9	0.76	1.93	2.84	3.52
10	1.24	2.06	3.07	3.99
11	0.88	1.46	2.42	3.27
12	0.93	1.23	1.80	2.24
13	1.23	2.01	2.96	3.36
14	1.31	2.03	2.56	3.26

Crystal no.	Slope =growth rate μm/hr	intercept =initial size μm	Correlation coefficient
1	0.10	1.46	0.9971
2	0.17	0.01	0.9643
3	0.26	0.83	0.9817
4	0.31	1.17	0.9994
5	0.39	0.74	0.9854
6	0.17	0.27	0.9594
7	0.37	1.57	0.9999
8	0.18	2.91	0.9976
9	0.14	0.51	0.9981
10	0.14	0.84	0.9957
11	0.12	0.48	0.9894
12	0.07	0.70	0.9889
13	0.11	0.99	0.9968
14	0.10	1.09	0.9942

mean growth rate, μm/hr = 0.19

variance of growth rates, $\mu m^2/hr^2$ = 0.012

Run 25, T=40°C; ΔT=7°C; I/W=0.6

Crystal no.	Size, μm, at various times 0.5hr	4.17hr	8.5hr	12.25hr
1	1.43	5.26	9.32	14.05
2	3.62	8.72	11.66	18.52
3	2.97	10.42	12.67	19.96
4	1.73	4.81	9.03	13.95
5	4.32	10.66	14.53	21.02
6	2.06	11.43		30.71
7	3.61	11.99	18.64	27.26
8	1.83	3.79	7.62	10.53
9	2.63	4.12	8.02	11.49
10	3.41	4.96	7.52	9.03
11	3.56	12.73	25.77	30.62
12	2.41	3.06	4.51	6.22
13	0.98	1.46	2.58	3.96

Crystal no.	Slope -growth rate μm/hr	intercept -initial size μm	Correlation coefficient
1	1.06	0.79	0.9982
2	1.20	3.02	0.9846
3	1.24	2.74	0.8983
4	1.03	0.82	0.9952
5	1.36	4.00	0.9922
6	2.43	1.03	0.9999
7	1.96	2.95	0.9969
8	0.76	1.13	0.9959
9	0.86	0.78	0.9780
10	0.49	3.10	0.9972
11	2.39	3.00	0.9898
12	0.32	1.98	0.9843
13	0.25	0.63	0.9815

mean growth rate, μm/hr = 1.18

variance of growth rates, $\mu m^2/hr^2$ = 0.51

Run 26, T=40°C; ΔT=9°C; I/W=0.6

Crystal no.	Size, μm, at various times 0.5hr	2.75hr	6.2hr	8.5hr
1	2.74	5.62	9.11	17.62
2	3.62	9.72	14.33	26.22
3	4.58	10.52	15.63	26.77
4	5.62	13.62	23.72	32.03
5	3.72	12.43	21.72	30.22
6	2.76	10.93	19.42	29.66
7	3.63	9.78	17.51	26.30
8	4.62	11.73	18.62	28.03
9	2.74	12.63	19.99	31.02
10	5.62	16.32	24.63	38.66
11	4.62	9.70	12.22	19.71
12	3.03	8.63	12.24	22.66
13	3.78	6.42	10.33	18.46

Crystal no.	Slope -growth rate μm/hr	intercept -initial size μm	Correlation coefficient
1	1.73	1.01	0.9536
2	2.59	1.83	0.9645
3	2.57	2.83	0.9718
4	3.24	4.20	0.9991
5	3.23	2.59	0.9975
6	3.22	1.23	0.9937
7	2.74	2.00	0.9942
8	2.78	3.27	0.9908
9	3.32	1.72	0.9881
10	3.86	3.98	0.9850
11	1.71	3.91	0.9654
12	2.23	1.61	0.9615
13	1.73	2.00	0.9594

mean growth rate, μm/hr = 2.70

variance of growth rates, $\mu m^2/hr^2$ = 0.46

Run 27, T=40°C; ΔT=11°C; I/W=0.6

Crystal no.	Size, μm, at various times 0.4hr	1.5hr	3.25hr	5.0hr
1	5.03	10.14	15.22	23.62
2	2.74	9.62	14.33	20.51
3	3.64	11.72	16.03	24.81
4	6.04	12.04	18.41	25.63
5	2.03	8.41	12.12	17.51
6	2.71	7.92	11.23	15.66
7	6.94	10.72	15.76	18.41
8	3.72	11.66	16.24	23.91
9	5.42	9.63	19.06	26.03
10	3.02	8.22	16.42	24.01
11	4.63	8.99	16.94	24.72
12	6.61	10.72	15.24	23.02
13	3.72	5.93	9.72	12.93
14	3.62	9.22	18.48	25.72
15	2.73	8.65	16.62	25.02
16	2.72	4.72	7.34	10.43

Crystal no.	Slope -growth rate μm/hr	intercept -initial size μm	Correlation coefficient
1	3.91	3.59	0.9951
2	3.67	2.48	0.9874
3	4.30	3.13	0.9844
4	4.16	4.97	0.9975
5	3.19	1.86	0.9860
6	2.66	2.62	0.9846
7	2.51	6.60	0.9865
8	4.13	3.41	0.9849
9	4.09	5.68	0.9859
10	4.57	1.32	0.9998
11	4.40	2.66	0.9997
12	3.46	5.11	0.9939
13	2.02	2.95	0.9994
14	4.85	1.96	0.9984
15	4.80	1.07	0.9996
16	1.65	2.10	0.9994

mean growth rate, μm/hr = 3.65

variance of growth rates, $\mu m^2/hr^2$ = 0.97

Run 28, T=40°C; ΔT=5°C; I/W=0.9

Crystal no.	Size, μm, at various times 4.5hr	10.67hr	20.25hr	38.5hr
1	2.46	4.72	7.62	11.22
2	0.43	0.99	1.24	1.96
3	0.78	1.23	1.78	2.22
4	1.23	1.78	2.43	3.35
5	0.46	0.93	1.70	2.31
6	1.76	2.41	3.02	3.82
7	1.52	2.06	2.72	3.19
8	0.79		1.69	2.84
9	0.72	2.93	4.71	9.72
10	0.62	1.22	1.43	2.01
11	1.43	2.77	5.02	8.71
12	0.72	1.63	2.44	3.62
13	1.23	2.87	4.79	7.41
14	0.79	3.42	6.42	11.23
15	0.82	1.23	1.51	1.99
16	1.73	3.54	5.22	8.91
17	0.43	0.91	1.32	1.99
18	0.33	0.69	1.02	1.31

Crystal no.	Slope -growth rate μm/hr	intercept -initial size μm	Correlation coefficient
1	0.25	1.84	0.9899
2	0.042	0.38	0.9804
3	0.041	0.74	0.9669
4	0.061	1.07	0.9926
5	0.045	0.35	0.9754
6	0.058	1.68	0.9823
7	0.032	2.06	0.7587
8	0.06	0.50	0.9996
9	0.26	-0.24	0.9967
10	0.037	0.63	0.9620
11	0.21	0.52	0.9994
12	0.082	0.59	0.9849
13	0.18	0.79	0.9911
14	0.30	-0.09	0.9953
15	0.032	0.79	0.9800
16	0.22	1.05	0.9973
17	0.044	0.35	0.9880
18	0.027	0.33	0.9584

mean growth rate, μm/hr = 0.11

variance of growth rates, $\mu m^2/hr^2$ = 0.0091

Run 29 T=40°C; ΔT=7°C; I/W=0.9

Crystal no.	Size, μm, at various times 2.25r	9.5hr	16.17hr	21.0hr
1	2.72	4.56	6.22	8.91
2	1.78	5.62	6.99	9.43
3	1.72	4.63	6.72	9.54
4	1.23	3.72	4.73	6.81
5	1.03	3.21	4.50	6.34
6	0.87	1.56	2.41	3.99
7	1.24	1.96	2.55	3.42
8	1.36	1.88	2.43	3.28
9	2.68	4.87	6.33	8.72
10	2.43	4.52	5.96	7.32
11	1.24	4.06	5.07	6.38
12	2.63	4.63	6.03	
13	1.73	3.82	5.72	
14	2.43	2.89	3.91	5.42
15	1.73	5.62	8.02	11.63
16	1.63	5.06	7.42	10.56

Crystal no.	Slope -growth rate μm/hr	intercept -initial size μm	Correlation coefficient
1	0.32	1.74	0.9808
2	0.39	1.23	0.9858
3	0.40	0.73	0.9937
4	0.28	0.69	0.9863
5	0.27	0.44	0.9938
6	0.16	0.27	0.9588
7	0.11	0.92	0.9882
8	0.10	1.03	0.9777
9	0.31	1.89	0.9887
10	0.26	1.93	0.9984
11	0.26	0.97	0.9827
12	0.24	2.15	0.9970
13	0.29	1.09	0.9999
14	0.15	1.77	0.9502
15	0.51	0.56	0.9924
16	0.46	0.54	0.9910

mean growth rate, μm/hr = 0.28

variance of growth rates, $\mu m^2/hr^2$ = 0.015

Run 30, T=40°C; ΔT=9°C; I/W=0.9

Crystal no.	Size, μm, at various times 0.5hr	2.0hr	5.2hr	8.5hr
1	1.86	6.49	13.77	19.87
2	2.85	5.33	8.95	14.87
3	1.14	3.54	5.80	8.15
4	1.73	5.69	9.86	14.32
5	2.66	5.41	8.64	14.57
6	4.33	7.46	14.68	19.53
7	1.72		6.89	11.23
8	3.63	5.42	9.62	13.31
9	2.44	5.62	9.91	13.02
10	1.04		5.61	10.01
11	2.26	5.23	12.44	17.06
12	1.88	4.92	12.73	19.82

Crystal no.	Slope -growth rate μm/hr	intercept -initial size μm	Correlation coefficient
1	2.22	1.49	0.9957
2	1.47	2.07	0.9951
3	0.95	1.04	0.9932
4	1.62	1.49	0.9818
5	1.43	2.03	0.9929
6	1.93	3.69	0.9953
7	1.18	1.02	0.9987
8	1.22	3.05	0.9994
9	1.30	2.50	0.9886
10	1.11	0.29	0.9960
11	1.88	1.62	0.9945
12	2.27	0.65	0.9996

mean growth rate, μm/hr = 1.55

variance of growth rates, $\mu m^2/hr^2$ = 0.20

Run 31, T=40°C; ΔT=11°C; I/W=0.9

Crystal no.	Size, μm, at various times 0.4hr	2.5hr	4.25hr	6.5hr
1	1.72	4.87	7.65	10.22
2	2.63	6.94	9.72	13.62
3	3.64	7.84	9.96	14.02
4	2.72	10.48	17.62	23.61
5	3.04	8.96	14.32	19.44
6	4.02	9.64	13.62	18.01
7	2.31	3.62	6.04	8.42
8	4.31	7.62	10.41	14.57
9	2.06	8.41	12.21	16.40
10	3.41	6.72	9.49	12.98
11	4.02	8.69	11.22	15.06
12	4.71	10.72	15.06	19.22
13	2.61	5.41	9.22	13.06
14	2.03	3.21		6.03
15	3.61	7.07		17.21

Crystal no.	Slope -growth rate μm/hr	intercept -initial size μm	Correlation coefficient
1	1.41	1.31	0.9973
2	1.78	2.14	0.9986
3	1.66	3.19	0.9966
4	3.47	1.77	0.9961
5	2.71	2.18	0.9981
6	2.29	3.51	0.9971
7	1.03	1.57	0.9905
8	1.68	3.51	0.9991
9	2.33	1.81	0.9927
10	1.57	2.79	0.9999
11	1.78	3.67	0.9962
12	2.38	4.30	0.9946
13	1.75	1.60	0.9963
14	0.66	1.68	0.9985
15	2.27	2.18	0.9952

mean growth rate, μm/hr = 1.91

variance of growth rates, $\mu m^2/hr^2$ = 0.47

APPENDIX C: RAW DATA: MEAN SIZES, VARIANCES OF THE SIZE DISTRIBUTION OF THE NUCLEI, AND NUMBER OF THE NUCLEI GENERATED PER UNIT VOLUNME AT VARIOUS TIMES FROM THE BATCH EXPERIMENTS

Run 1, T=40°C; ΔT=1°C; I/W=0; Lmin=5μm

Time hr	Mean sizes μm	Variances μm^2	Number of nuclei per unit volume $\#/cm^3$
8.25[a]	6.21	0.83	2.78×10^3
12.50[b]	8.45	2.2	3.51×10^3
18.0 [c]	10.93	4.03	4.36×10^3

Size distributions of the nuclei analyzed at various times

a:	5.24	5.61	6.03	6.54	7.32	8.04	5.31
	5.48	6.79	6.21	7.59			
b:	5.08	5.42	5.46	5.93	6.02	6.31	6.22
	6.73	7.52	7.64	7.91	8.36	8.41	8.72
	8.75	9.41	9.32	9.67	9.89	10.62	10.51
	11.72	11.64	11.88	12.06			
c:	5.41	5.06	5.51	6.44	6.69	6.81	7.06
	7.51	7.58	7.69	8.71	8.88	9.91	9.06
	9.41	9.52	9.62	10.87	10.62	10.51	10.22
	11.09	11.63	12.54	12.66	12.93	13.64	13.75
	14.65	15.72	15.93	17.43	18.65	19.83	19.02

Run 2, T=40°C; ΔT=3°C; I/W=0; Lmin=5μm

Time hr	Mean sizes μm	Variances μm^2	Number of nuclei per unit volume $\#/cm^3$
4.5 [a]	7.39	1.79	5.62×10^3
7.5 [b]	14.44	6.34	6.86×10^3
10.9 [c]	17.03	7.73	1.32×10^4

Size distributions of the nuclei analyzed at various times

a: 5.06	5.23	5.76	6.41	6.09	6.25	7.24
7.69	9.43	8.65	8.06	9.52	10.66	
b: 5.72	6.94	6.66	8.72	8.76	9.43	20.73
22.94	23.06	24.96	17.84	10.72	12.54	10.63
12.66	20.62	13.78	15.96	19.88	22.43	
c: 5.23	6.94	6.66	7.53	9.87	10.62	14.32
15.76	20.88	25.43	22.73	20.62	25.72	27.66
16.32	18.72	26.41	25.06			

Run 3, T=40°C; ΔT=5°C; I/W=0; Lmin=5μm

Time hr	Mean sizes μm	Variances μm^2	Number of nuclei per unit volume $\#/cm^3$
3.26[a]	7.22	1.64	1.93×10^4
5.2 [b]	9.65	3.85	2.36×10^4
6.76[c]	14.16	6.02	3.56×10^4

Size distributions of the nuclei analyzed at various times

a:	5.36	5.42	5.06	6.74	6.34	8.92	7.32
	8.06	8.22	6.03	9.46	9.69		
b:	5.06	5.72	5.09	6.34	8.96	8.42	7.06
	10.72	11.64	11.06	13.65	15.84	15.92	
c:	5.04	5.02	6.94	7.22	9.68	9.11	11.54
	12.63	13.82	13.72	17.99	20.23	21.42	20.83
	18.55	18.06	20.44	22.56			

Run 4, T=40°C; ΔT=3°C; I/W=0.3; Lmin=5μm

Time hr	Mean sizes μm	Variances μm^2	Number of nuclei per unit volume $\#/cm^3$
6.17[a]	6.47	1.26	5.02×10^2
10.28[b]	9.33	2.82	9.41×10^2
15.2 [c]	12.68	4.65	2.19×10^3

Size distributions of the nuclei analyzed at various times

a:	5.42	5.62	5.02	5.65	6.73	6.24	7.63
	6.03	7.08	9.24				
b:	5.94	5.22	6.73	6.84	8.22	8.56	8.59
	10.24	10.06	11.21	12.56	13.22	12.96	
c:	5.24	5.31	7.89	7.64	9.59	9.06	10.87
	11.52	12.63	12.71	13.55	13.02	14.08	14.09
	16.42	17.61	19.52	17.60	17.88	20.21	

Run 5, T=40°C; ΔT=5°C; I/W=0.3; Lmin=5μm

Time hr	Mean sizes μm	Variances μm^2	Number of nuclei per unit volume $\#/cm^3$
6.42[a]	6.49	1.28	8.93×10^3
11.56[b]	9.80	3.57	1.73×10^4
16.20[c]	12.46	5.32	2.54×10^4

Size distributions of the nuclei analyzed at various times

a:	5.21	5.06	5.31	5.45	6.31	6.02	7.42
	7.61	8.41	8.06	9.62			
b:	5.34	5.09	5.82	6.02	6.41	8.72	8.56
	9.42	10.06	10.73	10.78	11.42	12.63	14.81
	14.22	16.72					
c:	5.21	5.46	6.71	7.42	7.06	7.22	9.82
	9.51	11.42	12.63	12.72	14.53	14.63	15.83
	16.72	17.93	19.02	20.43	22.51		

Run 6, T=40°C; ΔT=7°C; I/W=0.3; Lmin=5μm

Time hr	Mean sizes μm	Variances μm^2	Number of nuclei per unit volume $\#/cm^3$
3.73[a]	7.68	1.85	6.98×10^3
5.4 [b]	11.45	4.51	1.35×10^4
6.78[c]	16.49	9.01	1.97×10^4

Size distributions of the nuclei analyzed at various times

a:	5.06	5.32	5.42	6.73	6.22	7.34	8.42
	8.53	8.02	8.59	10.02	10.76	9.44	
b:	5.43	5.72	5.64	5.94	7.02	7.33	9.82
	8.64	9.99	10.64	12.52	12.71	12.83	13.81
	13.91	15.04	17.02	17.81	18.64	18.55	
c:	5.42	5.06	5.73	7.42	8.93	10.62	12.43
	15.72	18.92	17.63	20.59	22.51	23.87	25.91
	30.69	32.42					

Run 7, T=40°C; ΔT=9°C; I/W=0.3; Lmin=5μm

Time hr	Mean sizes μm	Variances μm^2	Number of nuclei per unit volume $\#/cm^3$
2.5 [a]	9.66	3.23	1.14×10^3
4.16[b]	11.38	4.76	2.59×10^3
5.5 [c]	13.62	6.62	4.17×10^3

Size distributions of the nuclei analyzed at various times

a:	5.72	5.68	5.34	7.32	8.94	8.06	8.98
	8.42	10.72	9.61	9.72	12.22	13.76	15.28
	15.09						
b:	5.22	5.09	5.20	6.43	8.24	8.61	7.22
	10.64	11.52	10.21	10.55	13.72	15.29	15.23
	12.09	13.06	18.12	18.76	20.93		
c:	5.32	5.24	5.16	5.22	6.73	8.76	8.09
	8.25	9.95	10.64	11.55	12.88	14.41	15.62
	15.73	17.82	19.29	19.61	19.24	23.52	22.71
	22.10	25.72					

Run 8, T=40°C; ΔT=5°C; I/W=0.6; Lmin=5μm

Time hr	Mean sizes μm	Variances μm^2	Number of nuclei per unit volume $\#/cm^3$
6.5 [a]	5.74	0.76	4.13×10^2
20.2 [b]	8.08	2.50	1.16×10^3
38.67 [c]	9.60	3.06	2.50×10^3

Size distributions of the nuclei analyzed at various times

a:	5.06	5.44	5.32	5.64	6.72	5.06	5.02
	6.98	6.41					
b:	5.05	5.46	5.32	6.72	8.93	8.64	10.72
	10.63	11.22					
c:	5.31	5.09	6.71	6.44	8.32	8.06	10.92
	11.42	11.81	11.50	12.21	12.89	14.10	

Run 9, T=40°C; ΔT=7°C; I/W=0.6; Lmin=5μm

Time hr	Mean sizes μm	Variances μm^2	Number of nuclei per unit volume $\#/cm^3$
4.2 [a]	7.99	2.69	4.03×10^3
7.65[b]	12.76	5.66	8.95×10^3
12.1 [c]	16.01	9.07	1.06×10^4

Size distributions of the nuclei analyzed at various times

a:	5.04	5.31	5.68	5.49	5.12	7.32	6.41
	6.58	9.71	10.62	10.21	10.09	12.24	12.01
b:	5.06	5.71	5.98	6.62	8.94	8.21	8.58
	10.72	13.41	12.62	13.55	15.11	15.06	16.61
	18.99	20.22	22.17	22.06			
c:	5.71	5.08	5.22	6.02	8.71	10.62	10.91
	12.71	11.50	14.62	17.51	18.06	22.38	22.94
	25.71	26.88	30.11	33.55			

Run 10, T=40°C; ΔT=9°C; I/W=0.6; Lmin=5μm

Time hr	Mean sizes μm	Variances μm^2	Number of nuclei per unit volume $\#/cm^3$
3.56[a]	6.53	1.49	1.17×10^4
5.16[b]	9.41	3.49	2.15×10^4
7.02[c]	14.60	7.41	2.97×10^4

Size distributions of the nuclei analyzed at various times

a:	5.17	5.26	5.23	5.09	6.71	6.24	8.09
	8.76	8.24					
b:	5.31	5.46	5.08	6.41	8.72	8.66	10.92
	12.41	13.69	12.71	14.01			
c:	5.01	5.42	5.06	5.22	6.71	9.72	10.46
	13.41	16.71	18.42	19.06	20.54	20.66	23.66
	22.01	22.75	23.40				

Run 11, T=40°C; ΔT=7°C; I/W=0.9; Lmin=5μm

Time hr	Mean sizes μm	Variances μm^2	Number of nuclei per unit volume $\#/cm^3$
9.66[a]	6.18	1.24	1.10×10^3
30.56[b]	7.38	2.07	3.54×10^3
56.21[c]	9.54	3.94	7.36×10^3

Size distributions of the nuclei analyzed at various times

a:	5.12	5.24	5.06	5.66	6.71	6.22	5.29
	6.06	7.48	8.92				
b:	5.02	5.41	5.32	5.08	7.42	7.69	6.31
	10.32	9.57	9.64	9.41			
c:	5.01	5.44	5.29	5.32	7.42	9.06	9.11
	9.89	11.64	10.20	13.41	15.46	16.82	

Run 12, T=40°C; ΔT=9°C; I/W=0.9; Lmin=5μm

Time hr	Mean sizes μm	Variances μm^2	Number of nuclei per unit volume $\#/cm^3$
7.83[a]	6.25	1.04	1.41×10^4
11.6 [b]	7.64	2.62	2.51×10^4
19.45[c]	11.34	5.99	3.92×10^4

Size distributions of the nuclei analyzed at various times

a:	5.32	5.06	5.41	5.91	7.81	5.32	5.64
	5.09	6.31	7.08	7.86			
b:	5.33	5.41	5.08	5.09	6.31	6.04	8.72
	10.66	11.45	11.62	8.31			
c:	5.08	5.49	5.21	5.14	7.22	6.31	6.06
	5.39	9.66	10.72	12.45	15.61	16.42	15.01
	15.32	18.48	20.56	18.33	20.40	22.31	7.08
	6.24	6.31					

Run 13, T=40°C; ΔT=10°C; I/W=0.9; Lmin=5μm

Time hr	Mean sizes μm	Variances μm^2	Number of nuclei per unit volume $\#/cm^3$
4.26[a]	7.58	2.49	1.15×10^4
8.22[b]	13.20	7.05	3.77×10^4
12.5 [c]	18.86	11.63	4.47×10^4

Size distributions of the nuclei analyzed at various times

a:	5.06	5.21	5.34	5.46	6.31	6.02	8.42
	8.69	10.33	11.42	11.09			
b:	5.09	5.38	5.06	5.24	6.32	6.09	8.42
	10.64	10.61	12.54	13.81	14.62	12.71	15.88
	15.94	17.82	22.31	24.56	25.08	25.91	
c:	5.64	5.09	5.21	5.17	5.65	6.08	6.84
	6.92	8.72	11.64	11.72	13.65	15.72	18.69
	20.08	22.54	22.91	25.31	27.42	27.66	29.34
	29.09	32.51	32.17	35.06	36.44	42.01	